Black Sea Production Centre
BLKSEA_REANALYSIS_PHYS_007_004

Issue: 3.1

Contributors: Bénédicte Lemieux-Dudon (CMCC), Leonardo Lima (CMCC), Andrea Storto (CMCC), Stefania Ciliberti (CMCC), Elisaveta Peneva (USOF), Simona Masina (CMCC)

Approval date by the CMEMS product quality coordination team: 09/12/2019

CHANGE RECORD

When the quality of the products changes, the QuID is updated and a row is added to this table. The third column specifies which sections or sub-sections have been updated. The fourth column should mention the version of the product to which the change applies.

Issue	Date	§	Description of Change	Author	Validated By
2.0	November 2017	all	First version of the document for V4	B. Lemieux-Dudon	
3.0	February 2018	all	Revision	E. Peneva	
3.1	April 2019	$VII	Adding SSH de-trended evaluation		
3.2	September 2019	$VII	Inclusion of the validation results for the extension period: 2016 to 2018		Mercator Ocean

APPLICABLE DOCUMENTS

	Ref	Title	Date / Version
DA 1	CMEMS-BS-ScQR	CMEMS Black Sea Scientific Qualification Report	Jan 2017
DA 2	CMEMS-BS ScVP	CMEMS Black Sea Scientific Validation Plan	Jan 2017
DA 3	CMEMS-BS-QUID_007_001	Black Sea QUID for BLKSEA_ANALYSIS_FORECAST_PHYS_007_001 for V2.2	Sep 2016

LIST OF FIGURES

LIST OF TABLES

GLOSSARY

CIL	Cold Intermediate Layer
EAN	Estimated Accuracy Number
EOFs	Emphirical Orthogonal Functions
IC	Initial Condition
MDT	Mean Dynamic Topography
PSU	Practical Salinity Unit
QNET	Surface Heat Flux
REA	REAnalysis
BS-RAN-V3	Black Sea reanalysis version V3
BS-RAN-V4	Black Sea reanalysis version V4
RMSD	Root Mean Square Difference
S	Salinity
SFW	Surface net Fresh Water flux
SL	Sea Level
SLA	Sea Level Anomaly
SSS	Sea Surface Salinity
SST	Sea Surface Temperature
STD	STandard Deviation
T	Temperature
TAC	Thematic Assembly Centre
UV	Zonal and meridional currents

TABLE OF CONTENTS

I EXECUTIVE SUMMARY

I.1 Products covered by this document

This document describes the quality of the product BLKSEA_REANALYSIS_PHYS_007_004, which includes 2D daily fields of sea surface height and 3D daily fields of temperature, salinity, meridional and zonal currents at about 3 km of horizontal resolution and 31 vertical levels. The available time series is 1992-2017.

The aim of the BLKSEA_REANALYSIS_PHYS_007_004 is to provide an integrated set of information coherent and consistent across space-time dimension, through an optimal combination of observations and appropriate space and time numerical model, covering the period 1995-2018.

I.2 Summary of the results

The quality of the BLKSEA_REANALYSIS_PHYS_007_004 has been assessed for the period 1995 to 2015 by comparing results with available observations and consolidated climatological products.

The quality of the product changes with time consistently with the increasing data availability, as shown in the assessment of ocean state variables (salinity, temperature), and the performance of the reanalysis increases with time, as the number of ocean observations increases. The assessment of the results suggests that the overall performance of the reanalysis is satisfactory: the ocean state is well constrained by data assimilation and the ocean physics appear well represented in many aspects.

Initial drifts in T/S are recovered by the data assimilation system during the reanalysis period with the increasing number of the in situ T/S profiles assimilated. A reduction of the drift is achieved by the mean of a) improvements of the T/S background error covariance structure, b) a better assessment of the MDT, c) a better SLA innovation bias correction and d) a retuned vertical physics parameterizations. But residual drifts still require to be investigated. As in BS-RAN-V3, a Large Scale Bias Correction (LSBC) restoring to T/S climatology is applied in BS-RAN-V4. But compared to BS-RAN-V3 the strength of the restoring factor is reduced in the first 1000.

The results are grouped by ocean state variables and summarized below. Note that the misfit skill scores are calculated before removing observation outliers. The performance is therefore under-evaluated compared to scores using the effective data assimilated by the system. In addition, the T/S misfit skill scores are downgraded by the early part of the reanalysis due to very sparse T/S in situ observations before 2005 in the Black Sea (see details in Table I-1)

Salinity (S) : The salinity RMS and BIAS with respect to in-situ data assimilated by the system are presented as profiles averaged over the whole domain (up to 800 m) and over the entire time period. RMS differences range from about 0.43 psu at the surface to a local maximum of 0.36 psu around 100 m depth and to less than 0.1 psu below 200 m. Salinity BIAS is very slightly positive in the first 25 m of the water column then negative at depths, peaking at -0.055 at 50 m and getting close to zero between 175 and 250 m . Below 300 m, the BIAS does not exceed 0.01 psu in absolute value.

Sea Level Anomaly (SLA) : the SLA RMS with respect to along-track data assimilated oscillates from about 3 to 6 cm with a mean of ~4.4 cm, comparable with the RMS of observations. The SLA bias is 0.05 cm. Importantly, the new SLA BS-RAN-V4 EANs cannot be compared to BS-RAN-V3 performance because of a necessary change in the SLA innovation bias removal (see discussion in section IV.6).

Sea Surface Temperature (SST) : SST RMS and BIAS with respect to gridded CMEMS objective analyses are presented as time series and horizontal maps. BIAS and RMS present a seasonal signal and remain quite stable all over the years, oscillating respectively around -0.08°C and 0.57°C.

Temperature (T) : The temperature RMS and BIAS with respect to in-situ data assimilated by the system are presented as profiles averaged over the whole domain (up to 800 m) and the entire reanalysis period. RMS differences along the water column range from the maximum value of 1.9°C at 30 m to less than 0.1°C below 200 m. In the surface layer, the BIAS is maximum with a positive value of ~0.39°C, while below 30 m the bias becomes negative. At around 50 m, the bias reaches -0.2°C which is the overall profile minimum bias. At depths, the bias always remains below -0.1°C, the lowest absolute values being found between 200 and 400 m.

I.3 Estimated Accuracy Numbers

The results for each variable assessed are presented in Table I-1. The skill scores are given for the full period of reanalysis (1995-2015) as well as for period 2005-2015 where the statistics are more relevant since before 2005 in situ profiles are very sparse.

Parameter	BIAS V4	RMS V4
SST [°C]	-0.07 / **-0.07**	0.58 / **0.59**
T [°C] 0-100	-0.02 / **0.025**	0.87 / **0.74**
T [°C] 100-300	-0.03 / **-0.003**	0.15 / **0.09**
T [°C] 300-800	-0.02 / **-0.02**	0.11 / **0.05**
S [psu] 0-100	-0.014 / **0.002**	0.33 / **0.26**
S [psu] 100-300	-0.006 / **0.009**	0.19/ **0.15**
S [psu] 300-800	-0.005 / **-0.002**	0.05 / **0.03**
SLA [cm]	0.055/ **0.045**	4.377/ **4.356**

Table I-1. **Summary of BLKSEA_REANALYSIS_PHYS_007_004 performance for different parameters and depth ranges over the entire time period 1995-2015 (first entry in red) and over 2005-2015 for temperature and salinity (second entry in blue).**

II PRODUCTION SYSTEM DESCRIPTION

II.1 Production centre details

In the following, a list of synthetic information related to Physics Production Unit:

- Production Center Name: BS-MFC PU-PHY
- Production Subsystem Name: BS-MFC Physical Reanalysis
- Production Unit: CMCC

The BLKSEA_REANALYSIS_PHYS_007_004 has been produced by Physics PU at CMCC by combining, the output of the ocean model, forced by atmospheric surface fluxes and relaxed to SST, and quality controlled ocean observations, through the data assimilation scheme.

II.2 Brief overview of the BS-MFC Physical Reanalysis System (BS-REA)

The Black Sea Physical Reanalysis system relies on five main components:

- **Ocean model** : is a hydrodynamic model, supplied by Nucleus for European Modelling of the Ocean (NEMO) ;
- **Data assimilation scheme** : is a variational data assimilation scheme (OceanVar) for temperature and salinity profiles, satellite Sea Level Anomaly along track data and satellite SST data ;
- **Assimilated data** : are in-situ temperature and salinity profiles, Sea Level Anomaly along track and satellite SST data ;
- R**estoring scheme** to SSS objective reanalysis and regridded satellite SST data with correction to the freshwater flux and heat flux, respectively
- **Large Scale Bias Correction** (LSBC) restoring to T/S climatology.

II.2.1 Circulation model component

The numerical ocean model for the BS-REA covers the entire Black Sea area and the hydrodynamic code is based on NEMO v3.4 (Nucleus for European Modeling of the Ocean, Madec et al., 2012). The primitive equations are discretized on a horizontal grid with 1/27° resolution in zonal direction and 1/36° resolution in meridional direction and a vertical grid of 31 levels with partial-steps, integrated in time using a linear free-surface formulation. The horizontal spatial resolution of 1/27°x1/36° is chosen in order to have the same Cartesian resolution in latitude and longitude, approximately 3 km at the model domain latitudes, which is conforming to the mesoscale eddy-resolving scale (Rossby radius of deformation in the Black Sea ~20 km). Bathymetry is based on GEBCO dataset (www.gebco.net).

The BS-REA configuration uses the ECMWF ERA-Interim atmospheric reanalysis (about 0.75° of spatial resolution). The atmospheric fields are provided 3-hourly. In particular, the atmospheric fields used are: zonal and meridional components of 10 m wind (ms^{-1}), total cloud cover (%), 2 m air temperature (K), 2 m dew point temperature (K) and mean sea level pressure (Pa). Precipitation fields over the basin are from GPCP rainfall monthly data (Adler et al., 2003; Huffman et al., 2009).

The atmospheric fields are used for computing the momentum, heat and water fluxes at the air-sea interface based on the Black Sea bulk formulae (Grayek et al., 2010).

Concerning the land forcing, in particular the river runoff contribution, an estimate of the inflow using monthly mean dataset provided by SESAME project (Ludwig et al., 2009) is used. The impact of the Bosporus Strait on the Black Sea dynamics is accounted for in terms of a surface boundary condition, taking into account the barotropic transport, which has been computed to balance the freshwater fluxes on monthly basis (Stanev and Beckers, 1999, Peneva et al., 2001).

II.2.2 Description of the data assimilation scheme

The data assimilation system of BS-REA is based on a three-dimensional variational (3DVAR) assimilation scheme, originally developed for the Mediterranean Sea (Dobricic and Pinardi, 2008) and later extended for the global ocean (Storto et al., 2011). The system is called OceanVar. The variational cost function is solved with the incremental formulation (Courtier, 1997). The pre-conditioning of the cost function minimization is achieved through a change-of-variable transformation.

In the BS-REA implementation of the OceanVar, the control vector in physical space is formed by the three-dimensional fields of temperature and salinity and sea surface height. The assimilation frequency is 3-daily, with a 6-day assimilation time-window. Background-error covariances are decomposed in vertical covariances and horizontal correlations. The former are modelled through 15-mode multi-variate Empirical Orthogonal Functions (EOFs). EOFs were calculated from a dataset of anomalies with respect to the long-term mean of a model simulation without data assimilation, using the full model resolution. Horizontal correlations are modelled through a first-order recursive filter (Farina et al., 2015), with spatially inhomogeneous correlation length-scales (Storto et al., 2014) specified as a function of the distance from coast, ranging approximately from 9 to 27 km. The assimilation of sea level anomaly (SLA) is performed by imposing local hydrostatic adjustments as multi-variate balance between the sea level innovation and vertical profiles of temperature and salinity (Storto et al., 2011).

The observations assimilated in the BS-Currents include: i) in-situ hydrographic profiles (mostly Argo floats) from the UK MetOffice Hadley Center EN4 dataset; ii) along-track sea level anomalies from all available missions, pre-processed and distributed by the CMEMS Sea level TAC. The mean dynamic topography for the assimilation of SLA is computed from a 10 year (1993-2012) model mean sea surface height; iii) gridded sea surface temperature (SST) observations provided by the CMEMS Ocean and sea ice TAC. The assimilation of SST assumes that satellite observations are co-located with the first model level. In BS-REA the observation pre-processing includes a background quality-check, which rejects observations whose square departure from the background exceeds the sum of background and observation error variances by a certain threshold. The threshold is currently set to 1 for SLA and 3.3 for the other observations. For satellite observations (SLA, SST), a horizontal thinning is also applied, approximately to retain one observation only every 6 km. The observational error specification is vertically varying for the in-situ and horizontally varying for the satellite observations, and is based on a prior analysis of the assimilation output statistics.

II.2.3 Large Scale BIAS Correction (LSBC)

Over time periods with very sparse in situ observations (before 2005), previous reanalysis exhibited a T/S drift with especially very high values of salt in the deeper layers. Experiments showed that the drift is systematically recovered after 2005 with the application of in situ T/S data in the DA system.

Sensitivity tests showed that the T/S drift is sensitive to: i) the MSSH and to ii) the EOFs dataset to assess the vertical background error covariance, iii) a better assessment and removal of the SLA innovation bias. A reduction of the salinity drift was achieved by these means. But residual drifts still require to be investigated. For those reasons, we still apply a Large Scale Bias Correction scheme but with a reduced strength. A T/S restoring term is applied to filter (both in space and time) the large scale model bias with respect to a monthly 1995-2015 climatology based upon a reanalysis that does not assimilate SLA data. The characteristic time scales of the restoring scheme range from 6 to 3 months with a stronger restroring factor at depths (transition depth being set to 800 m). A Shapiro filter is applied with a spatial length scale of about 2000 km.

II.2.4 Changes with respect to the operational system BS-Currents

There are six main changes of the BS-REA configuration with respect to the operational analysis and forecast system BS-Currents:

- The BS-REA is initialized on 1/1/1990 by a 2012-2016 January mean state from a previous assimilation experiment, followed by a 5 years spin-up, in the attempt of minimizing model biases at the beginning of the reanalysis period.
- In-situ observations are extracted from the U.K. MetOffice EN4 dataset, because the in-situ Copernicus TAC does not provide historical data before 2011 as of July 2016, unless extracting manually from individual platform files.
- The ERA-Interim atmospheric reanalysis replaces the operational ECMWF analyses and forecasts as surface forcing to ensure temporal consistency. Data are used 3-hourly.
- The Assimilation cycle is also changed: the assimilation frequency is every 3 days, with a 6-day assimilation time-window (i.e. "overlapping 3DVAR") in order to increase the observation coverage for each assimilation window.
- To lower the T/S drift connected to the lack of in situ observations between 1995 and 2005, a T/S climatological restoring term is applied to filter (both in space and time) the large scale model bias with respect to a monthly 1995-2015 climatology.
- The EOFs to assess vertical T/S background error covariances are now based on a dataset of weekly mean anomalies calculated from a 1995-2015 reanalysis.

ilated in the reanalysis system.

Table II summarizes the atmospheric forcing and data assimilated in the reanalysis system.

Table II-1. Atmospheric forcing and data assimilated details.

DATA TYPE	EXTERNAL PRODUCTS
ATMOSPHERIC FORCING	ECMWF ERA-INTERIM
SLA	SEALEVEL_BS_SLA_L3_REP_OBSERVATIONS_008_023 SEALEVEL_BS_SLA_MAP_L4_REP_OBSERVATIONS_008_031
In-situ profiles	UK MetOffice EN4.1.1
SST	SST_BS_SST_L4_NRT_OBSERVATIONS_010_006 SST_BS_SST_L4_REP_OBSERVATIONS_010_022 SST_BS_SST_L3S_NRT_OBSERVATIONS_010_013

III VALIDATION FRAMEWORK

The performance of the BLKSEA_REANALYSIS_PHYS_007_004 has been evaluated for the period 1st January 1995-31st December 2018 considering a set of standardized metrics grouped by ocean state variables and applied in order to assess different aspects that can affect the quality of the products.

All confrontations were undertaken from an "in-situ point of view", where the observational dataset were kept on their original position and the corresponding model estimates are interpolated to the sensor position.

The EANs have been computed using the misfits statistics. Misfits have been calculated before the data are inserted via data assimilation and the data can be considered as independent since the data are mostly sparse in space and time. The deviations between the datasets are quantified in terms of RMSD and BIAS, where RMSD provides estimates of the model precision while the BIAS indicates possible systematic errors in the model reanalysis, assuming that the observational dataset is correct. The RMSD and BIAS from temperature and salinity misfits are presented as monthly mean time series over 3 layers: L1) 0-100 m; L2) 100-300 m; L3) 300-800 m and as mean profile computed over the entire domain and the entire time period. Layers deeper than 800 m have not been considered because of the scarcicity of the observations. These three layers are also used in the metrics showing basin- and layer- averaged time-series.

Comparisons of the long-term mean with the reference climatology are performed on five depth levels, equal to 30, 70, 170, 440 and 1100 m of depth.

Trends are computed as linear trends from monthly mean outputs.

In the sea level comparison with observations, we compare the dynamic sea level only, defined as the difference between the full field of sea level and the time-varying basin-averaged mean sea level, to avoid that model drifts interfere in the validation.

The PU-PHY team is working, in collaboration with the Product Quality Responsible, to complete the evaluation of the system performances with respect to mixed layer depth, bottom temperature and currents as reported in [DA2]. In particular, for the newly introduced in V4 product Bottom Temperature, validation will be done against ARGO measurements and climate estimates for the deep part. Discussion on the possibility to use the geostrophic current anomaly from altimeter data for validation of the model surface currents will be initiated within the BS PQWG. This will be part of the updated version of the present QUID, since the numerical procedures for the BS-Currents are under development according to the evolution of the system.

IV VALIDATION RESULTS

IV.1 Sea Surface Temperature

Table IV summarizes the metrics and the observations used in the assessment of sea surface temperature.

Table IV-1. Metrics and observations used to assess sea surface temperature (continues in next page).

Name	Reference dataset	Quantity
SST-M-CLASS1-IRAD-MEAN_T	SST_BS_SST_L4_REP_OBSERVATIONS_010_022	Maps of long-term annual mean from reanalysis product and reference dataset
SST-M-CLASS4-IRAD-RMSD_XY	SST_BS_SST_L3S_NRT_OBSERVATIONS_010_013	Time series of RMS of reference dataset minus reanalysis
SST-M-CLASS4-IRAD-BIAS_XY	SST_BS_SST_L3S_NRT_OBSERVATIONS_010_013	Time series of BIAS of reference dataset minus reanalysis
SST-M-CLASS1-IRAD-RMSD_T	SST_BS_SST_L4_REP_OBSERVATIONS_010_022	Maps of annual mean RMS of reference dataset minus reanalysis product
SST-M-CLASS1-IRAD-BIAS_T	SST_BS_SST_L4_REP_OBSERVATIONS_010_022	Maps of annual mean BIAS of reference dataset minus reanalysis product
SST-M-CLASS1-IRAD-MEAN_XY	SST_BS_SST_L4_REP_OBSERVATIONS_010_022	Time series of domain averaged monthly SST computed from reanalysis product and reference dataset
QNET-M-NC-MEAN_XY	None	Time series of domain averaged surface heat flux
SST-M-CLASS1-IRAD-TREND	SST_BS_SST_L4_REP_OBSERVATIONS_010_022	Map of linear trend of SST

Figure IV (**SST-CLASS1-MEAN**) shows the SST comparison between annual mean computed from reanalysis product and from satellite observations. The spatial pattern of satellite observation is well reproduced by the reanalysis product with the typical zonal gradient in the eastern-most area and meridional gradient in the north-western region.

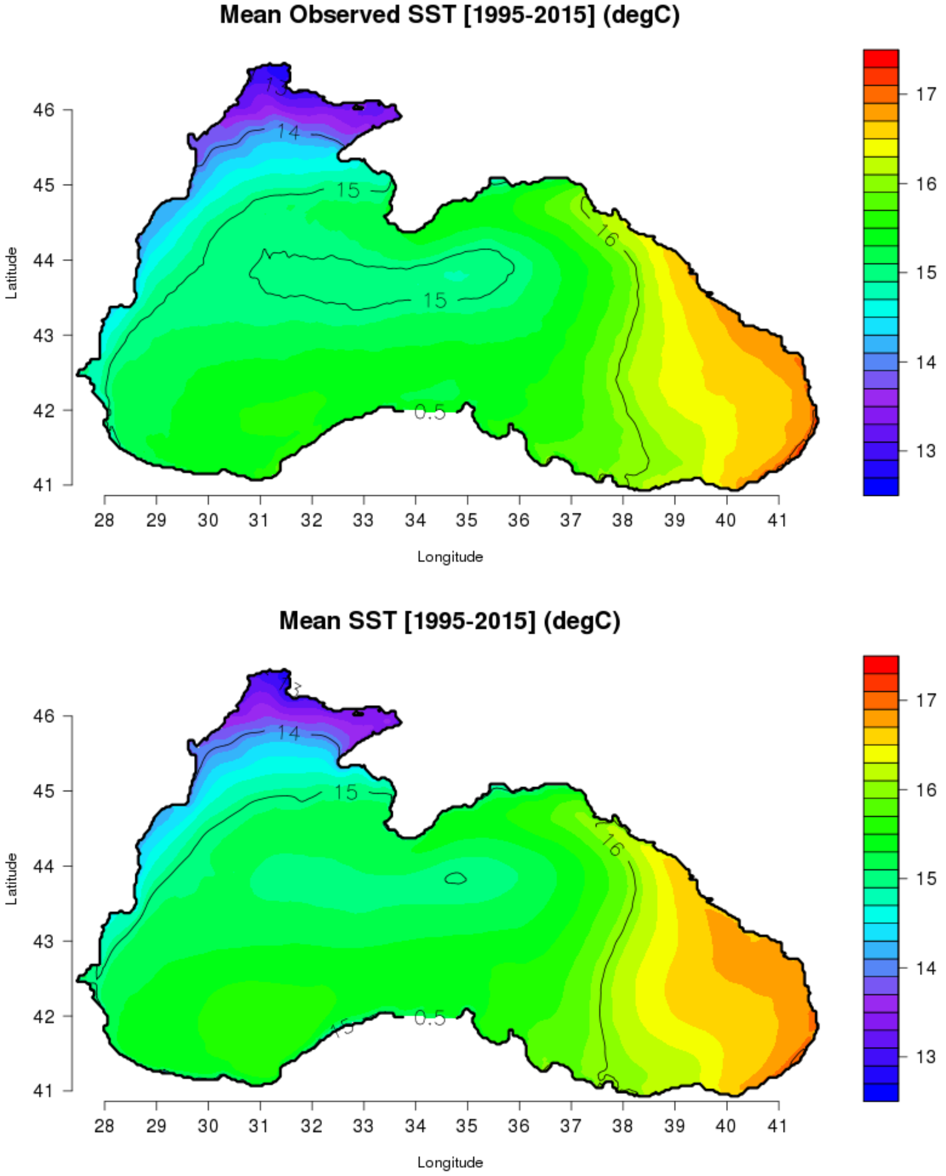

Figure IV-1. SST-CLASS1-MEAN Maps of long term annual mean from Satellite SST (top) and reanalysis product (bottom).

Figure IV (**SST-CLASS4-BIAS-MONTHLY** and **SST-CLASS4-RMS-MONTHLY**) shows the SST BIAS and RMSD of the differences between reanalysis product and satellite observations computed from monthly estimates over the time period 1995-2015. Both the statistics present a seasonal signal, with error increasing during summer period (up to 1.0°C). The RMSD oscillates between ~0.2 and 1.0°C around an average value of 0.57°C. The BIAS is positive during summertime and negative during wintertime. It oscillates between -0.5 and 0.025°C with an average of -0.074°C.

Figure IV (**SST-CLASS1-BIAS and SST-CLASS1-RMS**) shows maps of the SST BIAS and RMS computed over the period 1995-2015. The horizontal maps highlight the areas where the major model deficiencies are located, i.e. the northern shallow area and the eastern most part of the domain where the BIAS and RMSE peak to 0.24 and 0.28°C , respectively.

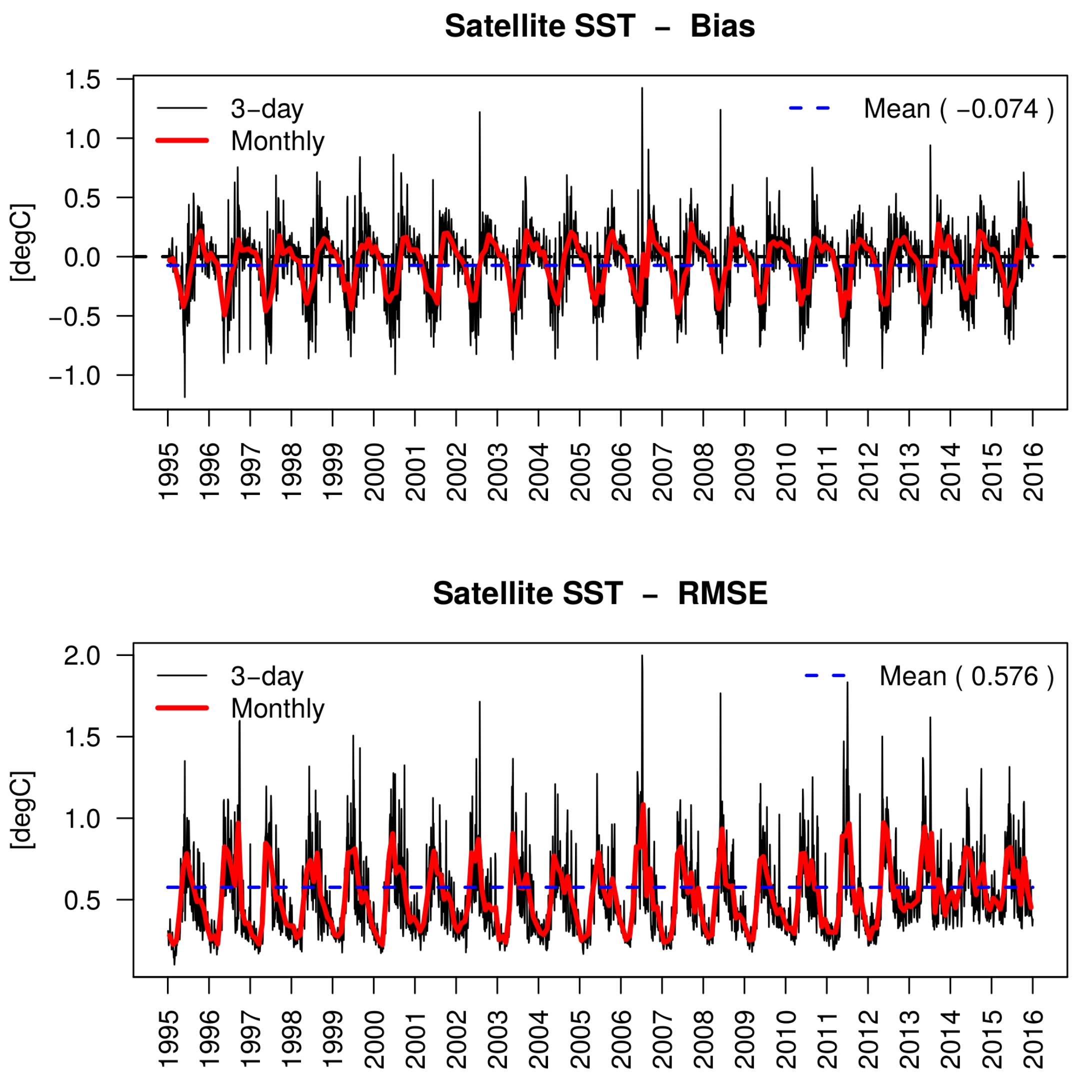

Figure IV-2. SST-CLASS4-RMS-MONTHLY (top panel) and SST-CLASS4-BIAS-MONTHLY (bottom panel) showing time series of basin averaged SST misfit BIAS and RMS computed from reanalysis product and satellite observations.

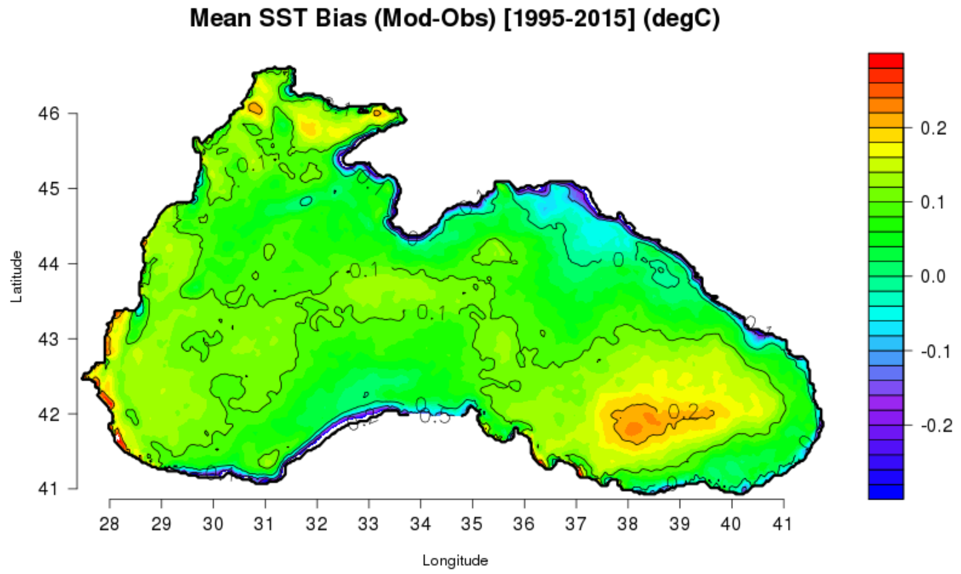

(a)

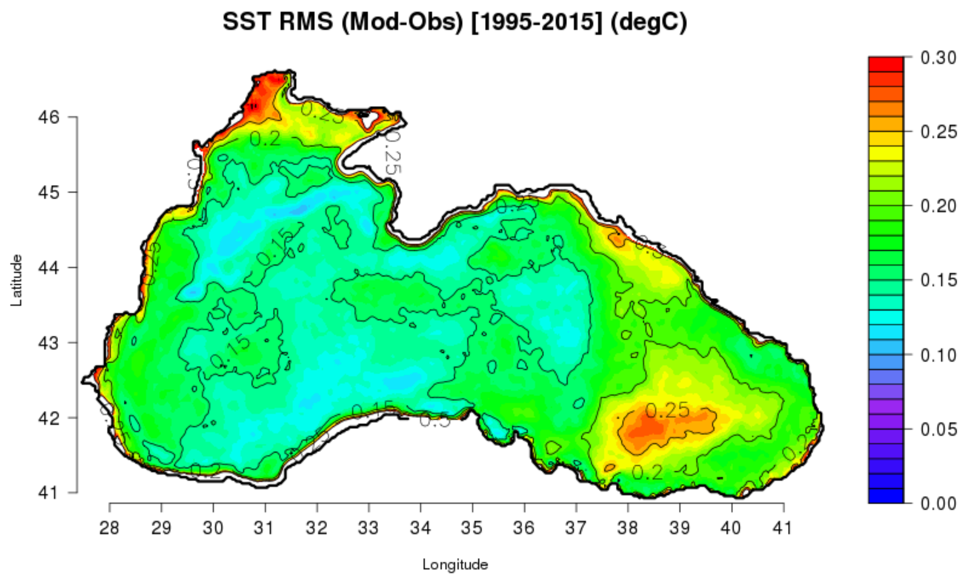

(b)

Figure IV-3. SST-CLASS1-BIAS (top panel) and SST-CLASS1-RMS (bottom panel) showing the maps of the BIAS and RMS computed from reanalysis product against satellite observations over period 1995-2015.

Figure IV (**SST-CLASS3-2DMEAN**) shows the time series of basin averaged monthly mean SST computed from reanalysis product and from satellite observations over the whole period. The multiyear mean for the reanalysis product is 15.46°C, while for the observations is 15.38°C.

Figure IV (**QNET-CLASS3-2DMEAN**) shows the multiyear monthly mean net heat flux. The net heat budget is equal to 20.2 W/m^2. The blue line shows the Damping Heat flux associated to the NEMO SST restoring term. The reanalysis SST surface temperature (ie, first model level temperature) are in average too high compared to the SST_L4 regridded satellite observation. A systematic negative heat flux correction is applied to the net downward heat flux. This correction is slightly reduced compared to BS-RAN-V3.

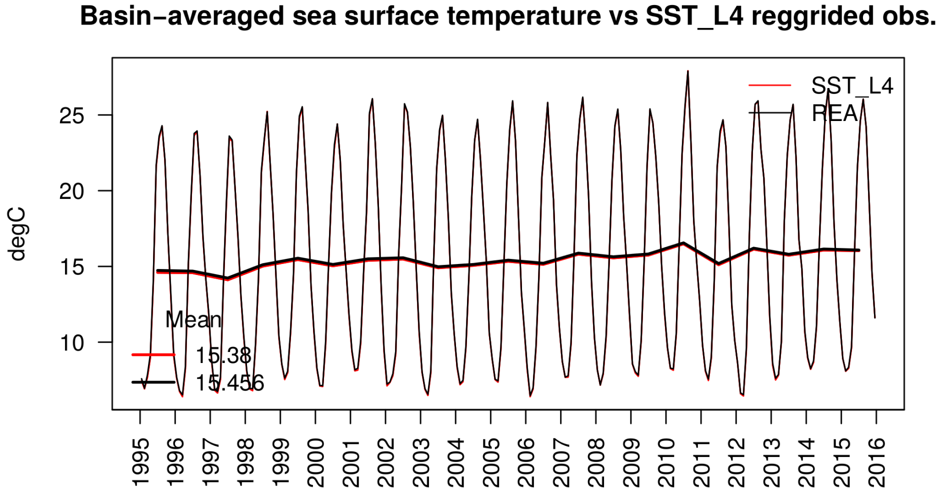

Figure IV-4. SST-CLASS3-2DMEAN Basin averaged monthly mean SST computed from reanalysis product (REA) and from satellite observations (SST_L4)

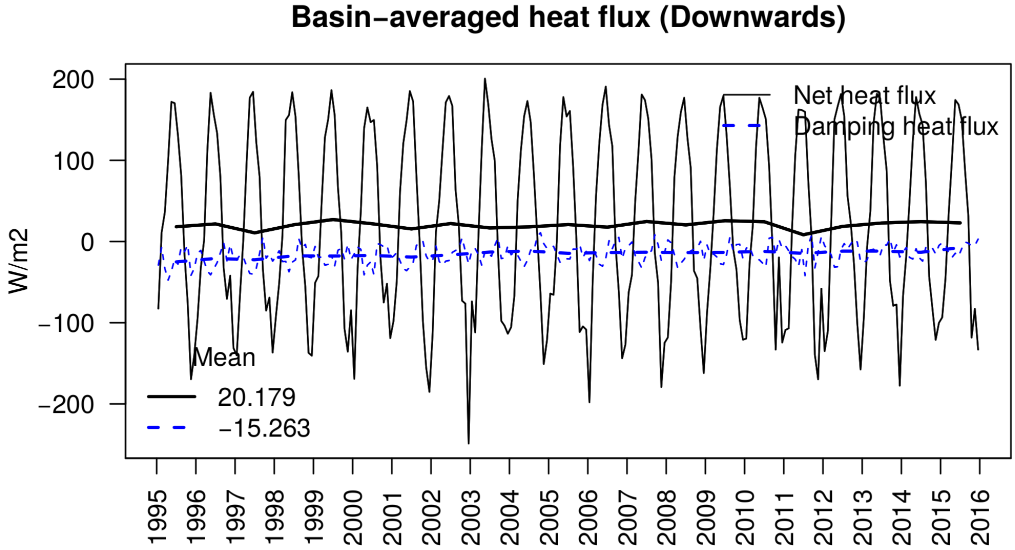

Figure IV-5. QNET-CLASS3-2DMEAN Time series of basin averaged surface net heat flux computed from reanalysis product.

Figure IV and Figure IV-1 (**SST-CLASS1-TREND**) show the linear trends of SST over period 1995-2015 for the reanalysis product and for the SST reference dataset. It highlights the close reproduction of the observed trend by the reanalysis product with a rate ranging from 0.8 to 1°C per decade.

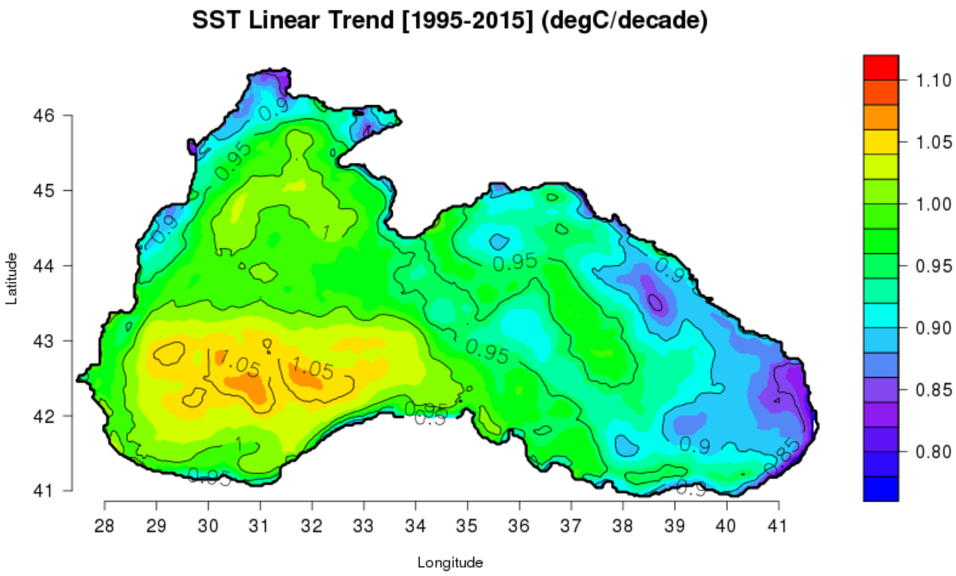

Figure IV-6. SST-CLASS1-TREND Map of the SST linear trend over period 1995-2015 from the reanalysis product.

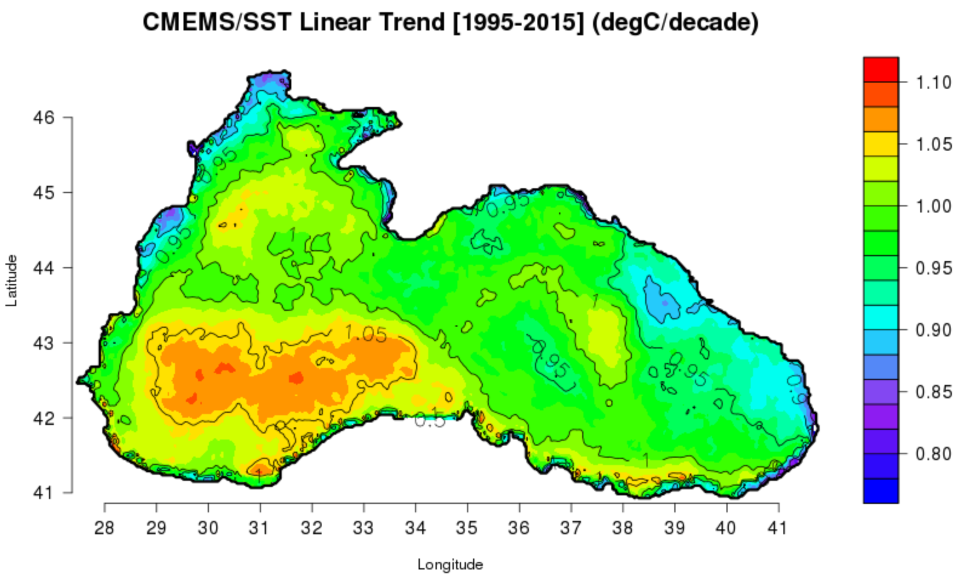

Figure IV-1. Map of the SST linear trend over the period 1995-2015 from the CMEMS SST reference dataset

IV.2 Temperature

Table IV-1 summarizes the metrics and the observations used in the assessment of the reanalysis performance for the temperature.

Table IV-1. Metrics and observations used to assess temperature

Name	Reference dataset	Quantity
T-30 m-M-CLASS1-CLIM-MEAN_T And more generally: T-<DEPTH>-M-CLASS1-CLIM-MEAN_T With <DEPTH> to be replaced by 30 m, 70 m, 170 m, 440 m or 1100 m.	Simonov A. I. and E. N. Altman, Editors. 1991. Hydrometeorology and hydrochemistry of the USSR seas. Vol. IV, The Black Sea, Gidrometeoizdat, 430 pp.	Maps of long-term annual mean from reanalysis product at different depths
T-30 m-M-CLASS1-CLIM-BIAS_T And more generally: T-<DEPTH>-M-CLASS1-CLIM-BIAS_T With <DEPTH> to be replaced by 30 m, 70 m, 170 m, 440 m or 1100 m.	Simonov A. I. and E. N. Altman, Editors. 1991. Hydrometeorology and hydrochemistry of the USSR seas. Vol. IV, The Black Sea, Gidrometeoizdat, 430 pp.	Maps of long-term annual mean difference between the reanalysis product and the reference dataset at different depths
T-M-<LAYERS>-NC-MEAN_XY With <LAYERS> to be replaced by 0_100 m, 100_300 m or 300_800 m	None	Time series of temperature computed from reanalysis product at different layers
T-PROF-M-NC-IC-BIAS_XY	None	Water column differences between monthly basin averaged reanalysis temperature profiles and the IC
T-<LAYERS>-M-INNO-PROF-RMS With <LAYERS> to be replaced by 0_100 m, 100_300 m or 300_800 m	UK MetOffice EN4	Time series of RMS computed from misfits in different layers
T-<LAYERS>-M-INNO-PROF-BIAS With <LAYERS> to be replaced by 0_100 m, 100_300 m or 300_800 m	UK MetOffice EN4	Time series of BIAS computed from misfits in different layers
T-PROF-M-INNO-PROF-RMS	UK MetOffice EN4	Mean RMS profiles
T-PROF-M-INNO-PROF-BIAS	UK MetOffice EN4	Mean BIAS profiles

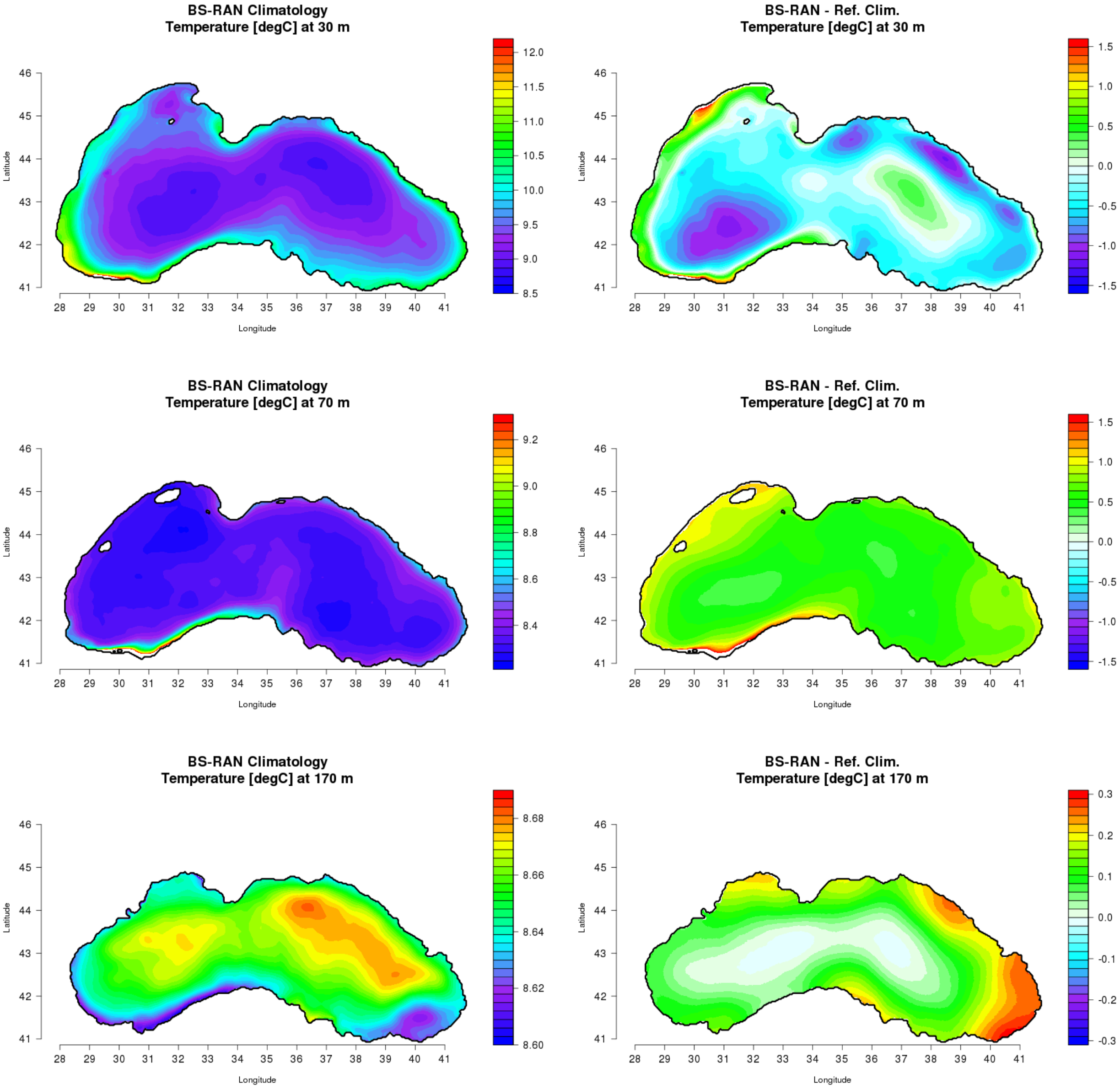

Figure IV-2. T-CLASS1-MEAN-DEPTHS Maps of the reanalysis product temperature climatology (left panels) and difference between reanalysis and reference dataset climatology (right panels) at 30, 70, 170, 440, 1100 m of depth (continues in next page).

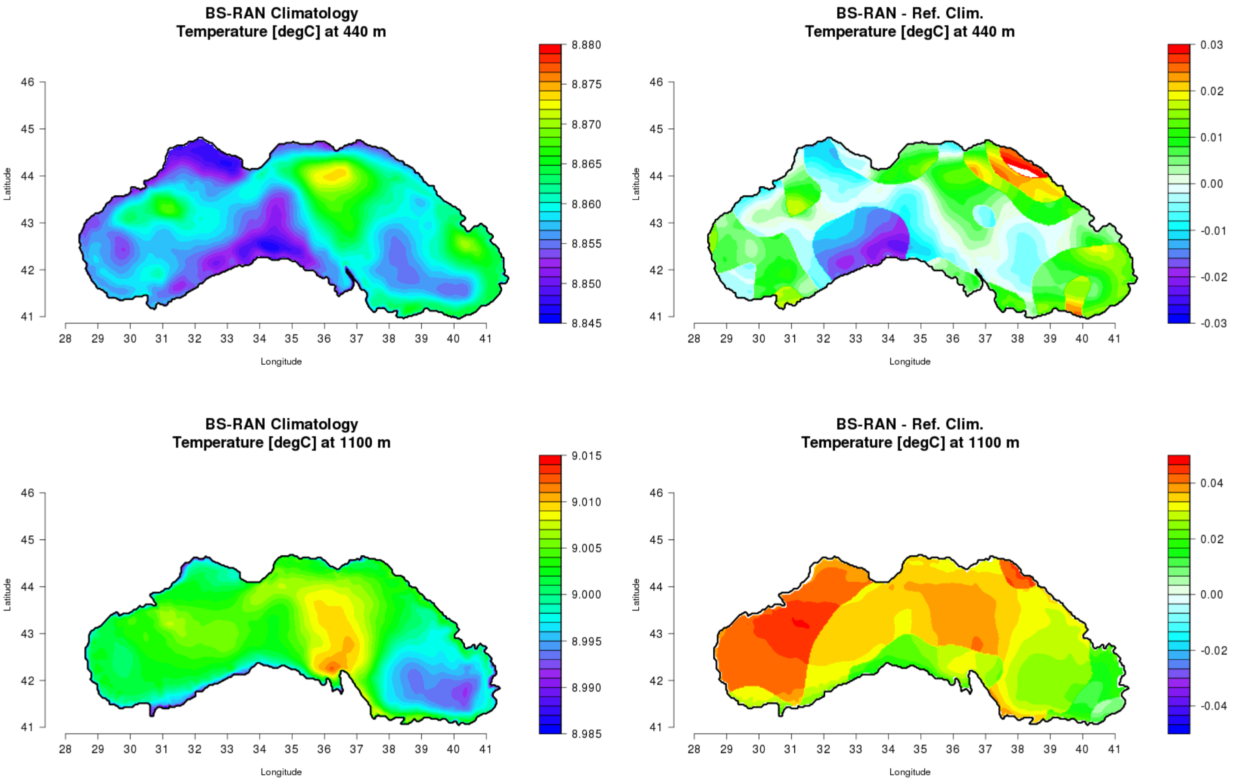

Figure IV-3. T-CLASS1-MEAN-DEPTHS Maps of the reanalysis product temperature climatology (left panels) and difference between reanalysis and reference dataset climatology (right panels) at 30, 70, 170, 440, 1100 m of depth.

Figure IV-2. T-CLASS1-MEAN-DEPTHS Maps of the reanalysis product temperature climatology (left panels) and difference between reanalysis and reference dataset climatology (right panels) at 30, 70, 170, 440, 1100 m of depth (continues in next page).

shows the maps of the 1995-2015 climatology from BS REA (left panels) and the difference between the reanalysis climatology and the reference dataset (right panels) at the five selected levels at 30, 70, 170, 440 and 1100 m of depth.

Differences at 30 m of depth indicate that the reanalysis is on the average colder than the reference climatology in the western area and warmer in the interior of the eastern area, with absolute differences generally below 0.8°C, except i) in the shallow north-western area with biases up to 1.4°C; and ii) in the south-western interior with negative biases down to -1.2°C. At deeper levels, the reanalysis is warmer than the reference dataset with differences of the order of magnitudes 0.5, 0.2, 0.02 and 0.04 °C, at 70, 170, 440 and 1100 m of depth, respectively.

Figure IV-4 shows the basin-averaged temperature values in the three selected layers (0-100, 100-300, 300-800 m of depth). The upper layer proves rather stable with a pronounced seasonal variability, oscillating between 8 and 12°C with an average value of 9.8°C. The layer 100-300 m shows a small initial increase of the layer-averaged temperature (+0.12°C over period 1995-2015). Similarly, the 300-800 m layer is stable in average showing values in between 8.87 to 8.90°C. The layers 100-300 and 300-800 m exhibit two abrupt but moderate cooling events, over periods 2002-2003 and 2006-2007. .

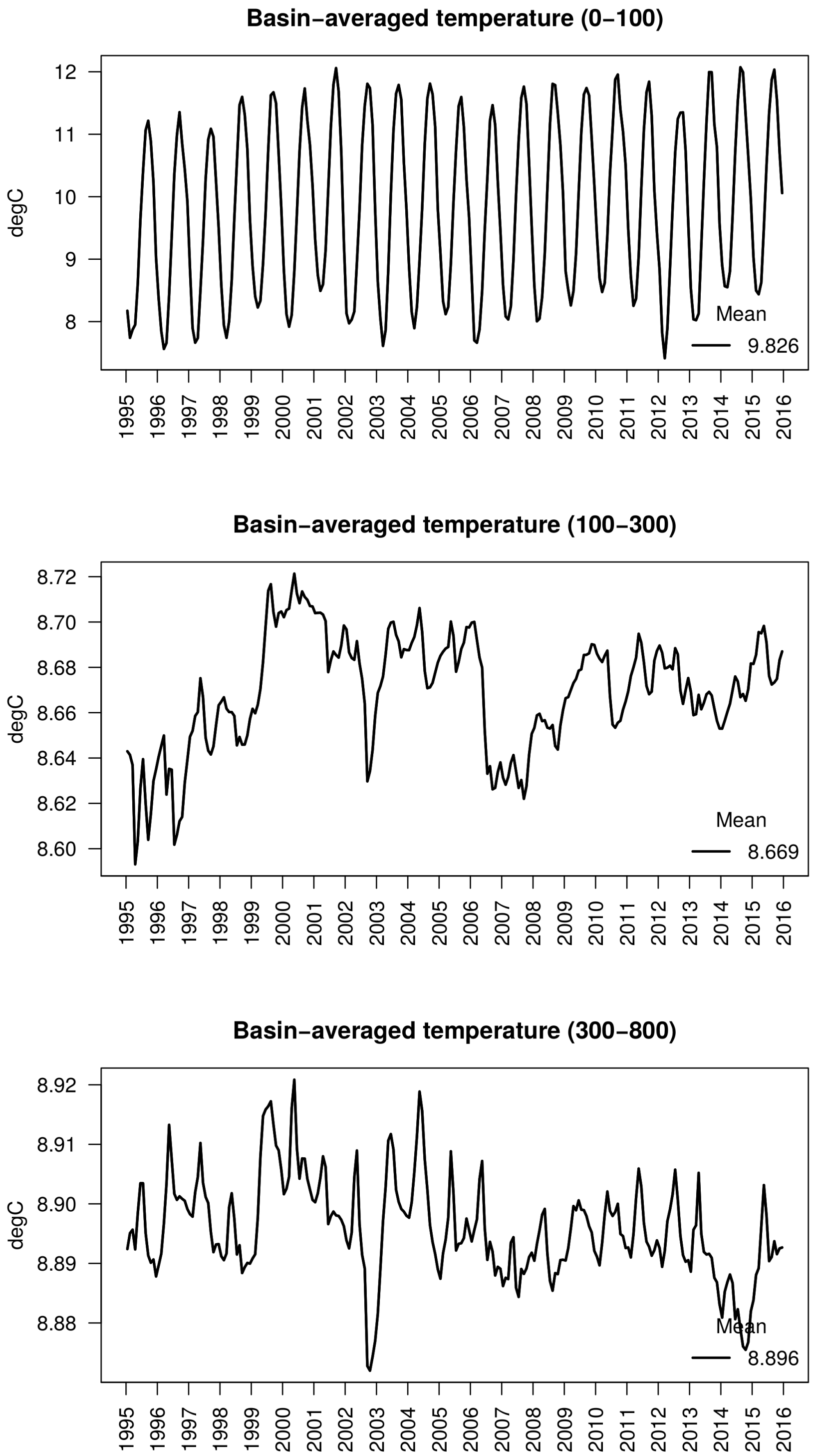

Figure IV-4. T-CLASS3-LAYERS Basin averaged layer temperature in the three selected layers 0-100 m, 100-300 m, 300-800 m.

Figure IV-5 (**T-CLASS3-IC-CHANGE**) shows the basin averaged monthly mean temperature (top panel) and the changes with respect to the initial conditions (bottom panel). The former highlights the penetration of the seasonal cycle, which tends to disappear below 100 m of depth and the evolution of the Cold Intermediate layer (CIL). The changes with respect to the initial conditions plot shows a small cooling after 2005 in correspondence with the deployment of the Argo floats.

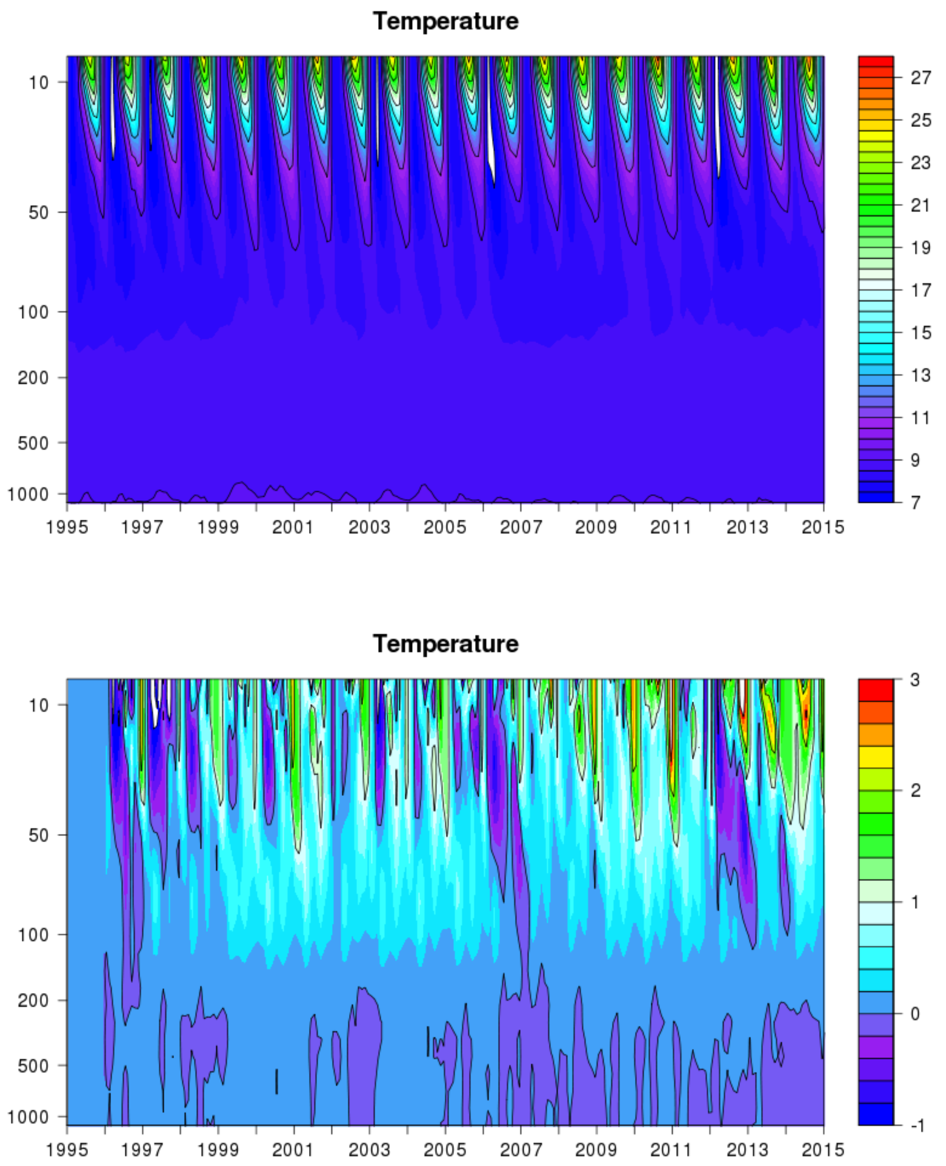

Figure IV-5. T-CLASS3-IC-CHANGE Domain average temperature monthly means as a function of depth and time (top) and changes with respect to the initial conditions

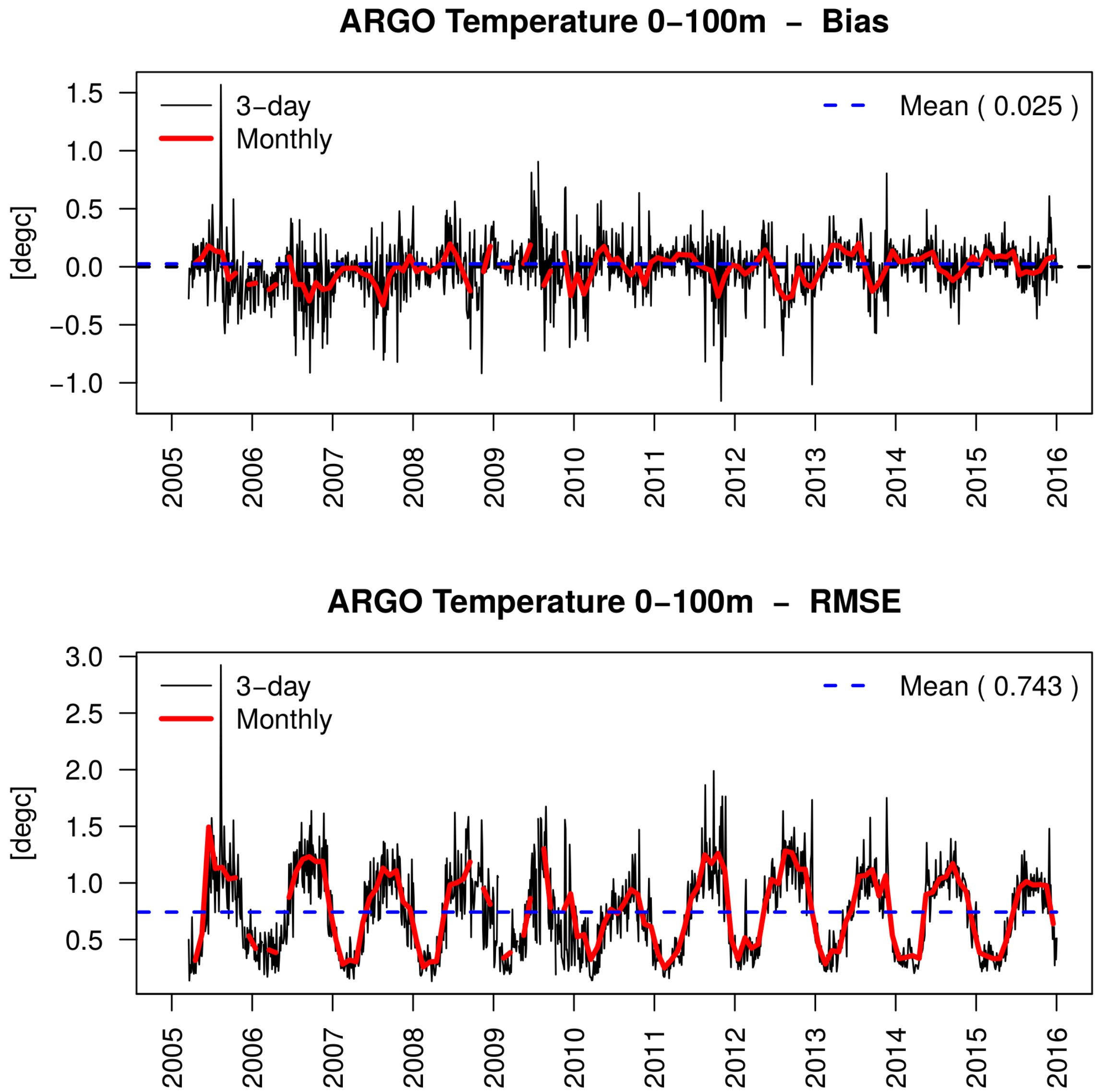

Figure IV-6. T-CLASS4-BIAS-LAYERS and T-CLASS4-RMSE-LAYERS : time series of the BIAS and RMSE computed from the misfits between temperature observations and reanalysis product in the three different layers 0-100 m, 100-300 m and 300-800 m. Black and red lines refer to 3-day and monthly statistics, respectively (continues in next page).

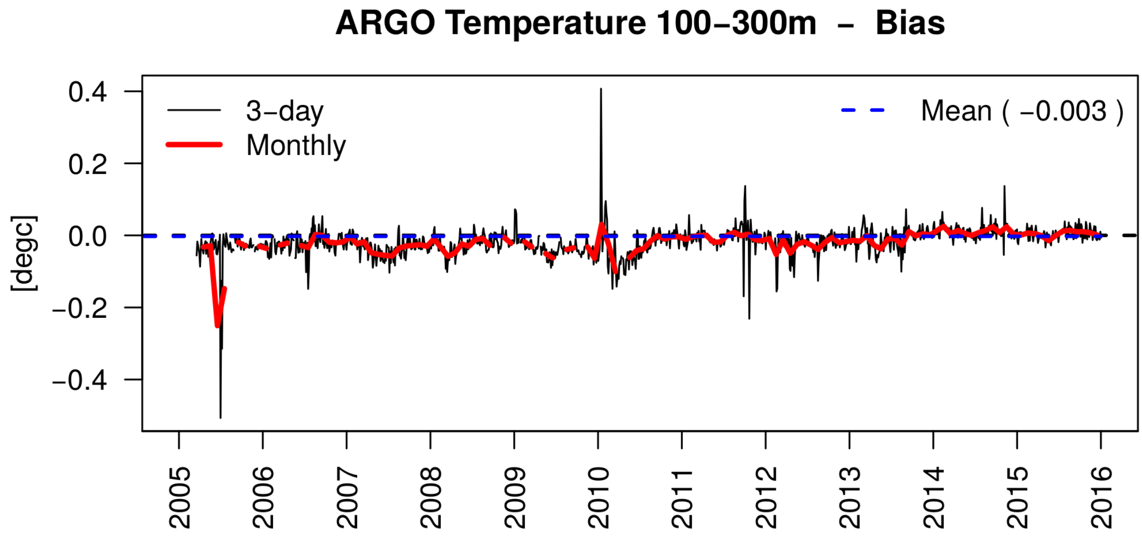

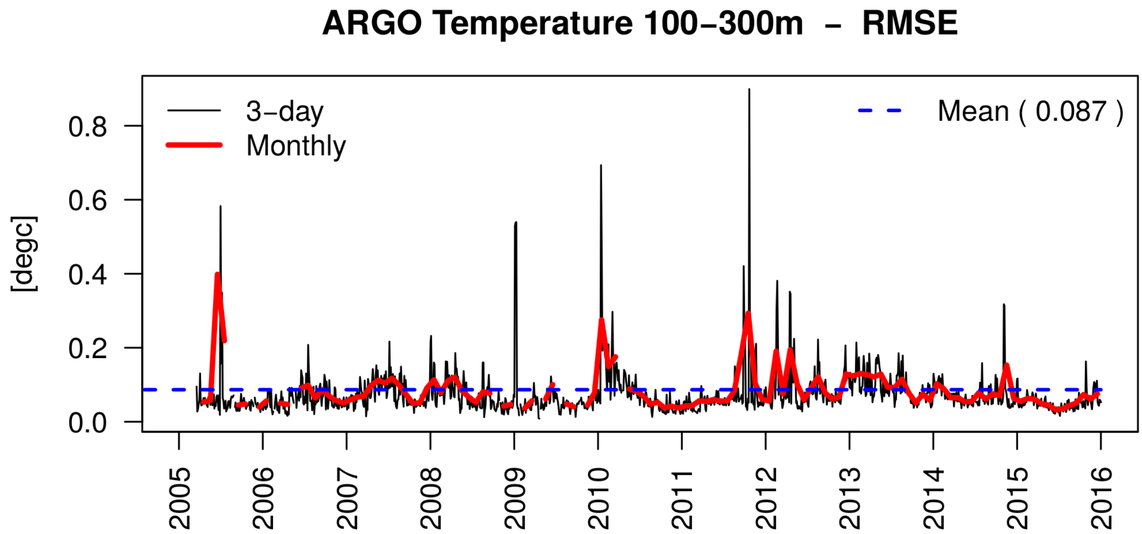

Figure IV-7. T-CLASS4-BIAS-LAYERS and T-CLASS4-RMSE-LAYERS : time series of the BIAS and RMSE computed from the misfits between temperature observations and reanalysis product in the three different layers 0-100 m, 100-300 m and 300-800 m. Black and red lines refer to 3-day and monthly statistics, respectively (continues in next page).

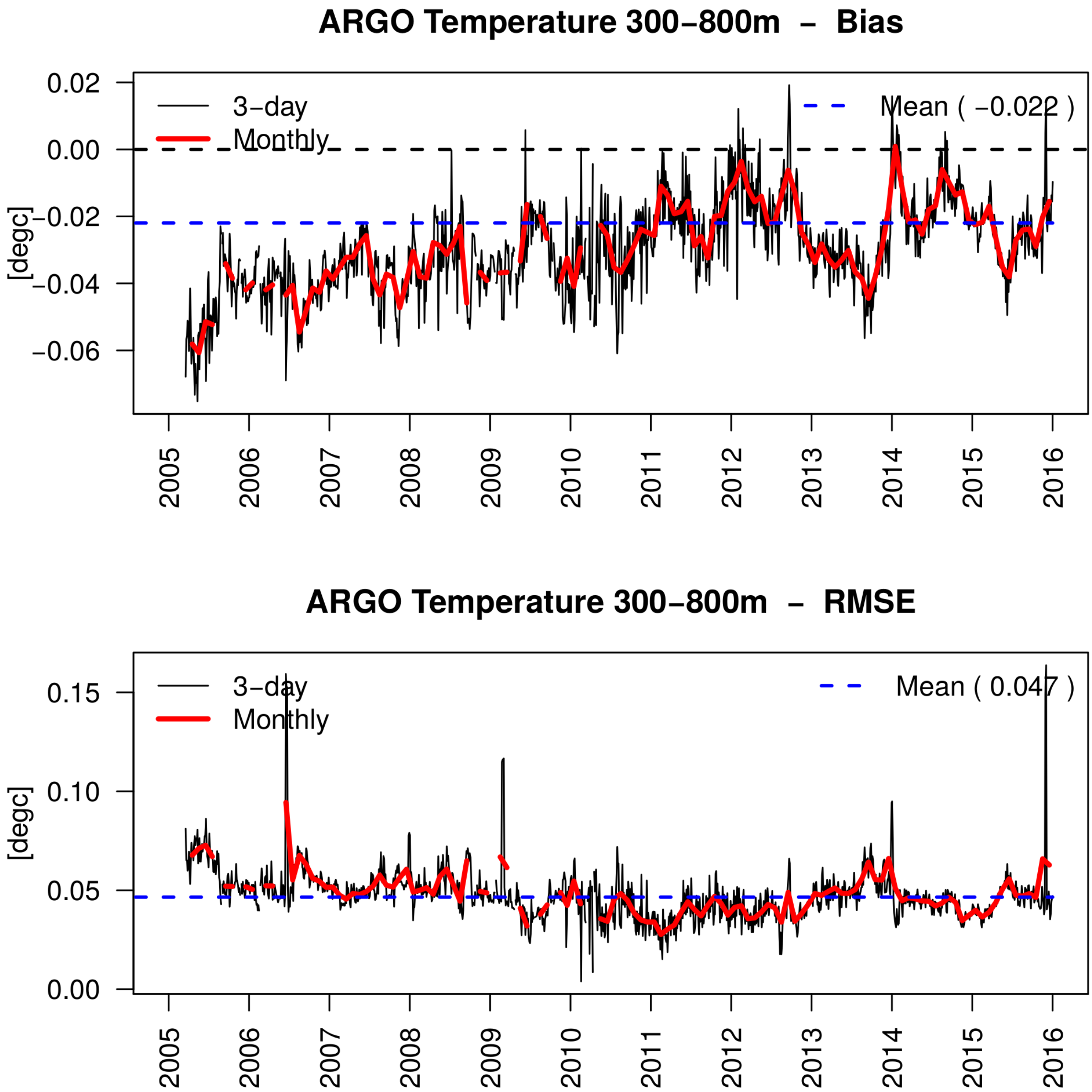

Figure IV-8. T-CLASS4-BIAS-LAYERS and T-CLASS4-RMSE-LAYERS : time series of the BIAS and RMSE computed from the misfits between temperature observations and reanalysis product in the three different layers 0-100 m, 100-300 m and 300-800 m. Black and red lines refer to 3-day and monthly statistics, respectively

Figure IV-8 shows time series of the BIAS and RMSE skill scores for temperature. The scores are computed from the misfits between observation and reanalysis. They are grouped in three layers (0-100 m, 100-300 m, 300-800 m). They are shown for period 2005-2015 since before 2005 scores are not relevant because in T/S situ observations are very sparse. In Appendix, the BIAS and RMS scores are shown over the full reanalysis period on Figure VIII-3. The bias is here defined as difference between observations and model equivalents. The upper ocean statistics are characterized by a small bias (-0.025°C) and by a RMSE with a pronounced seasonal signal, i.e. larger (up to 1.4°C) towards the end of the summer and smaller (0.3°C) in wintertime with an average value of 0.74°C. For the layer 100-300 m, the average RMSE is 0.087°C with a very small BIAS of -0.003°C. The statistics are downgraded over period 1995-2015 due to the in situ profile sparseness (RMSE and BIAS are 0.155°C and -0.032°C, respectively). The 300-800 m layer is characterized by a cold bias (-0.022°C) which is partially absorbed along time. This layer exhibits RMSE average values of 0.047°C and 0.11°C over period 2005-2015 and 1995-2015, respectively. Again, the skills are downgraded by the early part of reanalysis.

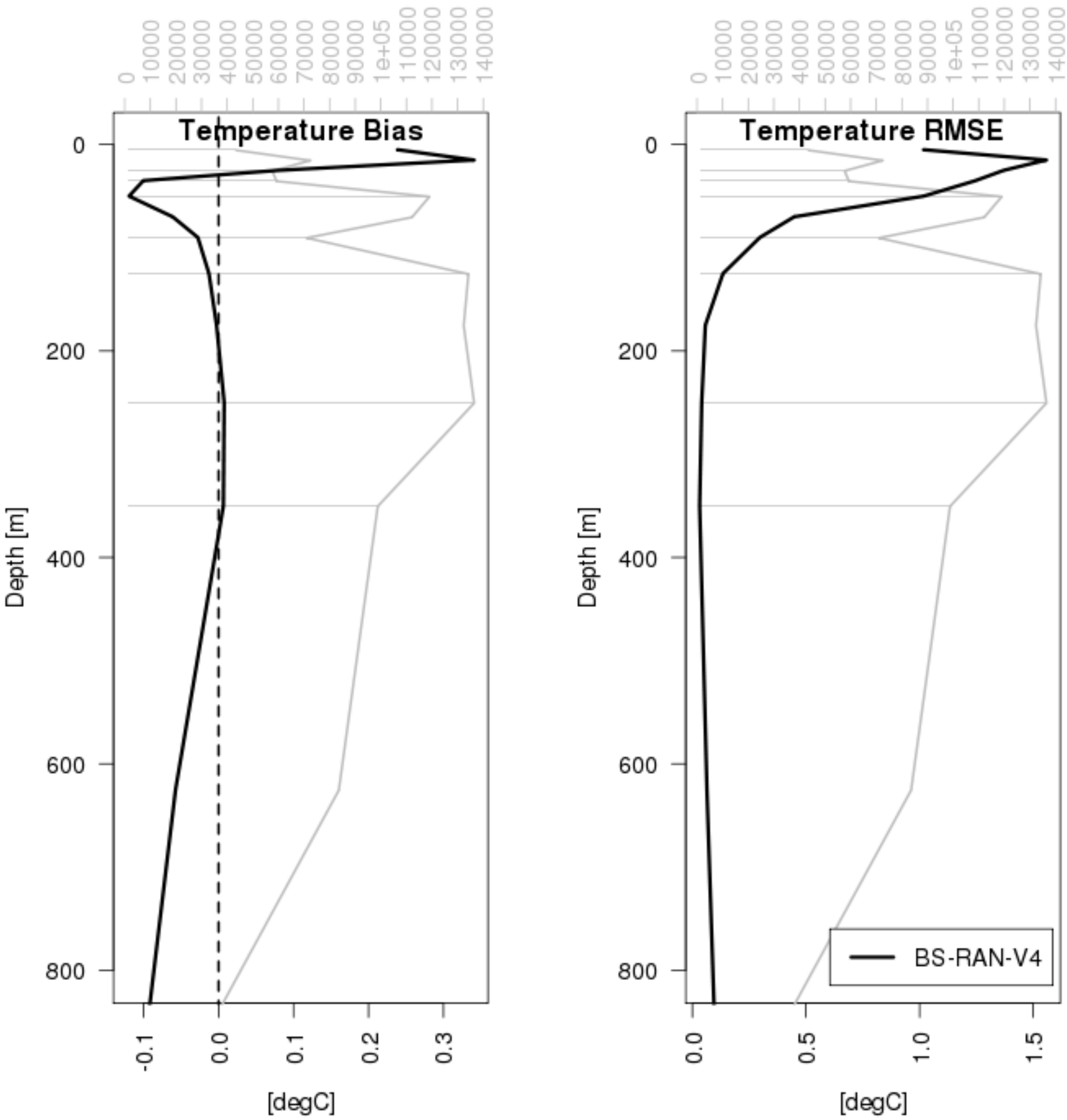

Figure IV-9. T-CLASS4-BIAS-DEPTH and T-CLASS4-RMS-DEPTH : BIAS and RMS computed from the T reanalysis misfits. Number of observations is shown in gray.

Figure IV-9 (**T-CLASS4-BIAS-DEPTH** and **T-CLASS4-RMS-DEPTH**) displays temperature misfit BIAS (left) and RMS (right) profiles up to 800 m. The skill scores are shown for period 2005-2015. The same statistics are given for the entire reanalysis period 1995-2015 in Appendix on Figure VIII-4. The skill scores below 800 m are not shown due to data sparseness. The BIAS exhibits a maximum positive value at 20 m depth (~0.3°C) indicating that the model is too cold. Below 40 m, the BIAS becomes negative (~-0.1°C). Between 200 and 400 m, the Bias reaches its minimum absolute value, to further slowly increase again at depths, reaching a negative bias value of -~0.1°C at 800 m. Around 30 m of depth, the RMS peaks at 1.5°C and quickly decreases in the deeper layers. The same trends can be observed for the statistics calculated over period 1995-2015 (see Figure VIII-4 in Appendix), but again scores are downgraded .

The total EANs, BIAS and RMS for temperature are included in Table IV-2. The skill scores are given for the full period of reanalysis 1995-2015 as well as for period 2005-2015, period for which the statistics are more relevant owing to the deployment of the Argo float in the Black Sea in 2005 and onward.

Table IV-2. Temperature misfit EANs for period 1995-2015 (in black) and period 2005-2015 (in blue)

TEMPERATURE [°C]	BIAS	RMS
0 -100 m	-0.02 / **0.025**	0.87 / **0.74**
100 -300 m	-0.03 / **-0.003**	0.15 / **0.09**
300-800 m	-0.02 / **-0.02**	0.11 / **0.05**

IV.3 Sea Surface Salinity

Table IV-3 summarizes the metrics and the observations used in the assessment of Sea Surface Salinity.

Table IV-3. Metrics and observations used to assess sea surface salinity

Name	Reference dataset	Quantity
SSS-M-NC-MEAN_XY	None	Averaged monthly mean over the Black Sea
FWNET-M-NC-MEAN_XY	None	Black Sea averaged monthly fresh water flux
SSS-M-NC-TREND	None	Linear trend of SSS

Figure IV-10 (**SSS-CLASS3-2DMEAN**) shows the basin averaged sea surface salinity (SSS) temporal evolution. The SSS has a multiyear average of 17.8 psu and oscillates between 17.4 and 18.2 psu. From 1995 to 1999the SSS decreases of about 0.4 psu, increases back to its initial value in 2004 and finally exhibits some small wiggles till the end of 2015. The net upwards water flux Figure IV-11 (**SFW-CLASS3-2DMEAN**) is negative on the average (-0.001 10^{-3} Kg/m2/s) indicating a net gain of water. The Damping freshwater flux associated to the NEMO SSS restoring scheme is shown in blue with a positive correction in average indicating that the model SSS is too warm compared to the SSS regridded observations (EN4 objective reanalysis). Figure IV-12 compares the maps of the model and observation SSS trend over the period 1995-2015 .

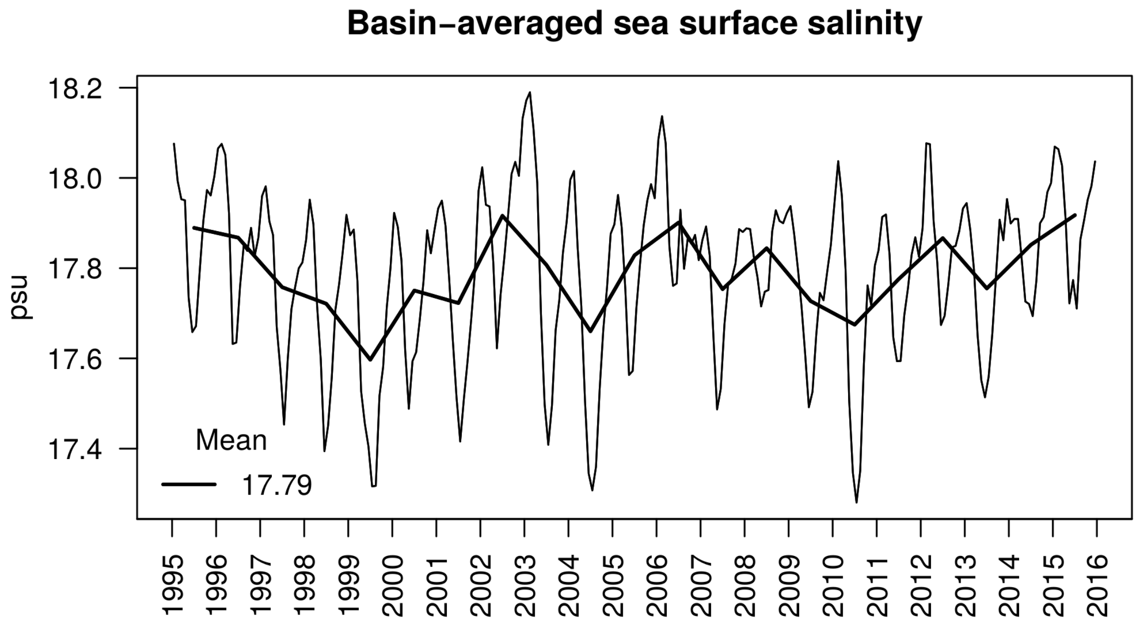

Figure IV-10. SSS-CLASS3-2DMEAN : Basin averaged monthly mean SSS.

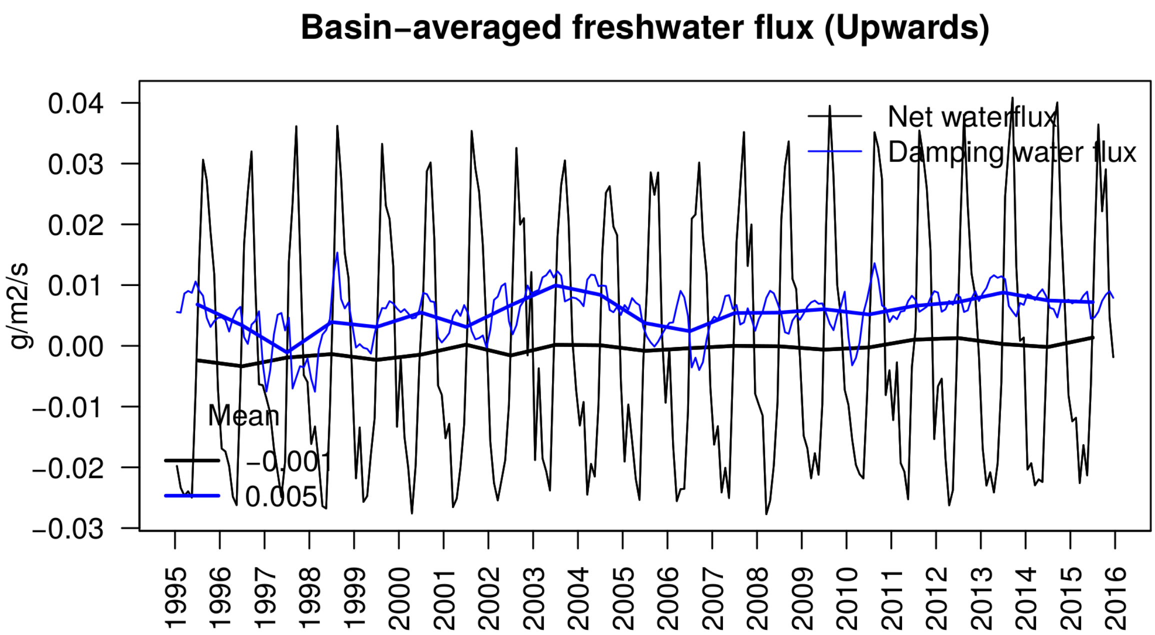

Figure IV-11. SFW-CLASS3-2DMEAN Basin averaged upward freshwater flux and water flux correction (restoring scheme to EN4 SSS objective reanalysis) in g/m²/s.

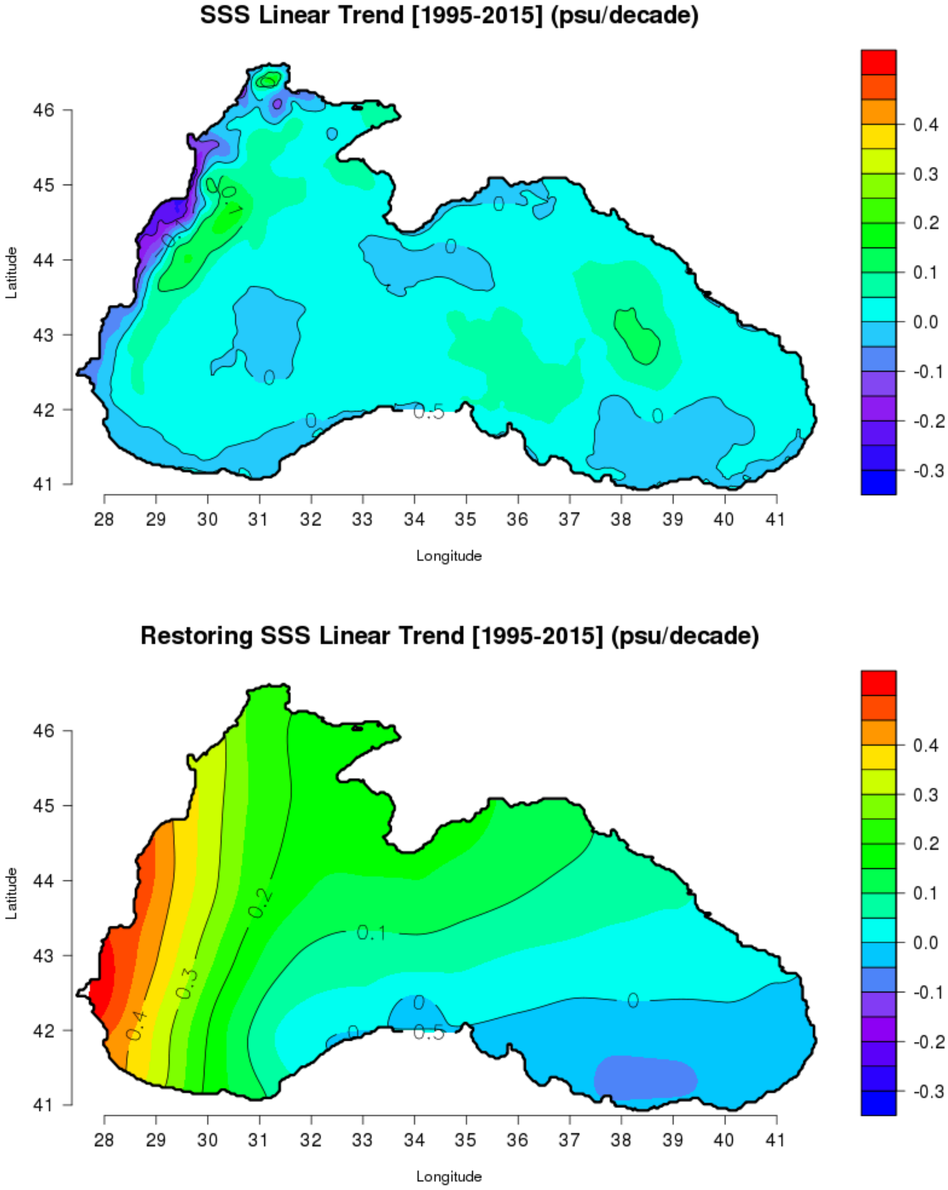

Figure IV-12. SSS-CLASS1-TREND Linear trend of SSS over the period 1995-2015 for the reanalysis product (top) and the reference dataset (bottom).

IV.4 Salinity

Table IV-4 summarizes the metrics and the observations used in the assessment of Salinity.

Table IV-4. Metrics and observations used to assess salinity.

Name	Reference dataset	Quantity
S-30 m-M-CLASS1-CLIM-MEAN_T And more generally: S-<DEPTH>-M-CLASS1-CLIM-MEAN_T With <DEPTH> to be replaced by 30 m, 70 m, 170 m, 440 m or 1100 m.	Simonov A. I. and E. N. Altman, Editors. 1991. Hydrometeorology and hydrochemistry of the USSR seas. Vol. IV, The Black Sea, Gidrometeoizdat, 430 pp.	Maps of long-term annual mean from reanalysis product at different depths
S-30 m-M-CLASS1-CLIM-BIAS_T And more generally: S-<DEPTH>-M-CLASS1-CLIM-BIAS_T With <DEPTH> to be replaced by 30 m, 70 m, 170 m, 440 m or 1100 m.	Simonov A. I. and E. N. Altman, Editors. 1991. Hydrometeorology and hydrochemistry of the USSR seas. Vol. IV, The Black Sea, Gidrometeoizdat, 430 pp.	Maps of long-term annual mean difference between the reanalysis product and the reference dataset at different depths
S-<LAYERS>-M-NC-MEAN_XY With <LAYERS> to be replaced by 0_100 m, 100_300 m or 300_800 m	None	Time series of salinity computed from reanalysis product at different layers
S-PROF-M-NC-IC-BIAS_XY	None	Water column differences between monthly basin averaged reanalysis salinity profiles and the IC
S-<LAYERS>-M-INNO-PROF-RMS With <LAYERS> to be replaced by 0_100 m, 100_300 m or 300_800 m	UK MetOffice EN4	Time series of RMS computed from misfits in different layers
S-<LAYERS>-M-INNO-PROF-BIAS With <LAYERS> to be replaced by 0_100 m, 100_300 m or 300_800 m	UK MetOffice EN4	Time series of BIAS computed from misfits in different layers
S-PROF-M-INNO-PROF-RMS	UK MetOffice EN4	Mean RMS profiles
S-PROF-M-INNO-PROF-BIAS	UK MetOffice EN4	Mean BIAS profiles

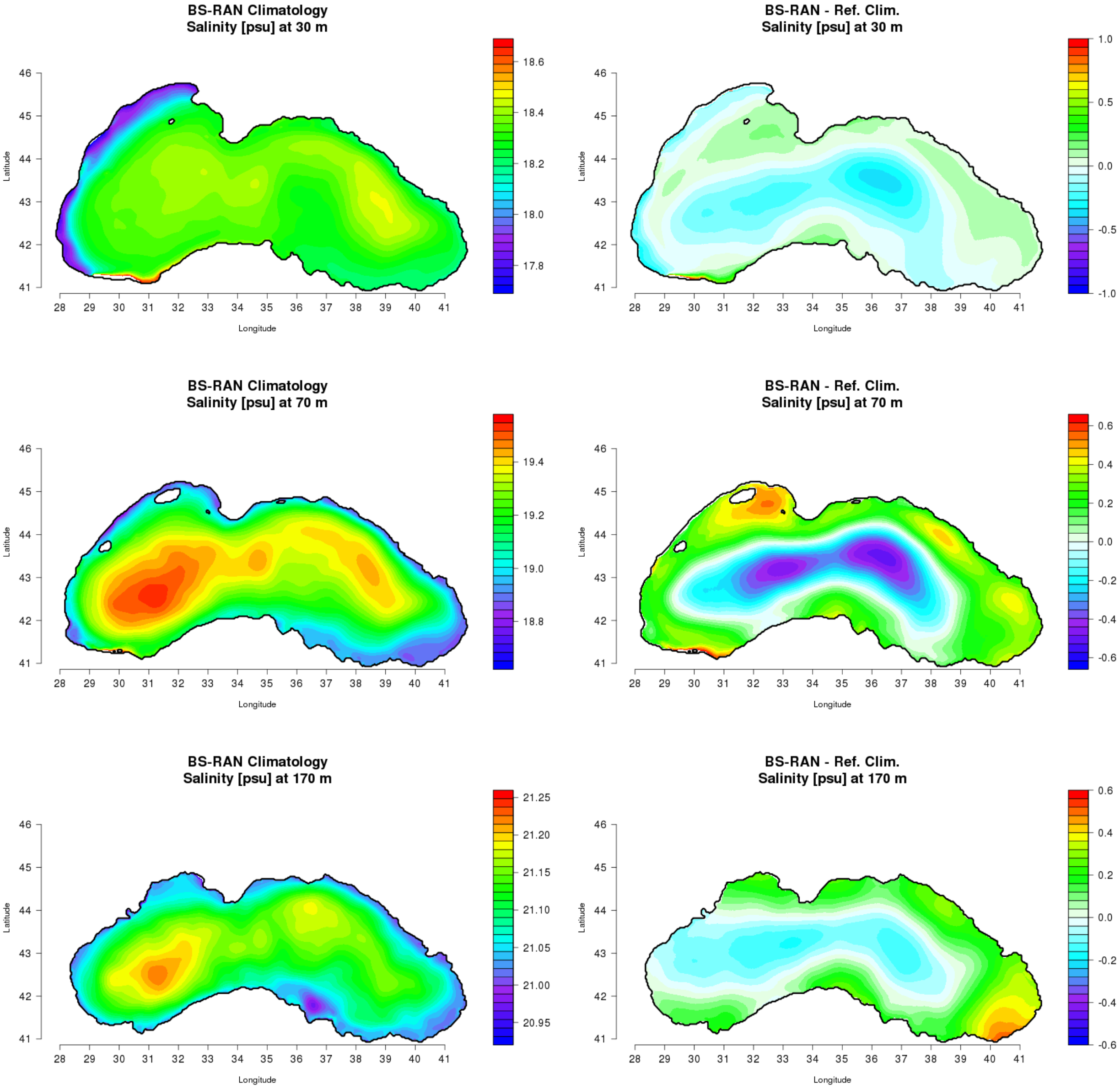

Figure IV-13. S-CLASS1-MEAN-DEPTHS Maps of reanalysis climatology for salinity (left panels) and difference between reanalysis and reference dataset climatology (right panels) at 30, 70, 170, 440 and 1100 m of depth (continues in next page).

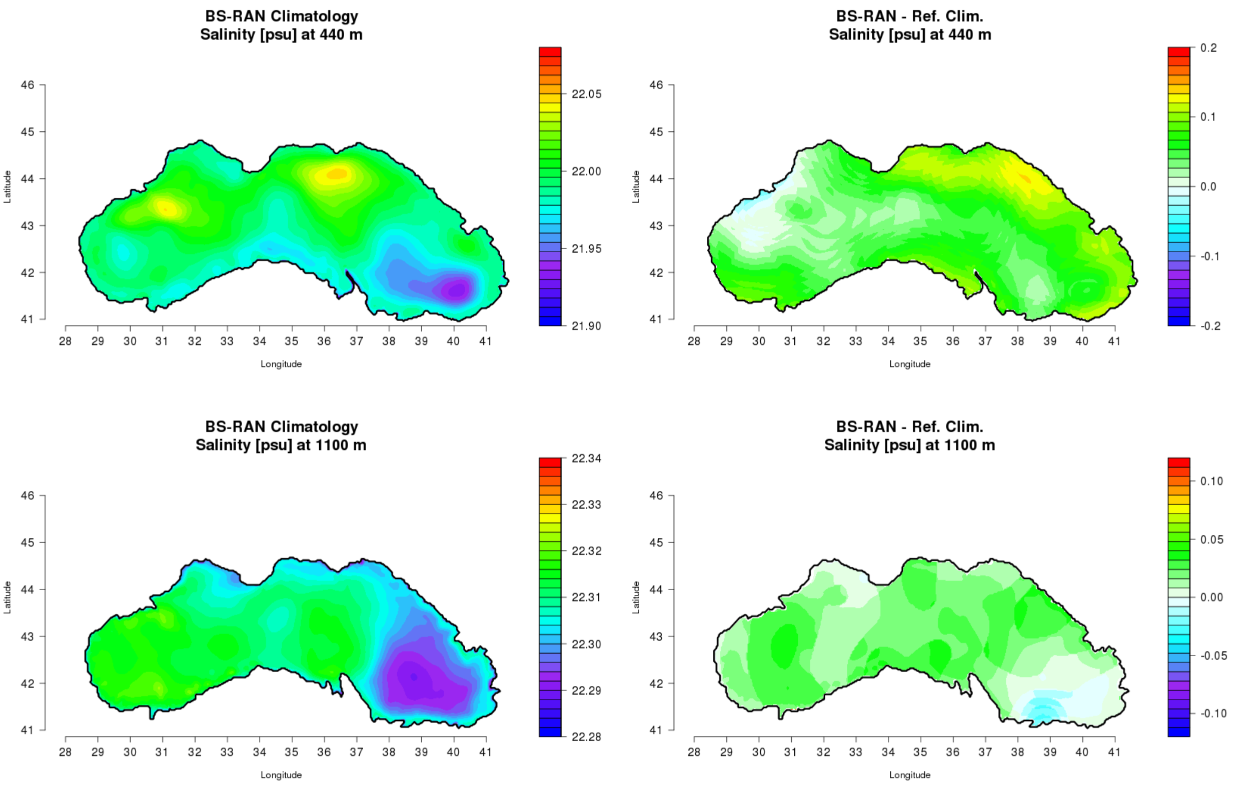

Figure IV-14. S-CLASS1-MEAN-DEPTHS Maps of reanalysis climatology for salinity (left panels) and difference between reanalysis and reference dataset climatology (right panels) at 30, 70, 170, 440 and 1100 m of depth.

Figure IV-13. S-CLASS1-MEAN-DEPTHS Maps of reanalysis climatology for salinity (left panels) and difference between reanalysis and reference dataset climatology (right panels) at 30, 70, 170, 440 and 1100 m of depth (continues in next page).

shows the BS-REA 1995-2015 climatology and the difference between the BS-REA climatology and reference dataset climatology at the five selected levels at 30, 70, 170, 440 and 1100 m of depth.

Differences at 30 m of depth indicate that the reanalysis is on the average fresher than the reference climatology in the interior of the Black Sea (up to 0.3 psu) and slightly saltier near the northern and south-western coasts (~+0.1 psu). At 70 and 170 m, the reanalysis is again fresher in the interior Black Sea (up to -0.5 and -0.1 psu, at 70 m and 170 m, respectively), while it saltier in the coastal areas. At deeper levels, the reanalysis is generally saltier than the reference dataset with differences of the order of 0.1 psu at 440 m. At 1100 m of depth, the differences becomes very tiny in absolute value (less than 0.05 psu).

Figure IV-16 shows the basin-averaged salinity values in the three selected layers (0-100, 100-300, 300-800 m of depth). The upper layer exhibits a small freshening (~-0.3 psu) during the first part of the timeseries (1995-1999) and a later salinification with abrupt events in periods 2002-2003 and 2005-2007, interspersed by a maximum freshening in 2004 (~18.6 psu). The intermediate layer 100-300 m shows a similar but smoother trend with a freshening (~-0.2 psu) till 2005 and a salinification onward (~+0.3 psu) with an average value of about 21.2 psu. This pattern is probably due to a moderate model drift corrected by the assimilation of the T/S in situ profiles after 2005. However the range of variation of the signal remains small for both layers (order of +/-0.3psu) over 1995-2015. On the contrary, the deeper layer (300-800) first shows a small salinification trend (~+0.1 psu) followed by an abrupt freshening event in period 2002-2003 that is recovered onward. The variation of the signal is also small in that layer : 0.1 psu over 1995-2015.

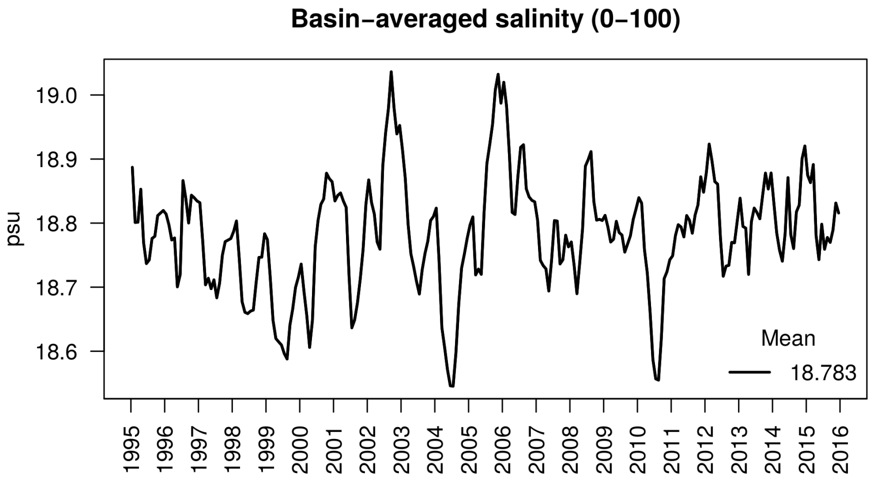

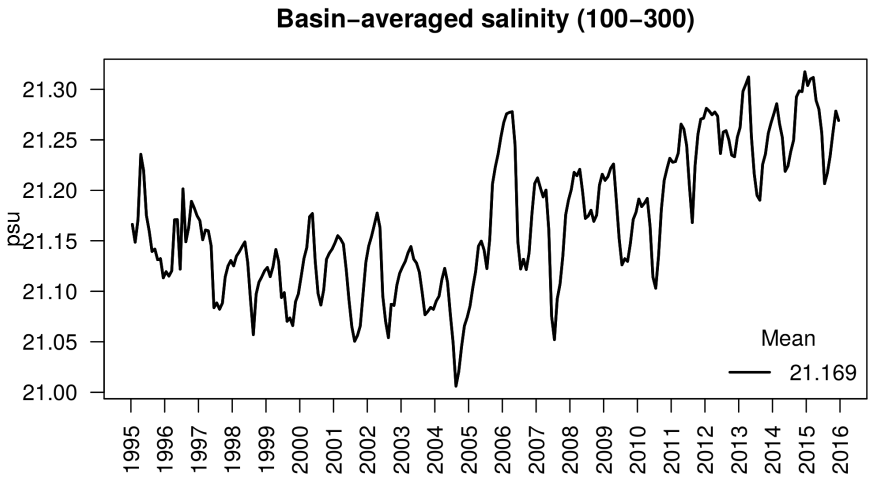

Figure IV-15. S-CLASS3-LAYERS Basin averaged salinity in the three selected layers from 1995 onwards (0-100 m, top; 100-300 m, middle; 300-800 m, bottom) (continue in next page).

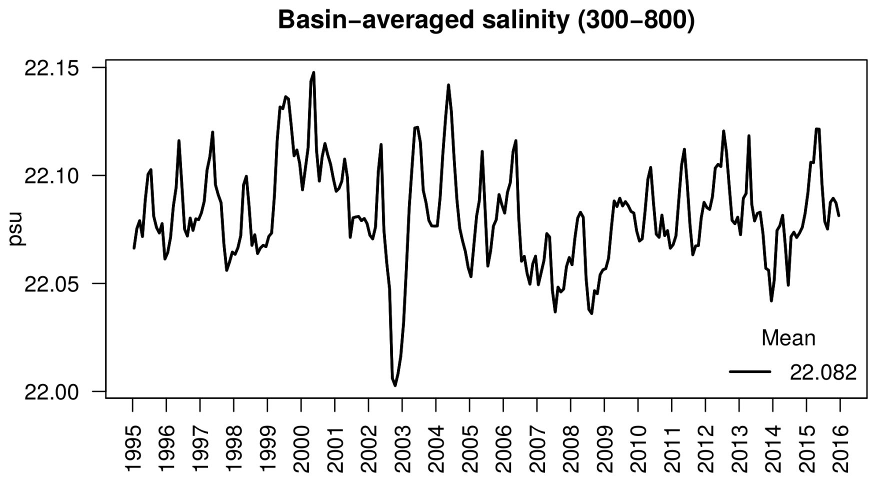

Figure IV-16. S-CLASS3-LAYERS Basin averaged salinity in the three selected layers from 1995 onwards (0-100 m, top; 100-300 m, middle; 300-800 m, bottom)

Figure IV-17 (**S-CLASS3-IC-CHANGE**) shows the evolution of the domain averaged salinity computed as function of time in different layers. The two plots exhibit some seasonal cycles in the top layers with some stronger salinification events for time periods 2002-2003 and 2005-2007. As mentioned earlier, these event are also visible on Figure IV-16 showing the time series of salinity (salinification in layer 0-100 m, and a concomitant small freshening in layer 300-800 m for the event 2002-2003, and traces of salinifications in layer 100-300 m for the event 2005-2007). In parallel, the time series of the basin average temperature on Figure IV-4, exhibits a drop in temperatures in all layers for the 2002-2003 event, while this drop only shows up in the top layers for event 2005-2007. Interestingly, over the period of time 2002-2003, Figure IV-11 shows an evidence of a fresher model SSS (ie, computed as the first model level salinity) compared to the SSS regridded observations. Indeed, a higher positive water flux correction (~+0.004g/m2/s) is applied to the net upward freshwater flux (ie, restoring term to EN4 SSS objective analysis). On the contrary, in period 2006-2007 this restoring term decreases (~-0.004g/m2/s). This suggests that after 2005, owing to the deployment of the Argo floats the model salinity and temperature profiles are better constrained.

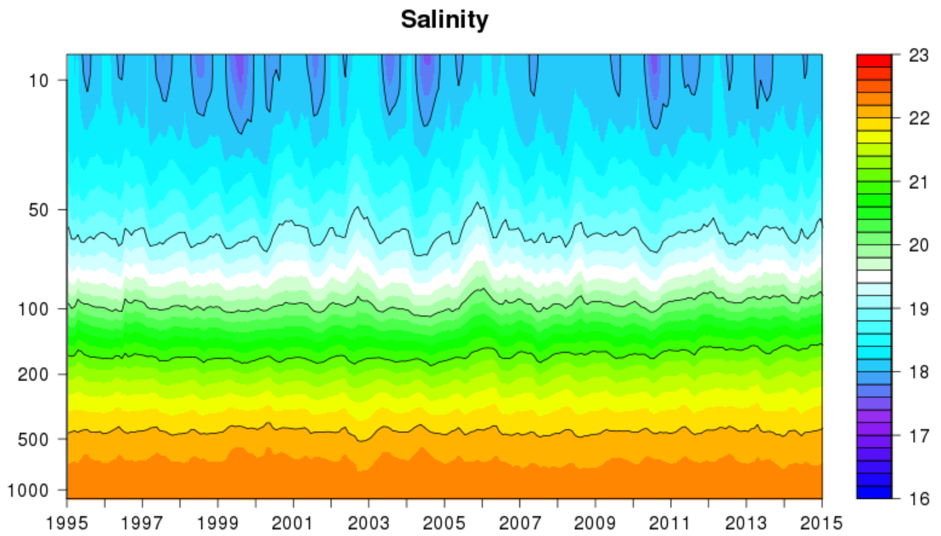

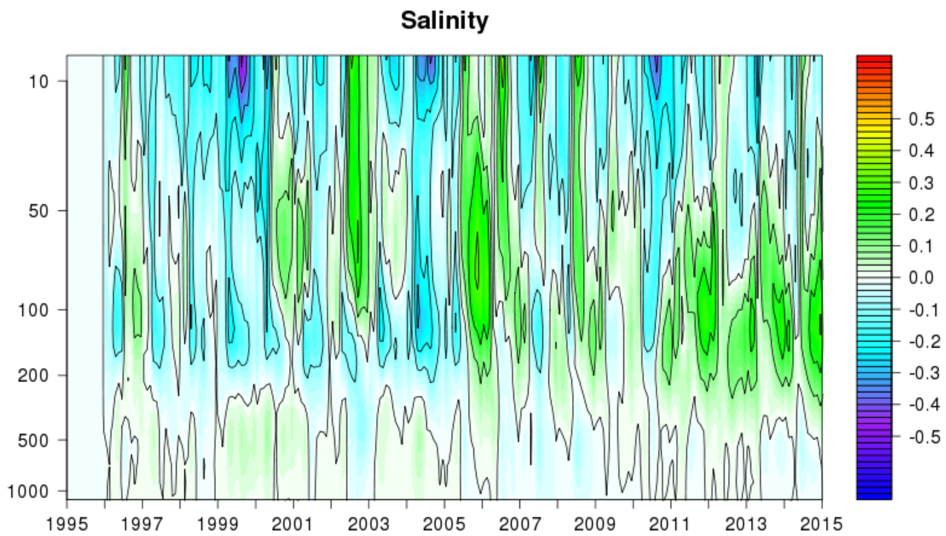

Figure IV-17. S-CLASS3-IC-CHANGE Basin average monthly mean salinity as a function of depth and time (top) and changes (bottom) with respect to the initial conditions

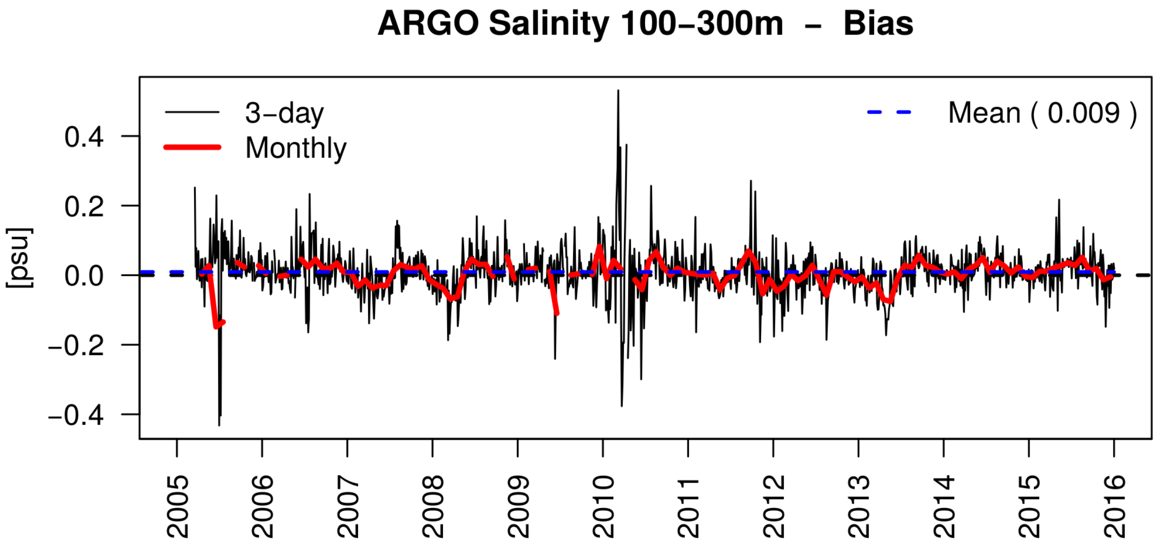

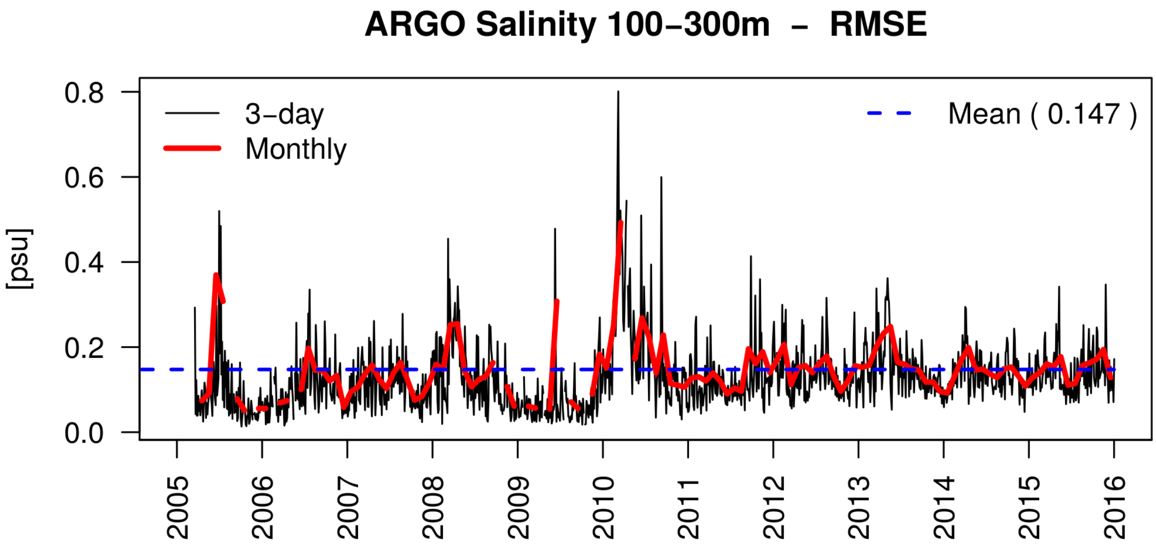

Figure IV-18. S-CLASS4-BIAS-LAYERS (top) and S-CLASS4-RMS-LAYERS (bottom) computed from misfits of reanalysis product in different layers (continues in next page).

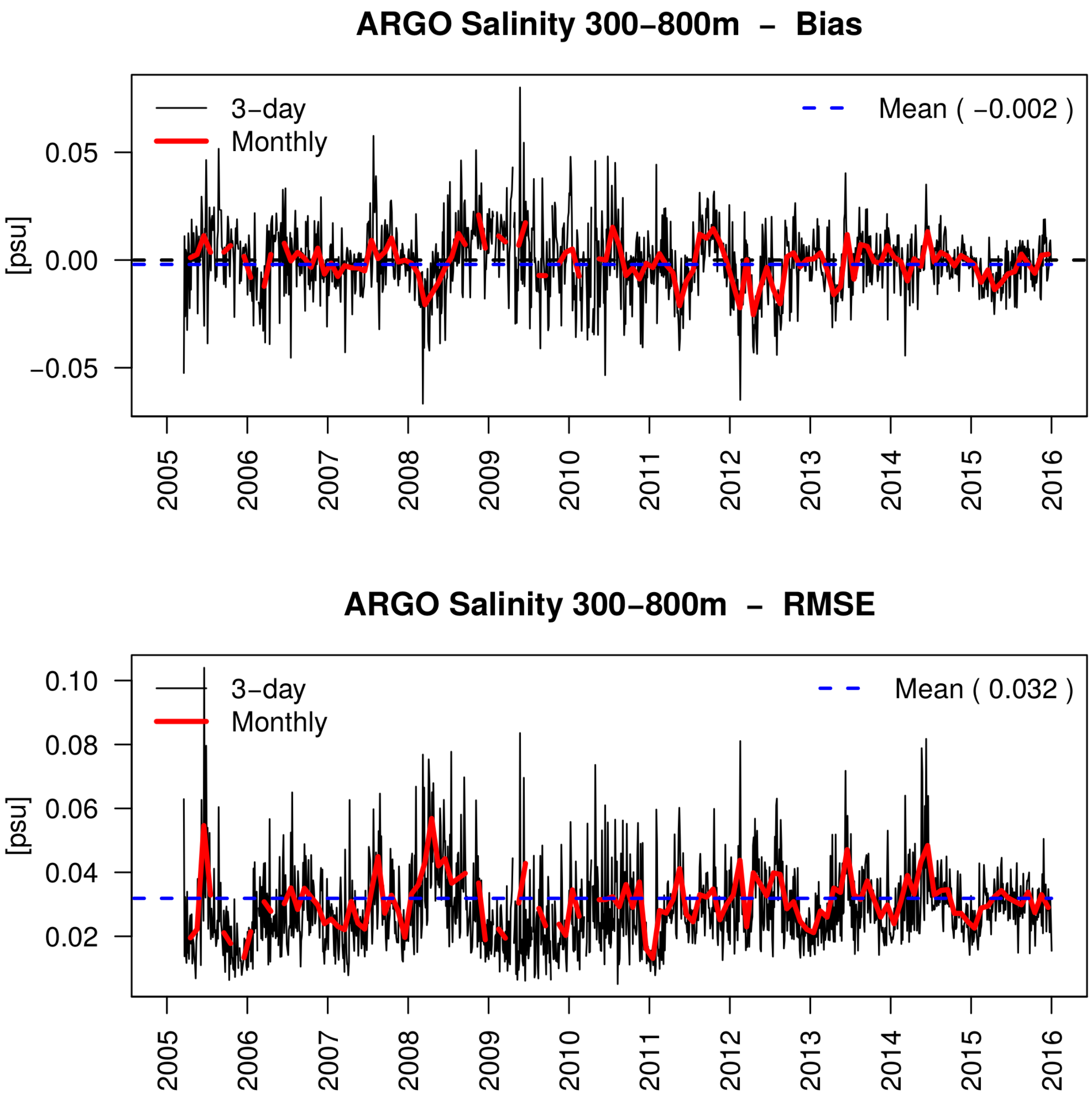

Figure IV-19. S-CLASS4-BIAS-LAYERS (top) and S-CLASS4-RMS-LAYERS (bottom) computed from misfits of reanalysis product in different layers

Figure IV-19 (**S-CLASS4-RMS-LAYERS and S-CLASS4-BIAS-LAYERS**) presents the salinity misfit BIAS and RMS computed in different layers at observation location for the three layers 0-100, 100-300 and 300-800 m and for period 2005-2015. In Appendix, Figure VIII-7 shows the same statistics for the full reanalysis period.

Skill scores in the upper layer are rather stable over time, with an averaged BIAS and RMS of 0.002 and 0.26 psu, respectively. Again due to the lack of in situ observation before 2005, statistics over the full reanalysis time period are downgraded (BIAS of -0.014 and RMS of 0.33 psu). The 100-300 m layer exhibits similar results, with a bias of 0.009 psu and a RMSE of 0.15 psu.

In the deep layer 300-800 the averaged BIAS and RMSE are -0.002 and 0.032 psu, respectively. In all layers, the salinity innovation BIAS and RMS tend to diminish at the end of the reanalysis period.

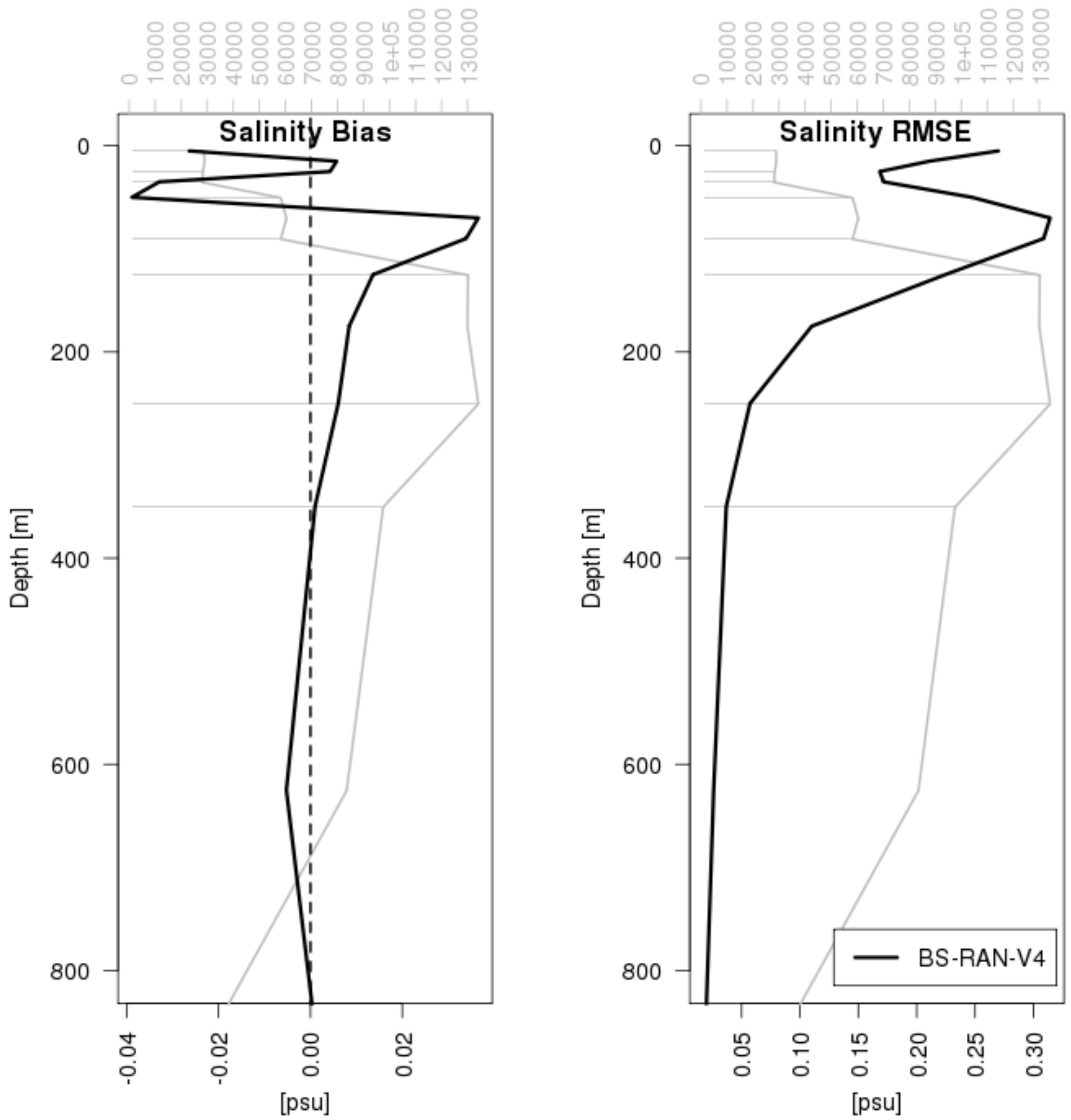

Figure IV-20. S-CLASS4-BIAS-DEPTH and S-CLASS4-RMS-DEPTH computed from reanalysis misfits. Number of observations is shown in gray.

Figure IV-20 (**S-CLASS4-BIAS-DEPTH** and **S-CLASS4-RMS-DEPTH**) displays the BIAS and RMS profiles computed from the salinity misfits over period 2005-2015. Figure VIII-8 in Appendix shows the same statistics over the full reanalysis period. The misfit BIAS is negative at the surface (slightly below -0.25 psu) and after wiggling back to a near zero bias at 20 m, it reaches -0.038 psu at 50 m, which is the maximum bias of the whole profile in absolute value (ie, the reanalysis is too salty compared to the observations). Between about 60 and 350 m, the BIAS becomes positive again (reanalysis is too fresh) with a maximum value of 0,03 psu at about 80 m. Below the bias remains slightly positive but never exceeds 0.005 psu. The RMS difference is 0.27 psu at the surface, decreases till 30 m and increases again to reach the maximum value along the profile (0.32 psu) at about 80 m of depth. Below the RMS constantly decreases (less than 0.1 psu at 200 m, 0.02 psu at 800 m). Note again that statistics are downgraded when calculated over period 1995-2015 due to the sparseness of in situ profile before 2005. The total EANs, BIAS and RMS for salinity are included in Table IV-5. Salinity misfit EANs for time period 1995-2015 (black) and time period 2005-2015 (blue). The skill scores are given for the full period of reanalysis 1995-2015 as well as for period 2005-2015 where the statistics are more relevant (sparseness of the in situ profiles before 2005).

Table IV-5. Salinity misfit EANs for time period 1995-2015 (black) and time period 2005-2015 (blue)

Salinity [psu]	BIAS	RMS
0-100 m	-0.014 / **0.002**	0.33 / **0.26**
100-300 m	-0.006 / **0.009**	0.19/ **0.15**
300-800 m	-0.005 / **-0.002**	0.05 / **0.03**

IV.5 Currents

Table IV-6 summarizes the metrics and the observations used in the assessment of currents.

Table IV-6. Metrics and observations used to assess the currents

Name	Reference dataset	Quantity
UV-15m-M-NC-MEAN_T	None	Maps of Black Sea surface mean currents at 15 m
EKE-15m-M-CLASS3-ALT-MEAN_T	SEALEVEL_BS_SLA_MAP_L4_REP_OBSERVATIONS_008_031	Maps of Black Sea Eddy Kinetic Energy at 15 m

Figure IV-21 (**UV-CLASS1-15M-MEAN**) displays maps of surface mean currents at 15 m of depth computed from reanalysis product over 1995-2015. The mean surface circulation is in agreement with the literature and presents the well-known Black Sea surface circulation features with in particular the Western and Eastern cyclonic gyres. Compared to reanalysis BS-RAN-V3, the Batumini area circulation is modified, the South-East branch of the Eastern gyre being moved to the North West.

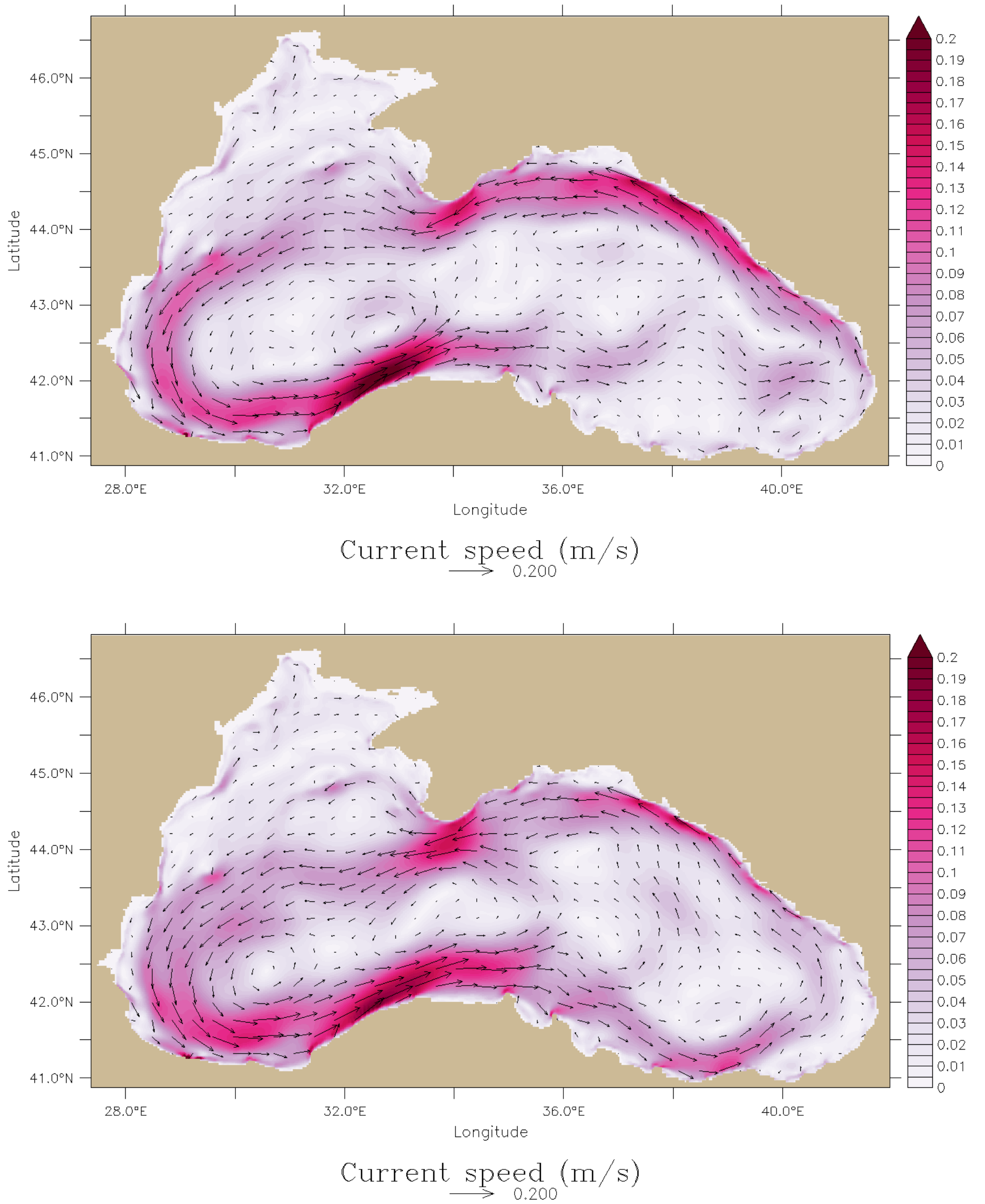

Figure IV-21. UV-CLASS1-15M-MEAN Average surface currents for period 1995-2015 : reanalysis BS-RAN-V4 (upper panel) and BS-Ran-V3 (lower panel).

IV.6 Sea Level

Table IV-7 summarizes the metrics and the observations used in the assessment of Sea Level.

Table IV-7. Metrics and observations used to assess the sea level

Name	Reference dataset	Quantity
SL-M-CLASS4-RMSD_XY	SEALEVEL_BS_SLA_L3_REP_OBSERVATIONS_008_023	SL RMSD averaged over the whole domain
SL-M-CLASS1-ALT-TREND	SEALEVEL_BS_SLA_MAP_L4_REP_OBSERVATIONS_008_031	Linear Trend of dynamic sea level

Figure IV-22 (**SL-CLASS4-RMS**) presents the SLA RMS computed along track over the reanalysis period on a daily and monthly basis. On monthly basis, the RMS difference oscillates between 3 and 6 cm, with an average value of 4.38 cm. The mean misfit BIAS is 0.05 cm. The scores are apparently downgraded compared to BS-RAN-V3. As we demonstrate in the following, the apparent downgrade is due to a necessary change in the SLA misfit bias calculation and removal. On the contrary to BS-RAN-V3, the new bias calculation and removal process now result in a non null bias, which de facto increases the RMS scores.

It is worth it to note that the misfit RMS and BIAS statistics are calculated over the entire pool of SLA observations before the observation screening step (i.e., rejection of outliers) and before the data assimilation. When assimilating SLA observations it is mandatory to assess and remove the bias of the SLA misfit before feeding it to the data assimilation system. (Dee et al, 2005). In the BS-RAN-V3 system, the SLA misfit bias was calculated over the entire pool of SLA observations, and further removed before calculating the BIAS and RMS SLA misfit EANs. The removal of such a bias artificially reduces the BIAS score to zero in the EANs statistics. On the contrary, the BS-RAN-V4 calculates the bias after the observation screening step.

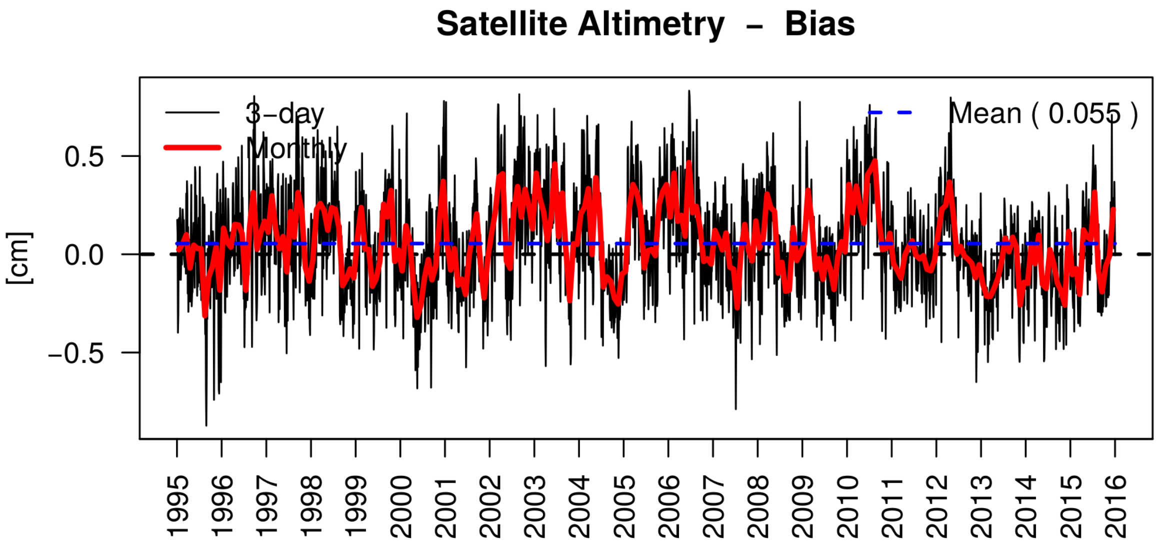

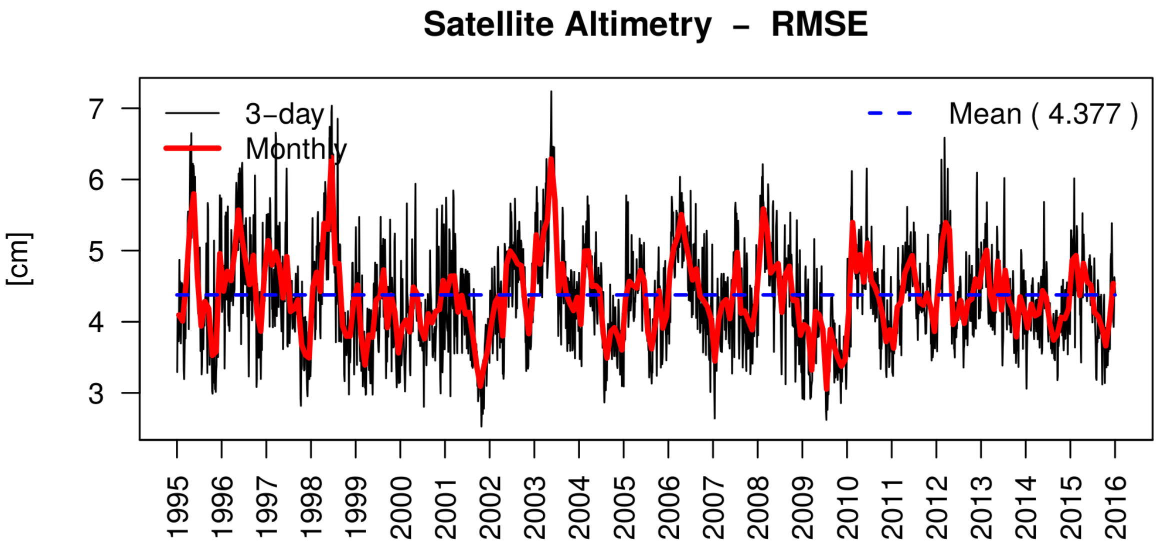

Figure IV-22. SL-CLASS4-RMS. Time series of the BIAS and RMS difference of the SLA misfit (altimetry data minus model) before the observation screening step.

Figure IV-23 and **Errore. L'origine riferimento non è stata trovata.** show the RMS and BIAS misfit for both BS-RAN_V3 and BS-RAN-V4 after the screening of observations and after the data assimilation, respectively. By construction, the BS-RAN-V4 BIAS is null on Figure IV-23 while it amounts -0.135 cm for BS-RAN-V3. This result demonstrates that the BS-RAN-V3 system was feeding the data assimilation system with a biased SLA misfit (which is in disagreement with the basic data assimilation hypothesis, and might result in a biased analysis, Dee et al, 2005). Interestingly, after minimization the BIAS and RMS scores (Figure IV-24) appears to be slightly better for V4 (0.014 and 1.571 cm, respectively) compared to V3 (0.004 and 1.645 cm, respectively). For those reasons, the BS-RAN-V4 SLA skill scores should not be considered as downgraded compared to V3 as would suggest Figure IV-22 and Tables **Errore. L'origine**

riferimento non è stata trovata. and Table V-1 Compared performance for reanalysis BS-RAN-V4 (new product), BS-RAN-V3 (previous QUID product) and BS-RAN-updV3 (previous delivered product) for different parameters and depth ranges over the entire time period 1995-2015 (first entry in red) and over 2005-2015 for temperature and salinity (second entry in blue). .

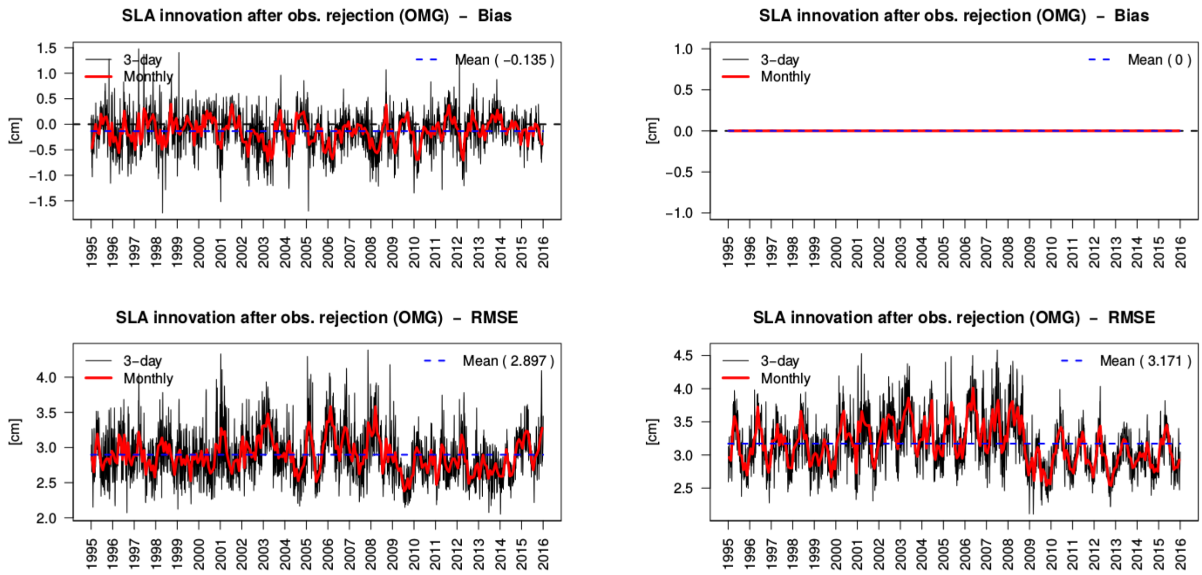

Figure : BS-RAN-V3ext Figure : BS-RAN-V4

Figure IV-23 RMS and BIAS misfit for both BS-RAN_V3 and BS-RAN-V4 after the screening of.

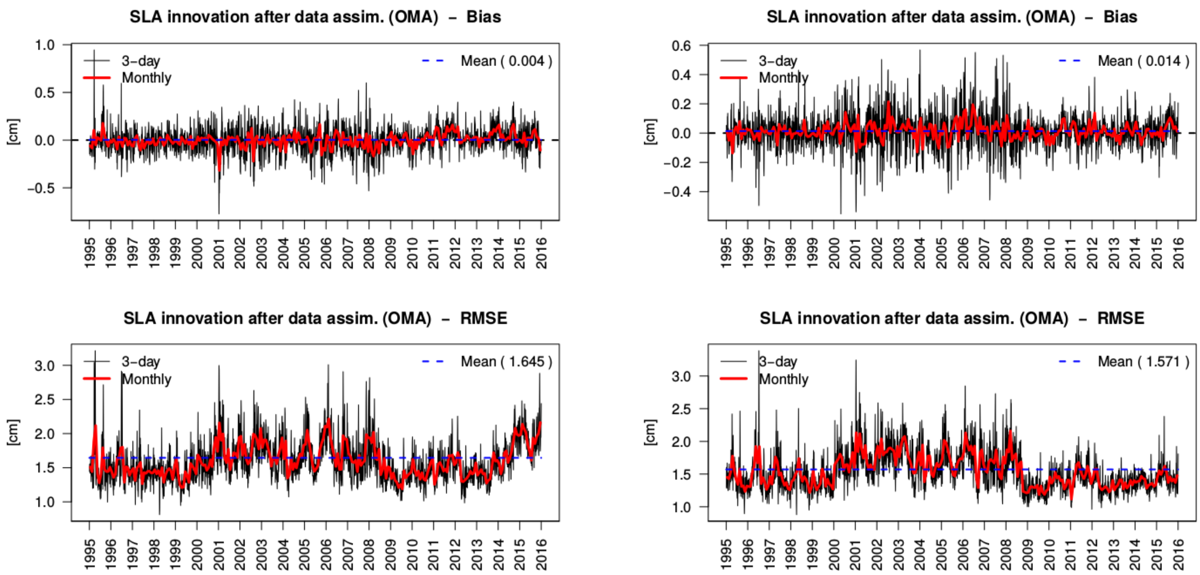

Figure : BS-RAN-V3ext Figure : BS-RAN-V4

Figure IV-24 RMS and BIAS misfit for both BS-RAN_V3 and BS-RAN-V4 after the data assimilation.

Figure IV-25 (SL-CLASS1-TREND) presents the linear trends of monthly means SL monthly computed respectively from BS REA (top panel) and reference altimetry regridded dataset (bottom panel). For this comparison, we use “dynamic sea level”, defined as the anomaly between the full sea level and the basin-averaged value, in order to exclude model drifts from the comparison. The comparison shows that BS REA is in qualitative agreement with the reference dataset to show a sea level rise on the very eastern and the north-western side of the domain (up to 0.015 m/decade = 1.5 mm/year for the far-eastern part), while the central-eastern region is locally characterized by sea level fall at a rate up to 0.015 m/decade.

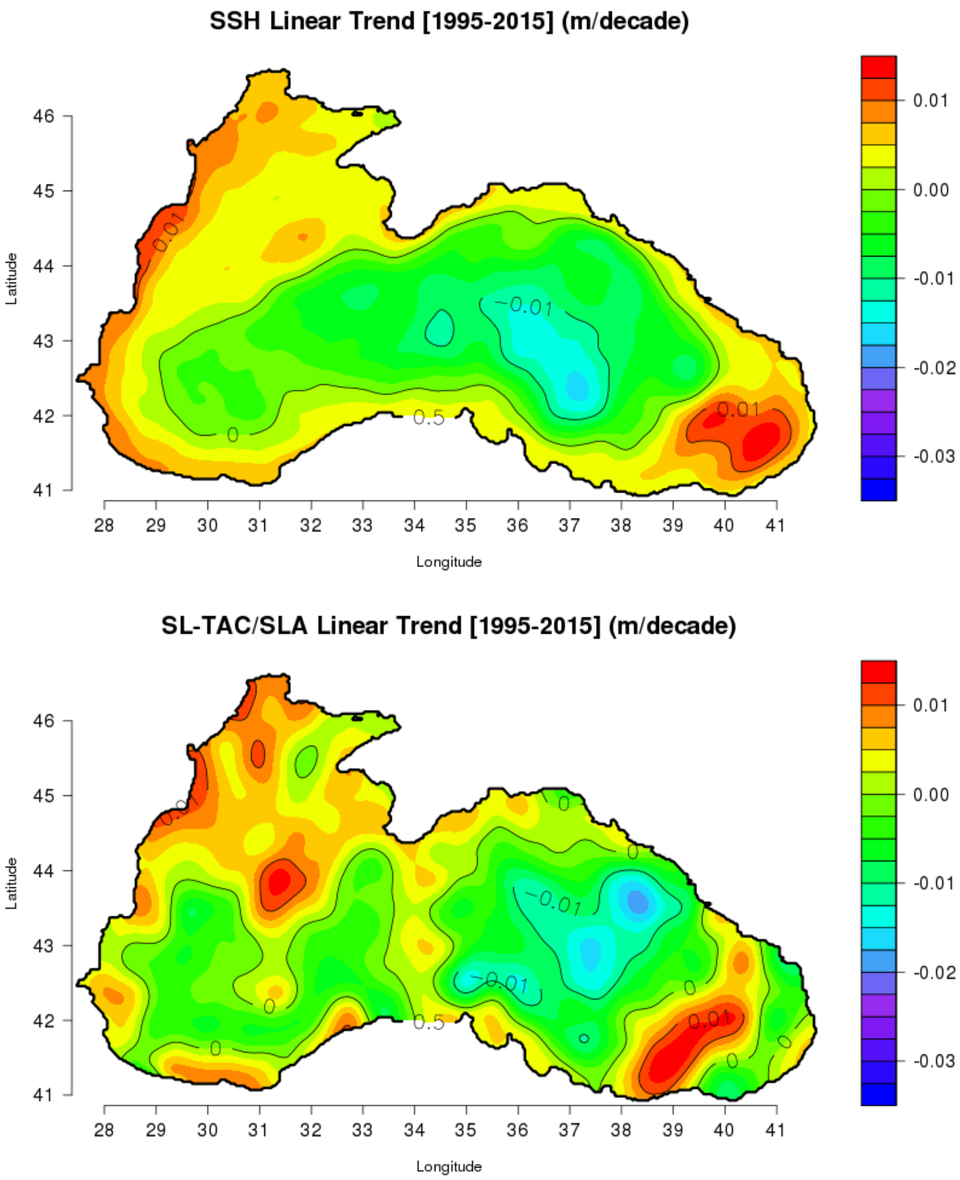

Figure IV-25. SL-CLASS1-TREND Maps of Sea Level linear trends over period 1995-2015 computed from the reanalysis BS-RAN-V4 (top panel) and from the CMEMS/SL-TAC reference dataset (bottom panel)

V COMPARATIVE PERFORMANCES BETWEEN BS-RAN-V4 AND BS-RAN-V3

Table V-1 Compared performance for reanalysis BS-RAN-V4 (new product), BS-RAN-V3 (previous QUID product) and BS-RAN-updV3 (previous delivered product) for different parameters and depth ranges over the entire time period 1995-2015 (first entry in red) and over 2005-2015 for temperature and salinity (second entry in blue). compares in detail the performance of the new BS-RAN-V4 reanalysis with respect to the previously delivered product BS-RAN-V3 (BS-RAN-updV3 being the effectively delivered reanalysis). The BS-RAN-V3 EANs are slightly improved, apparently except for the Satellite altimetry scores. As detailed in section IV.6, this apparent downgrade is due to a change in the SLA misfit bias calculation and removal. Owing to this change the performance of the BS-RAN-V4 system regarding the Altimetry cannot be achieved using the EANs scores provided in this table. We refer the reader to section IV.6 for a detailed discussion.

Parameter	**BIAS V4**	**BIAS upd-V3**	BIAS V3	**RMS V4**	**RMS upd-V3**	RMS V3
SST [°C]	-0.07 / -**0.068**	-0.08 / -0.075	-0.08 / X	0.576 / **0.586**	0.577 / 0.588	0.57
T [°C] 0-100	-0.02 / **0.025**	-0.06 / -0.015	-0.06 / -0.01	0.868 / **0.743**	0.879 / 0.752	0.87 / **0.76**
T [°C] 100-300	-0.03 / -**0.003**	-0.04 / -0.018	-0.04 / -0.02	0.155 / **0.087**	0.167 / 0.103	0.17 / **0.11**
T [°C] 300-800	-0.021 / -**0.022**	-0.024 / -0.027	-0.02 / -0.03	0.11 / **0.047**	0.112 / 0.05	0.10 / **0.05**
S [psu] 0-100	-0.014 / **0.002**	0.007 / 0.013	0.01 / 0.01	0.328 / **0.263**	0.349 / 0.292	0.36 / **0.31**
S [psu] 100-300	-0.006 / **0.009**	0.006 / 0.017	0.0 / 0.01	0.193/ **0.147**	0.203 / 0.171	0.20 / **0.17**
S [psu] 300-800	-0.005 / -**0.002**	0.002 / 0.005	0.004 / 0.007	0.047 / **0.032**	0.065 / 0.052	0.06 / **0.05**
SLA [cm]	0.055/ **0.045**	NA	NA	4.377/ **4.356**	3.679	4.38 3.68

Table V-1 Compared performance for reanalysis BS-RAN-V4 (new product), BS-RAN-V3 (previous QUID product) and BS-RAN-updV3 (previous delivered product) for different parameters and depth ranges over the entire time period 1995-2015 (first entry in red) and over 2005-2015 for temperature and salinity (second entry in blue).

VI SYSTEM'S NOTICEABLE EVENTS, OUTAGES OR CHANGES

Data assimilation system :

- Applies an ssh increment (EOFs statistical balance).
- New assessment of the Black Sea MDT based on a mean model SSH calculated over the reference time period 1992-2012.
- Modifies the SLA misfit bias calculation and removal.

Hydrodynamical model :

- Updated vertical diffusion parametrization.
- Strength of the restoring term to T/S climatology (LSBC) divided by a factor close to 2 between surface down to 800 m.

VII QUALITY CHANGES SINCE PREVIOUS VERSION

VII.1 Correction of the SSH trend

The BLKSEA_REANALYSIS_PHYS_007_004 product is proposed for the third time in the framework of Copernicus Marine Service with the aim to answer to the main user requirement, i.e. to have product time series of the last decades. The current delivered BS-RAN-V4 reanalysis extends back to 1995. A new set of EOFs is applied to assess the vertical T/S background error covariances. A new mean SSH was calculated over the reference period 1992-2012 to estimate the Black Sea MDT. Sea Surface Height increments are calculated and applied as a correction in NEMO. An improved SLA misfit bias calculation and removal is achieved to feed the data assimilation system. The BS-RAN-V4 EANs are slightly improved compared to the previous product BS-RAN-V3. The Satellite altimetry misfit skill scores appears downgraded but they cannot be compared between the two products owing to the change in the SLA misfit bias calculation. As detailed in section IV.6, the apparent downgrade is due to a necessary change in the SLA misfit bias calculation and removal. Owing to this change the Altimetry SLA scores cannot be compared with these scores. We refer the reader to section IV.6 for more information.

Due to the model constraint – the closed boundary at the Bosporus Strait – the SSH product is affected by a trend. This trend is in part due to the unbalance between the surface water flux and the flow conditions that are imposed at the Bosporus Strait, by using the current model configurations. We propose a de-trended product using a polynomial function to de-trend the model SSH, as shown in **Errore. L'origine riferimento non è stata trovata.**. In order to assess the accuracy of the SLA field (model SSH minus model MDT), the statistics are computed against the daily SLA gridded product (SEALEVEL_BS_PHY_L4_REP_OBSERVATIONS_008_042). We decide to validate the model SLA with respect to the gridded product because the de-trended approach is performed in the model space, as a post-processing step. That is, this approach considers the SSH values at the model grid, rather than at the along-track positions.

The use of the gridded product also allows a quasi-independent validation whereas it is possible to investigate how the model itself propagates the corrections from DA to other regions around the numerical domain. In contrast, there are a few along-tracks of SLA on the BS each day such that we expect sources of errors from the strategy that was employed to produce the daily gridded fields. The SLA gridded product provides spatial fields of errors and further information about its preparation can be found in http://marine.copernicus.eu/documents/QUID/CMEMS-SL-QUID-008-032-062.pdf. As a conclusion, the RMSD values that are presented in the Figure VII-3 can not directly be comparable with the values from the Figure IV-16, since the latter derive from misfits (altimetry data minus model at the observation locations) at the analysis step.

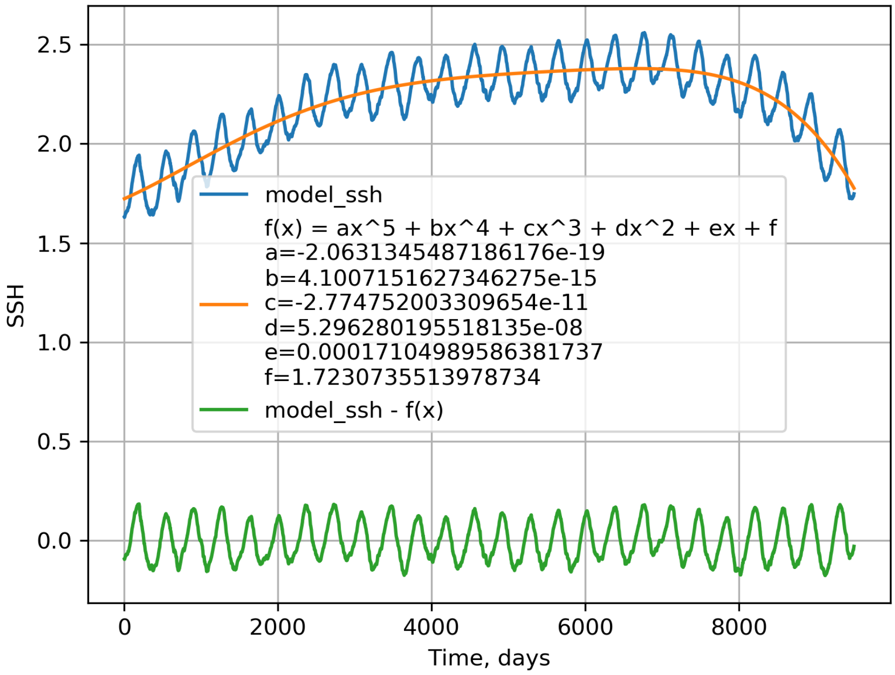

Figure VII-1. BS-PHY RAN basin-averaged SSH product time series (blue curve) and trend (orange curve) and after the de-trended procedure (green curve).

Figure VII-2. Basin-averaged SLA comparison using anomalies computed from BS-PHY RAN, by considering the detrended SSH (green line), original SSH fields (blue line). The red line indicates the SLA gridded product (SEALEVEL_BS_PHY_L4_REP_OBSERVATIONS_008_042).

shows the time series of the basin-averaged SLA from the BS-PHY RAN results and the SLA gridded product. The curves indicate that the de-trended SSH provides SLA fields in the same order of magnitude as compared to the SLA gridded product. Indeed, the values of SLA RMSD (Figure VII-3. SLA RMSE computed from the BS-PHY RAN results with respect to the SLA gridded product (SEALEVEL_BS_PHY_L4_REP_OBSERVATIONS_008_042), by considering the de-trended (green line) and original (blue line) SSH.

) computed from the BS-PHY RAN results against the gridded SLA exhibit that the application of the strategy to de-trend the SSH generates more accurate SLA fields, with the time-averaged RMSD indicating a reduction from 2.19 to 0.09 m.

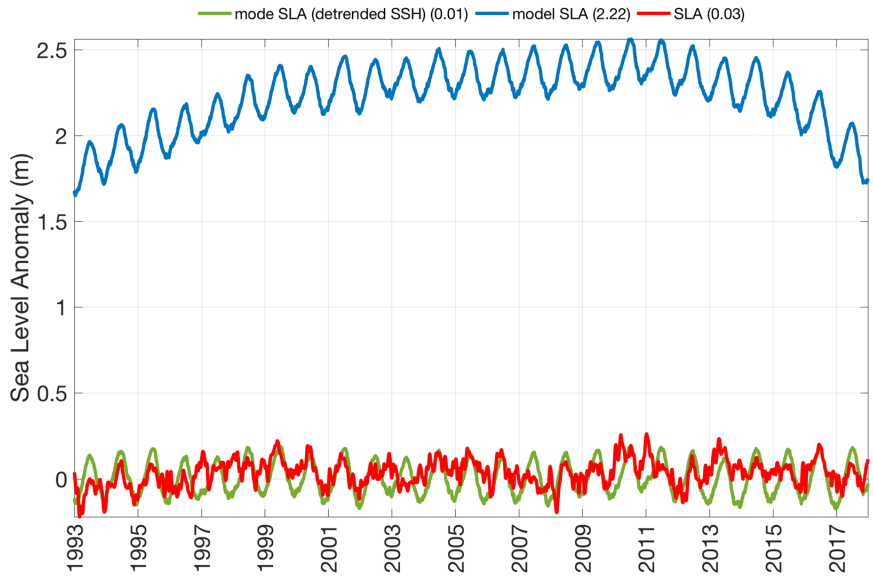

Figure VII-2. Basin-averaged SLA comparison using anomalies computed from BS-PHY RAN, by considering the detrended SSH (green line), original SSH fields (blue line). The red line indicates the SLA gridded product (SEALEVEL_BS_PHY_L4_REP_OBSERVATIONS_008_042).

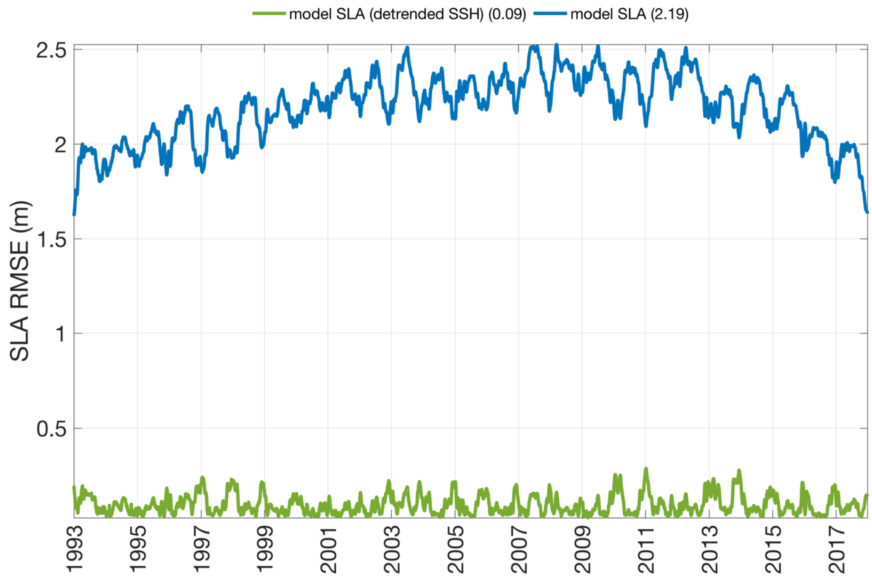

Figure VII-3. SLA RMSE computed from the BS-PHY RAN results with respect to the SLA gridded product (SEALEVEL_BS_PHY_L4_REP_OBSERVATIONS_008_042), by considering the de-trended (green line) and original (blue line) SSH.

VII.2 Validation results for the extension period: 2016 to 2018

Extension to year 2018 has been included to the previous reanalysis time series, that covered the time period between 1995 and 2015. After this extension, a consistency check was performed on the new years in order to assure the continuity in the quality of the reanalysis product. By using more robust tools to calculate the statistics, the results show that the quality of reanalysis did not changed significantly as it is shown in the Figures VII-4 to VII-13 and Table VII-1.

VII.2.1 Sea Surface Temperature

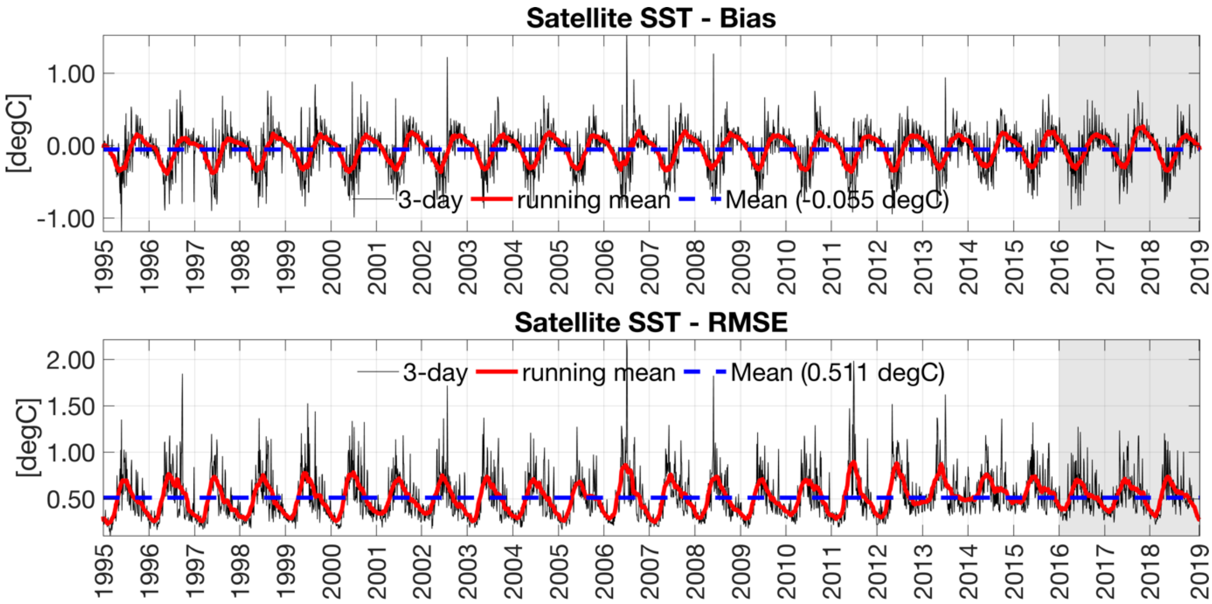

Figure VII-4. SST-CLASS4-BIAS-MONTHLY (top panel) and SST-CLASS4-RMSE-MONTHLY (bottom panel) showing time series of basin averaged SST misfit BIAS and RMSE computed from reanalysis product and satellite observations. The grey shading indicates the period of extension.

VII.2.2 Temperature

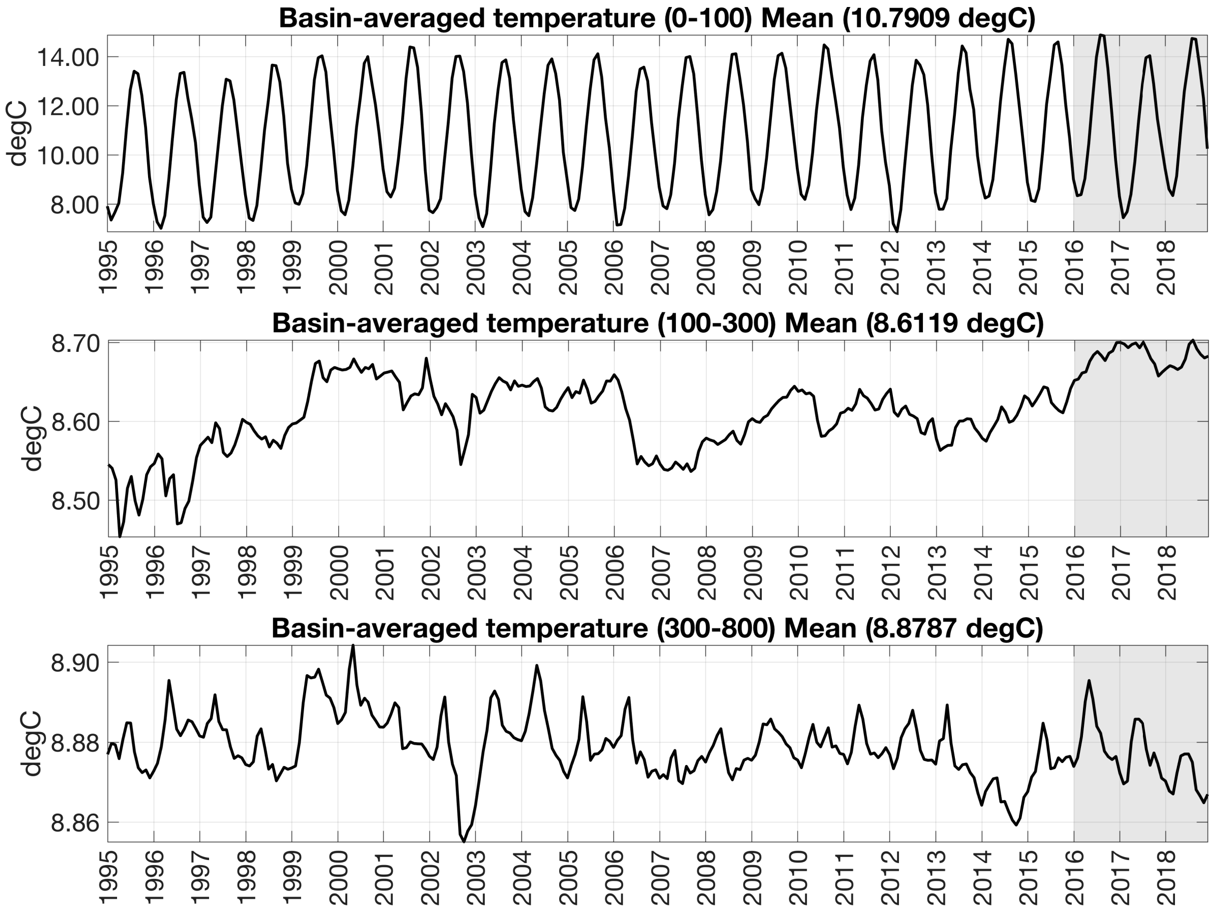

Figure VII-5. T-CLASS3-LAYERS showing the basin-averaged layer temperature in the three selected layers 0-100 m (top panel), 100-300 m (middle panel), 300-800 m (bottom panel). The grey shading indicates the period of extension.

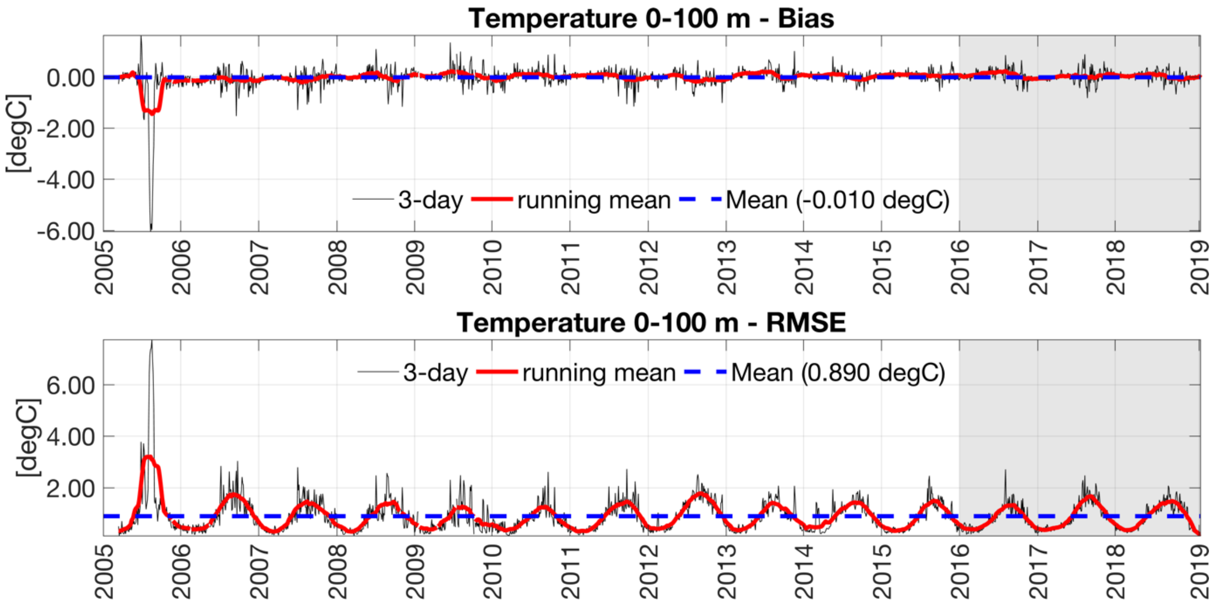

Figure VII-6. T-CLASS4-BIAS-LAYERS (top panel) and T-CLASS4-RMSE-LAYERS (bottom panel): time series of the BIAS and RMSE computed from the misfits between temperature observations and reanalysis product in 0-100 m. Black and red lines refer to 3-day and running mean statistics (15-day window), respectively. The grey shading indicates the period of extension.

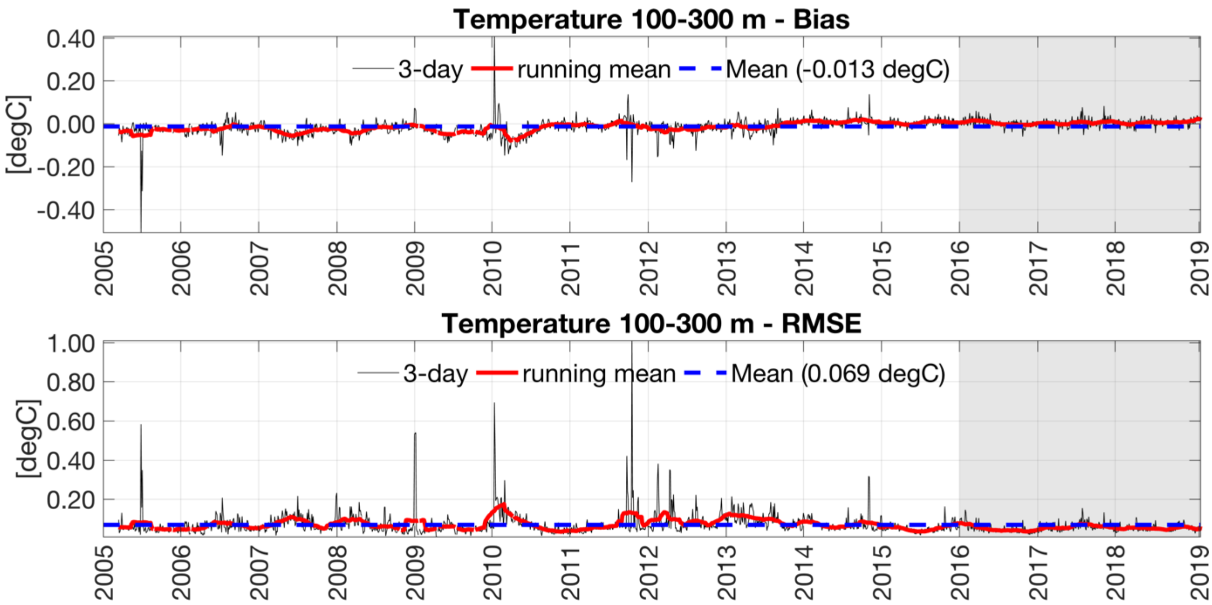

Figure VII-7. T-CLASS4-BIAS-LAYERS (top panel) and T-CLASS4-RMSE-LAYERS (bottom panel): time series of the BIAS and RMSE computed from the misfits between temperature observations and reanalysis product in 100-300 m. Black and red lines refer to 3-day and running mean statistics (15-day window), respectively. The grey shading indicates the period of extension.

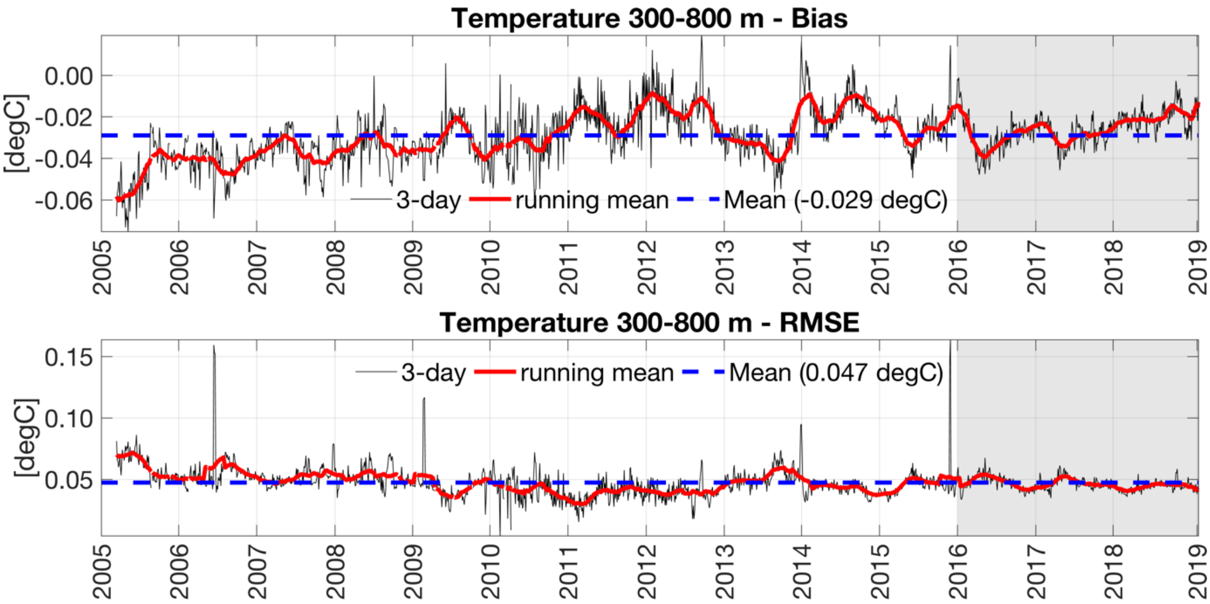

Figure VII-8. T-CLASS4-BIAS-LAYERS (top panel) and T-CLASS4-RMSE-LAYERS (bottom panel): time series of the BIAS and RMSE computed from the misfits between temperature observations and reanalysis product in 300-800 m. Black and red lines refer to 3-day and running mean statistics (15-day window), respectively. The grey shading indicates the period of extension.

VII.2.3 Salinity

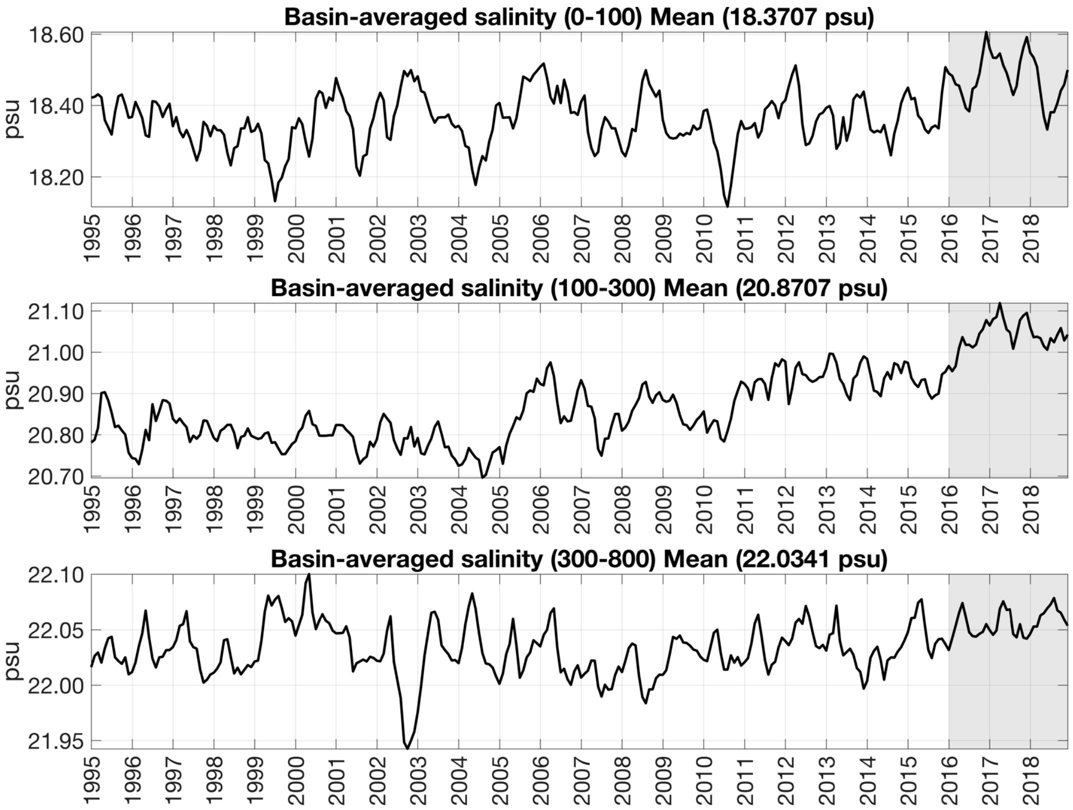

Figure VII-9. S-CLASS3-LAYERS showing the basin-averaged layer salinity in the three selected layers 0-100 m (top panel), 100-300 m (middle panel), 300-800 m (bottom panel). The grey shading indicates the period of extension.

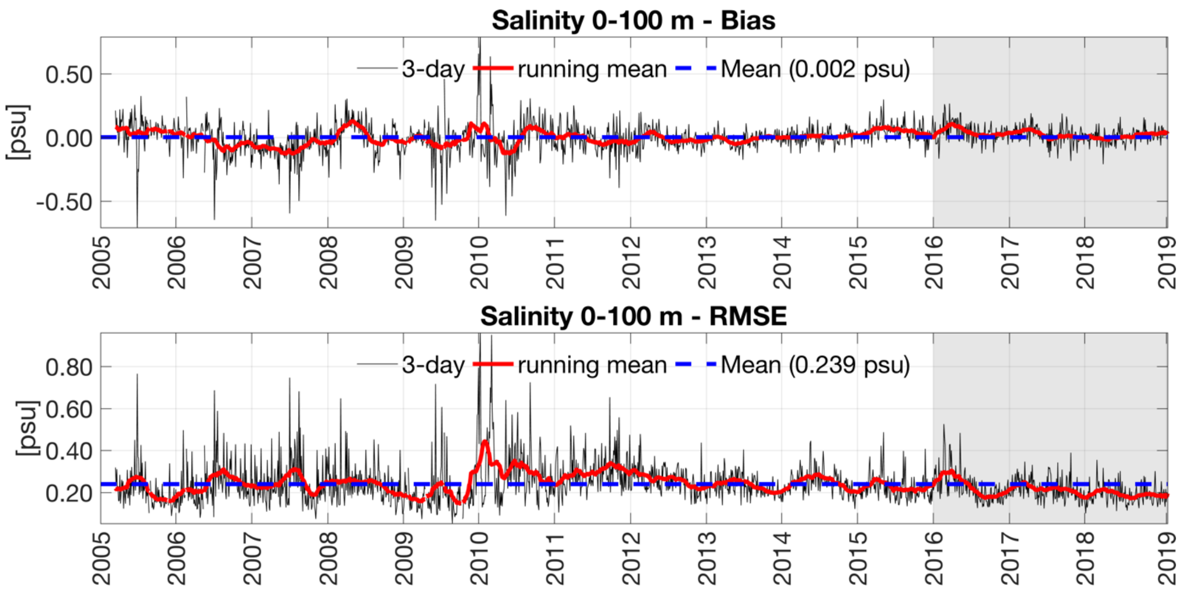

Figure VII-10. S-CLASS4-BIAS-LAYERS (top panel) and S-CLASS4-RMSE-LAYERS (bottom panel): time series of the BIAS and RMSE computed from the misfits between salinity observations and reanalysis product in 0-100 m. Black and red lines refer to 3-day and running mean statistics (15-day window), respectively. The grey shading indicates the period of extension.

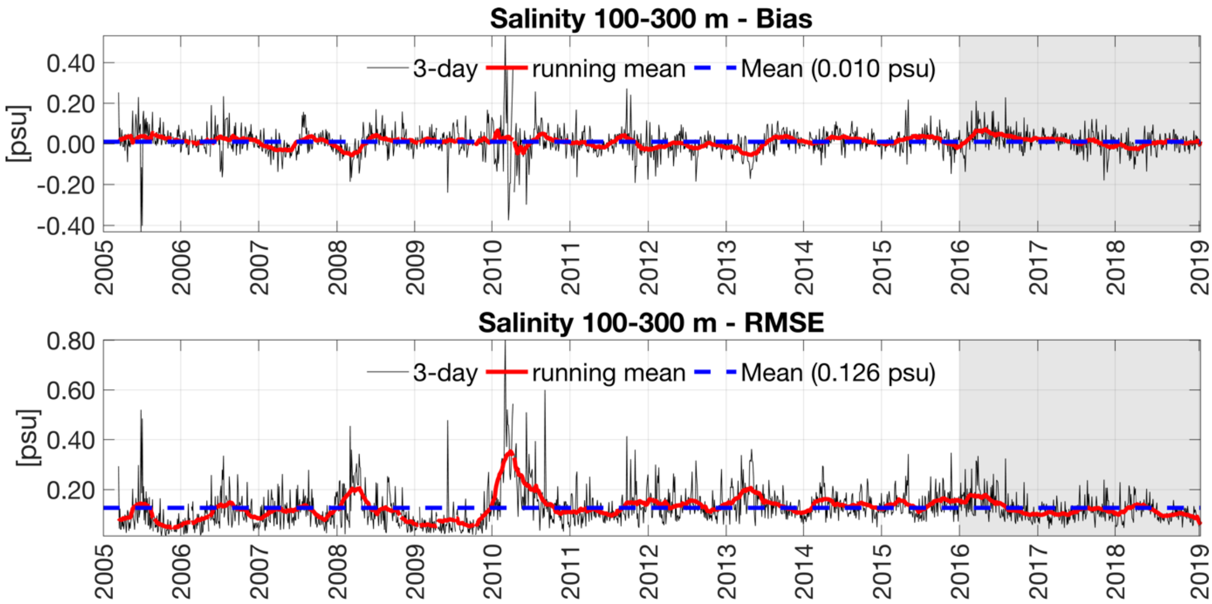

Figure VII-11. S-CLASS4-BIAS-LAYERS (top panel) and S-CLASS4-RMSE-LAYERS (bottom panel): time series of the BIAS and RMSE computed from the misfits between salinity observations and reanalysis product in 100-300 m. Black and red lines refer to 3-day and running mean statistics (15-day window), respectively. The grey shading indicates the period of extension.

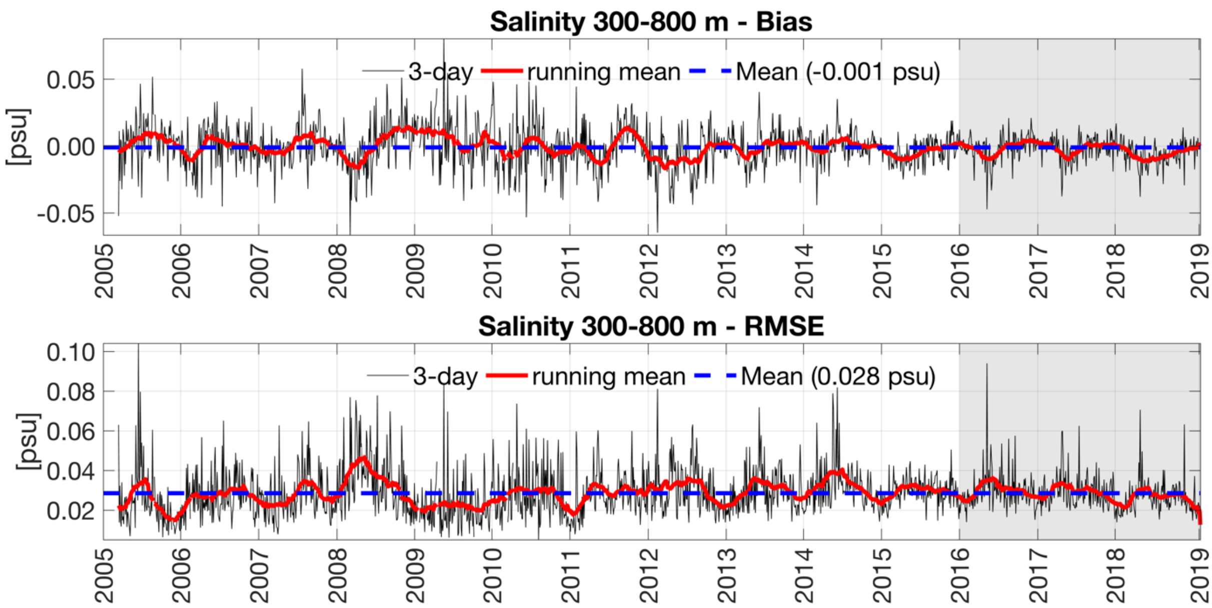

Figure VII-12. S-CLASS4-BIAS-LAYERS (top panel) and S-CLASS4-RMSE-LAYERS (bottom panel): time series of the BIAS and RMSE computed from the misfits between salinity observations and reanalysis product in 300-800 m. Black and red lines refer to 3-day and running mean statistics (15-day window), respectively. The grey shading indicates the period of extension.

VII.2.4 Sea Level

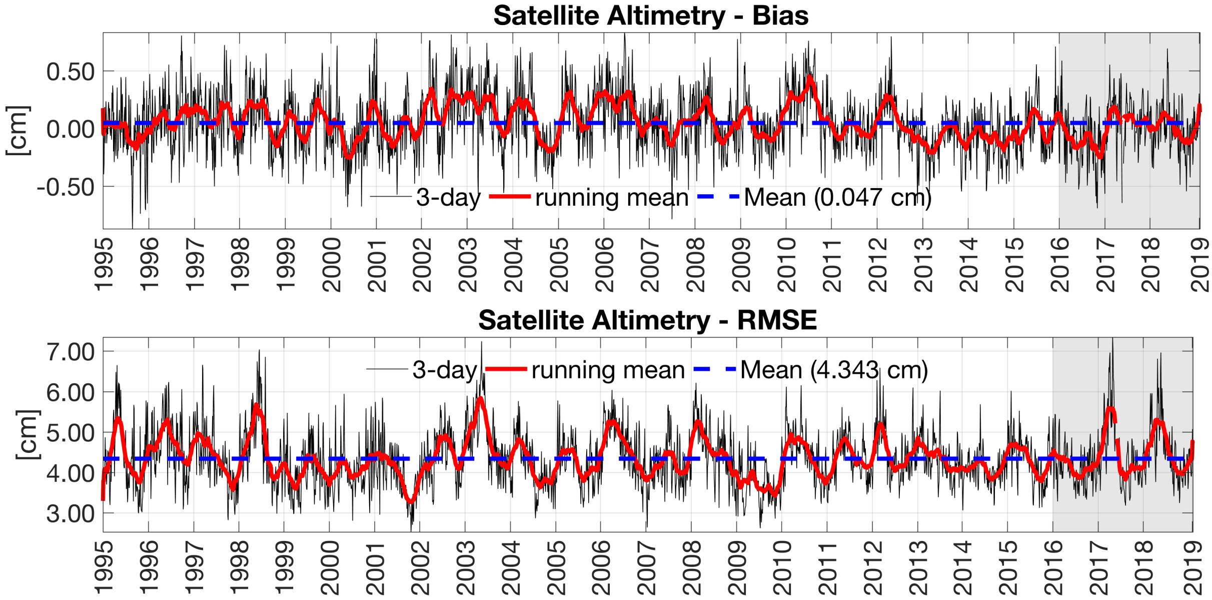

Figure VII-13. SL-CLASS4-BIAS-MONTHLY (top panel) and SL-CLASS4-RMSE-MONTHLY (bottom panel) showing time series of basin-averaged SLA misfit BIAS and RMSE computed from reanalysis product and satellite observations. The grey shading indicates the period of extension.

VII.2.5 Average Statistics

Table VII-1. Average statistics computed from the misfits (difference between observations and model at observations points). The black values indicate the statistics including the period of extension: the years 2016 to 2018 and January of 2019.

Parameter	Time period	BIAS	RMSE
SST [degC]	1995-2015	-0.074	0.576
	1995-Jan2019	-0.055	0.511
T [degC] 0-100 m	1995-2015	-0.018	0.868
	2005-2015	0.025	0.743
	2005-Jan2019	-0.010	0.890
T [degC] 100-300 m	1995-2015	-0.032	0.155
	2005-2015	-0.003	0.087
	2005-Jan2019	-0.013	0.069
T [degC] 300-800 m	1995-2015	-0.021	0.110
	2005-2015	-0.022	0.047
	2005-Jan2019	-0.029	0.047
S [psu] 0-100 m	1995-2015	-0.014	0.328
	2005-2015	0.002	0.263
	2005-Jan2019	0.002	0.239
S [psu] 100-300 m	1995-2015	-0.006	0.193
	2005-2015	0.009	0.147
	2005-Jan2019	0.010	0.126
S [psu] 300-800 m	1995-2015	-0.005	0.047
	2005-2015	-0.002	0.032
	2005-Jan2019	-0.001	0.028
SLA [cm]	1995-2015	0.055	4.377
	1995-Jan2019	0.047	4.343

VIII APPENDIX

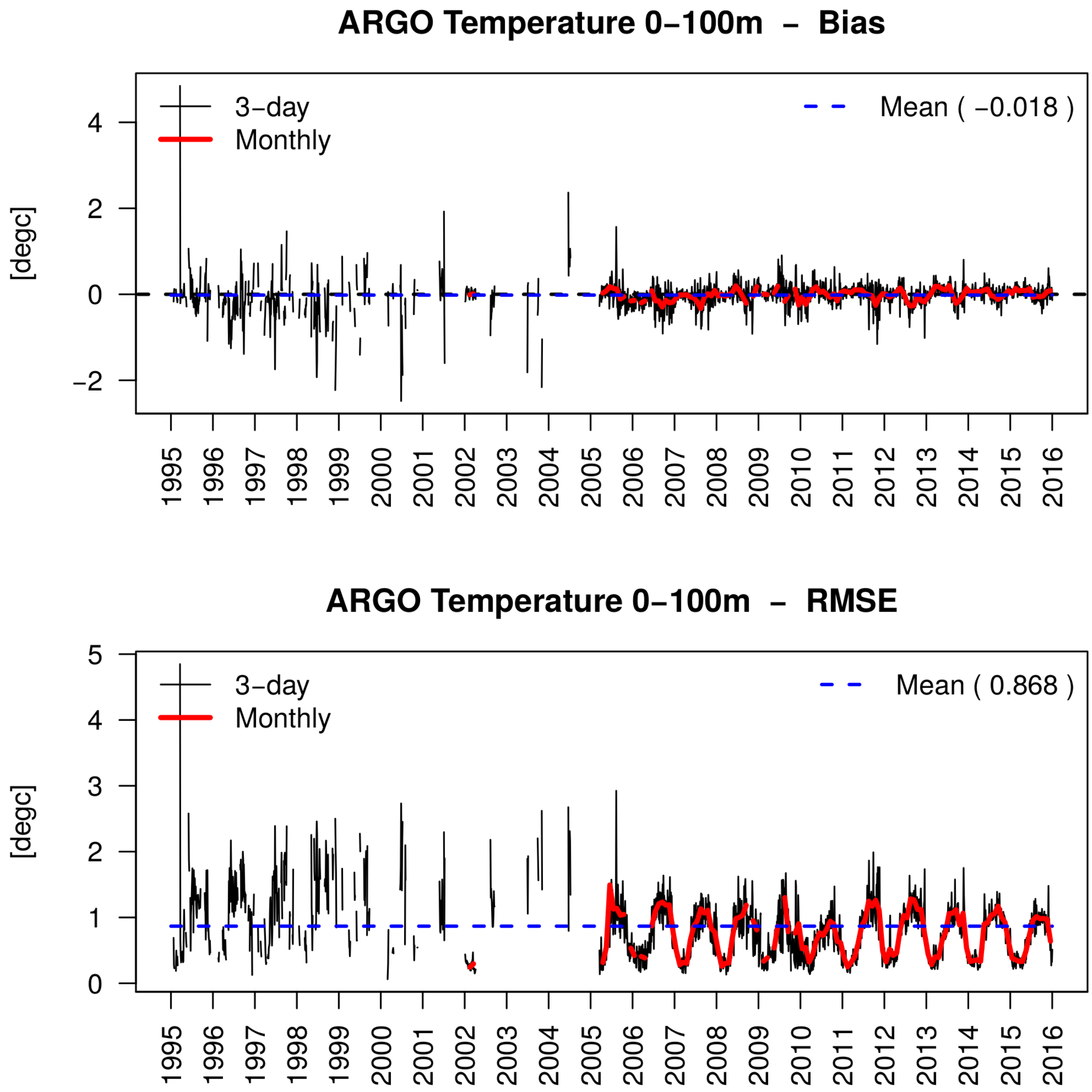

Figure VIII-1. T-CLASS4-BIAS-LAYERS and T-CLASS4-RMSE-LAYERS showing timeseries of BIAS and RMSE computed from misfits of temperature observations versus the reanalysis product in the three different layers 0-100 (1), 100-300 (2) and 300-800 (3) m over time period 1995-2015. Black and red lines refer to 3-day and monthly statistics, respectively (continues in next page).

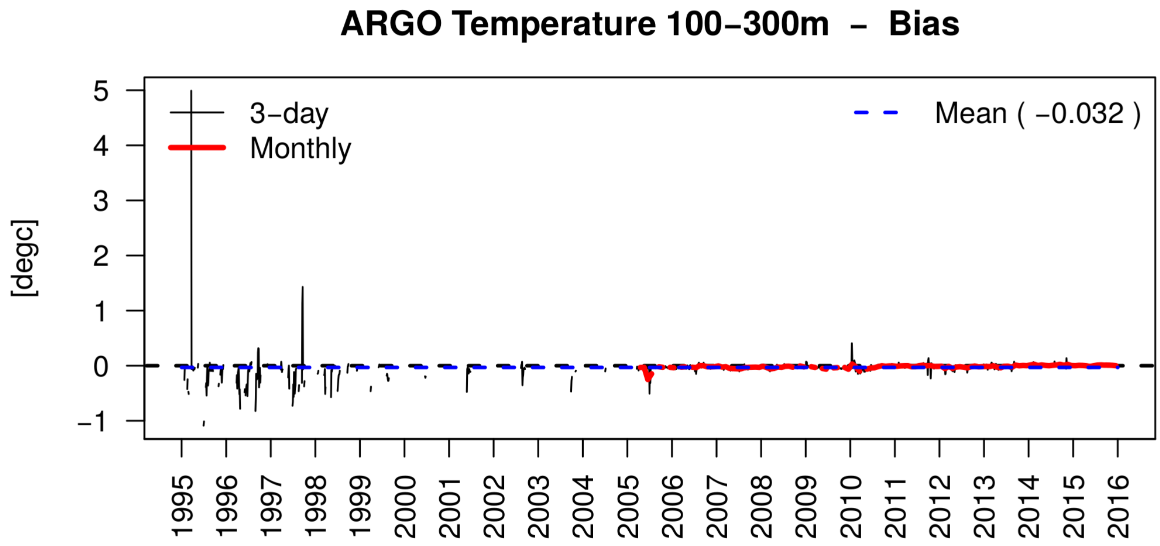

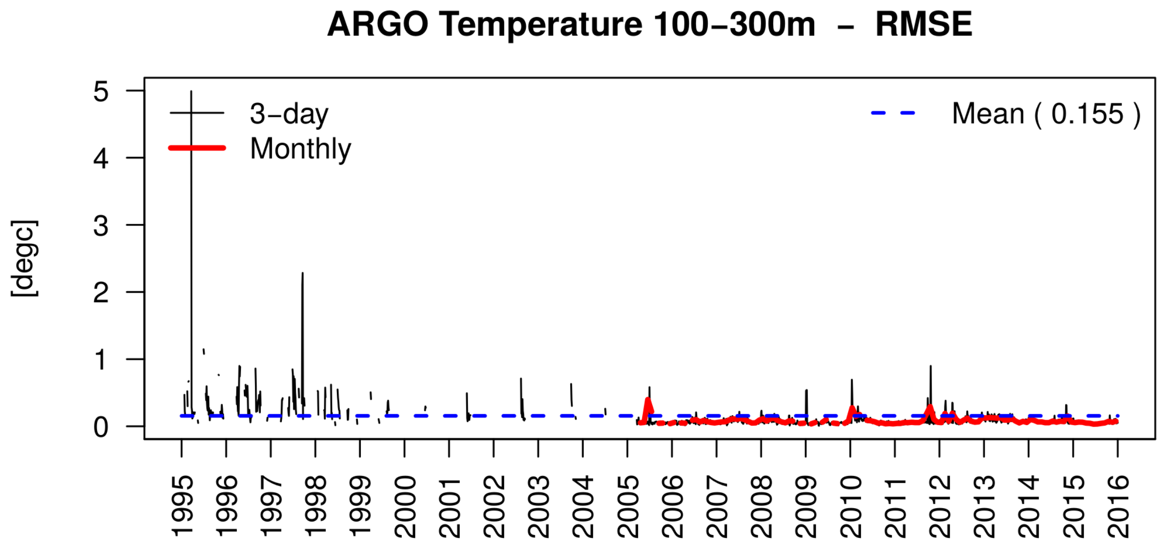

Figure VIII-2. T-CLASS4-BIAS-LAYERS and T-CLASS4-RMSE-LAYERS showing timeseries of BIAS and RMSE computed from misfits of temperature observations versus the reanalysis product in the three different layers 0-100 (1), 100-300 (2) and 300-800 (3) m over time period 1995-2015. Black and red lines refer to 3-day and monthly statistics, respectively (continues in next page).

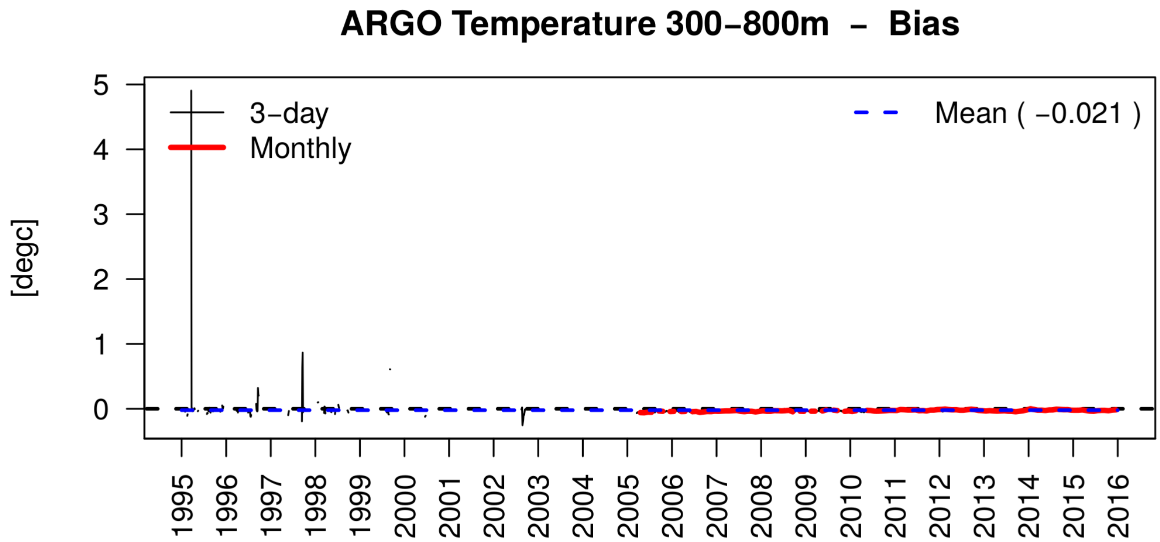

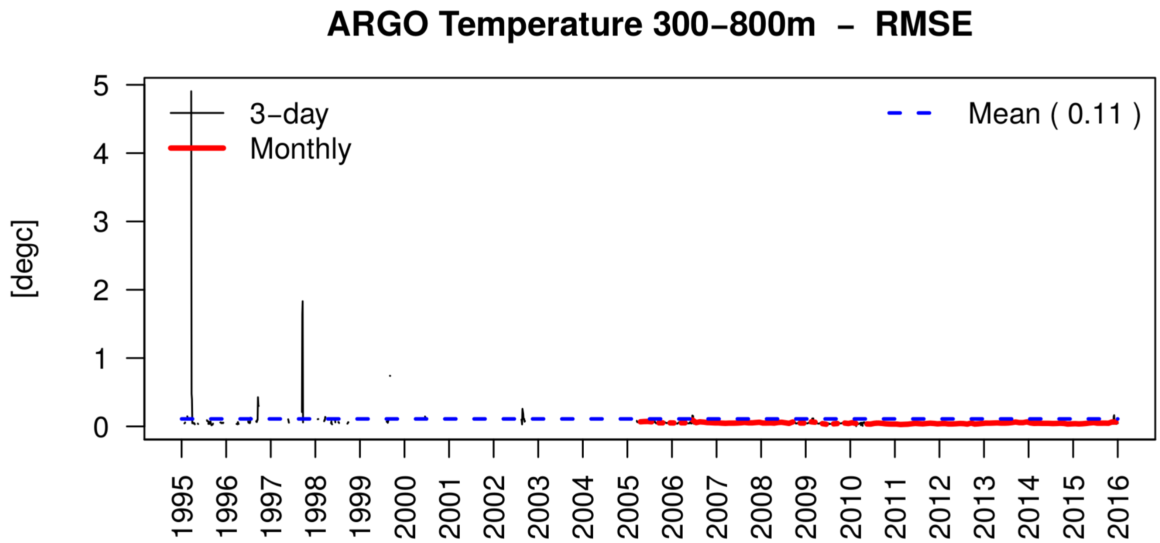

Figure VIII-3. T-CLASS4-BIAS-LAYERS and T-CLASS4-RMSE-LAYERS showing timeseries of BIAS and RMSE computed from misfits of temperature observations versus the reanalysis product in the three different layers 0-100 (1), 100-300 (2) and 300-800 (3) m over time period 1995-2015. Black and red lines refer to 3-day and monthly statistics, respectively.

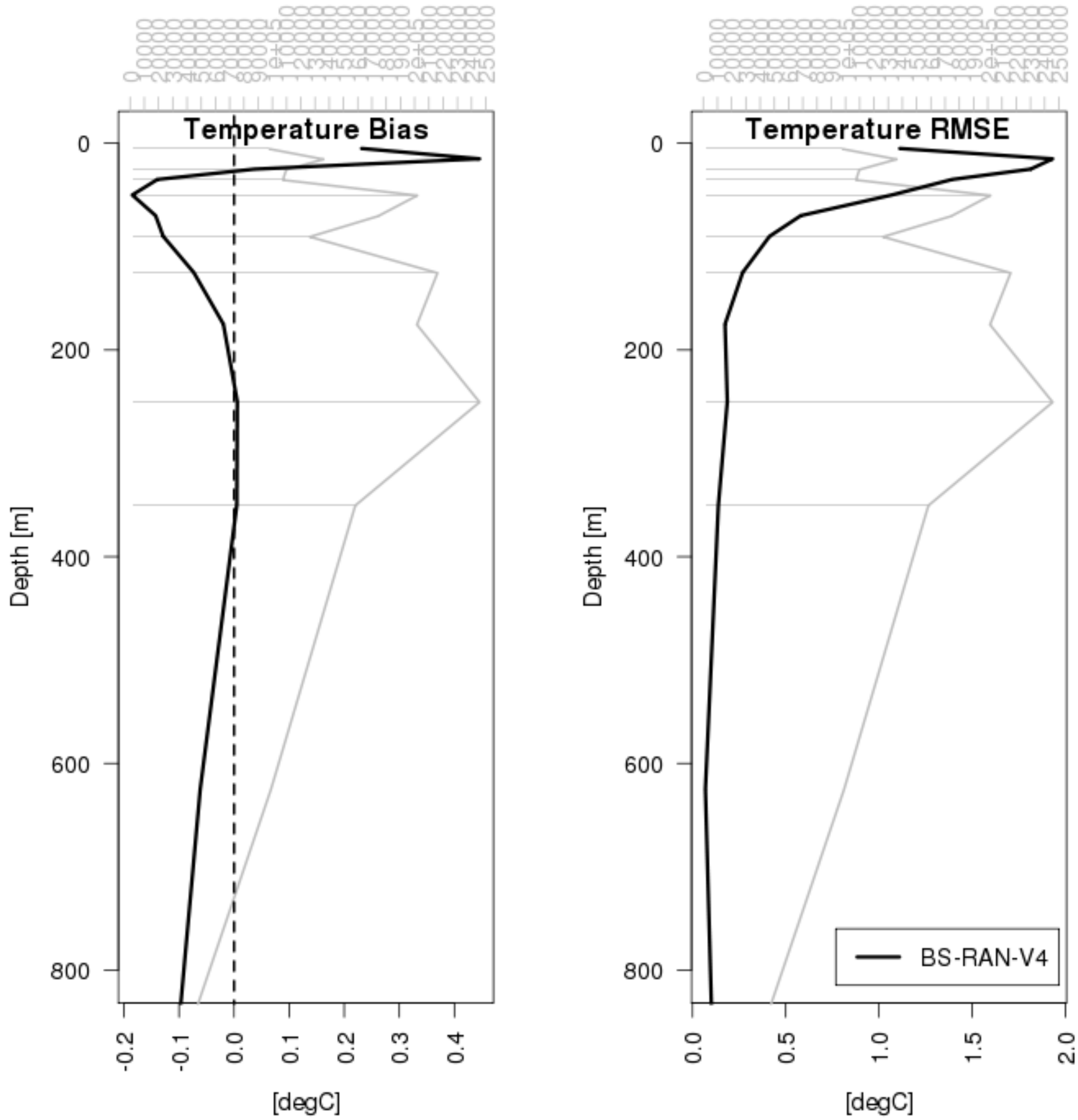

Figure VIII-4. T-CLASS4-BIAS-DEPTH and T-CLASS4-RMS-DEPTH computed from reanalysis misfits for time period 1995-2015. Number of observations is shown in grey.

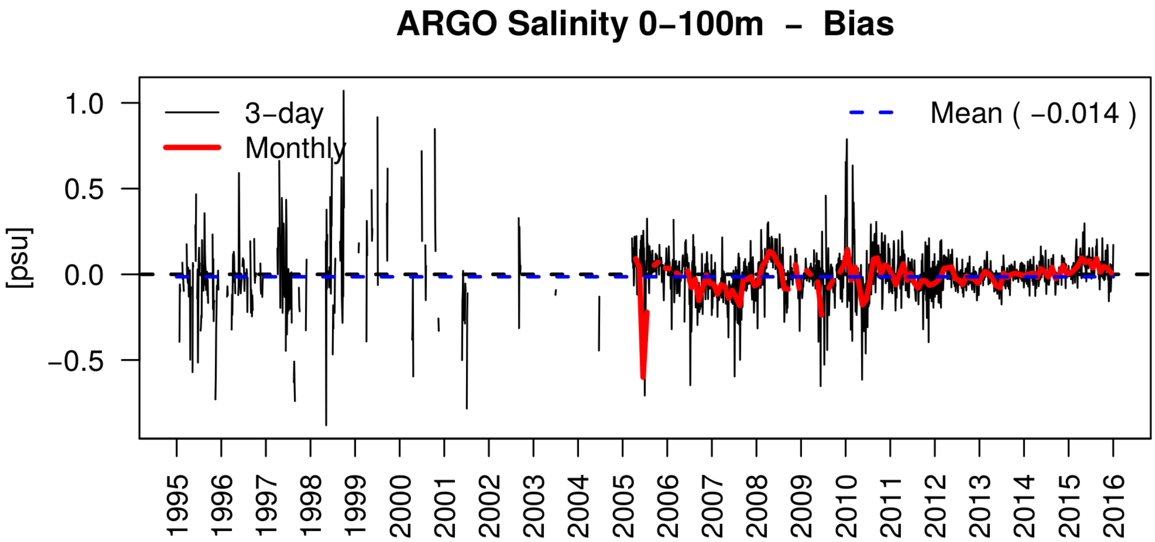

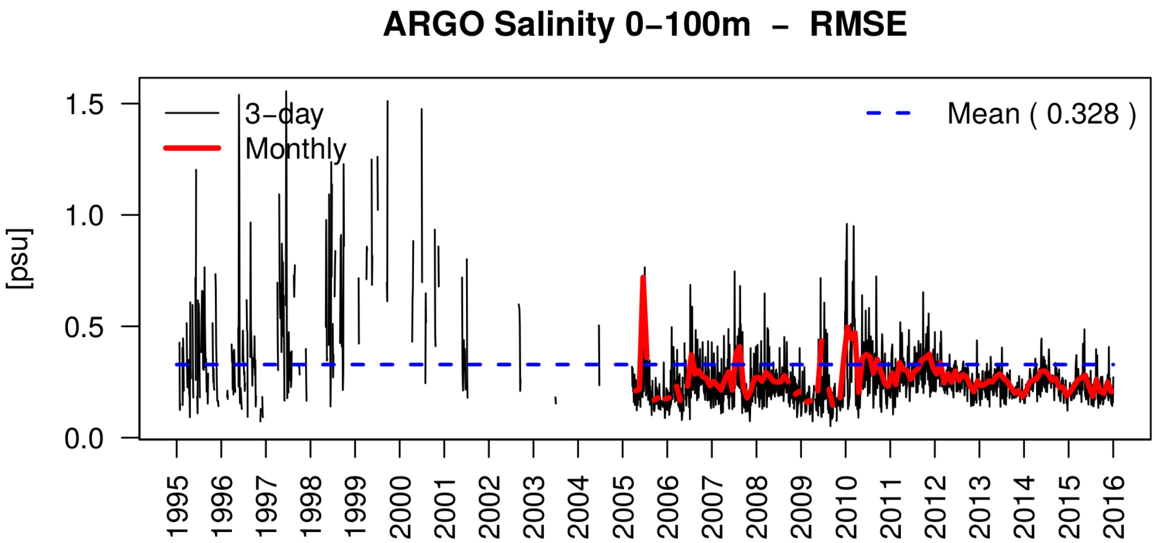

Figure VIII-5. S-CLASS4-RMS-LAYERS computed from misfits of reanalysis product in different layers for time period 1995-2015 (continues in next page).

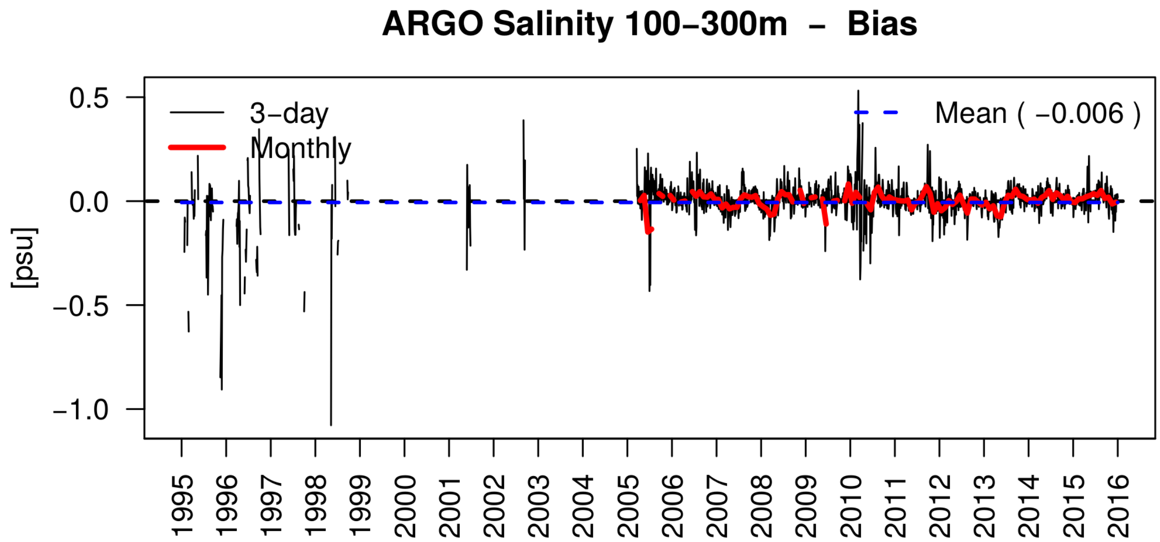

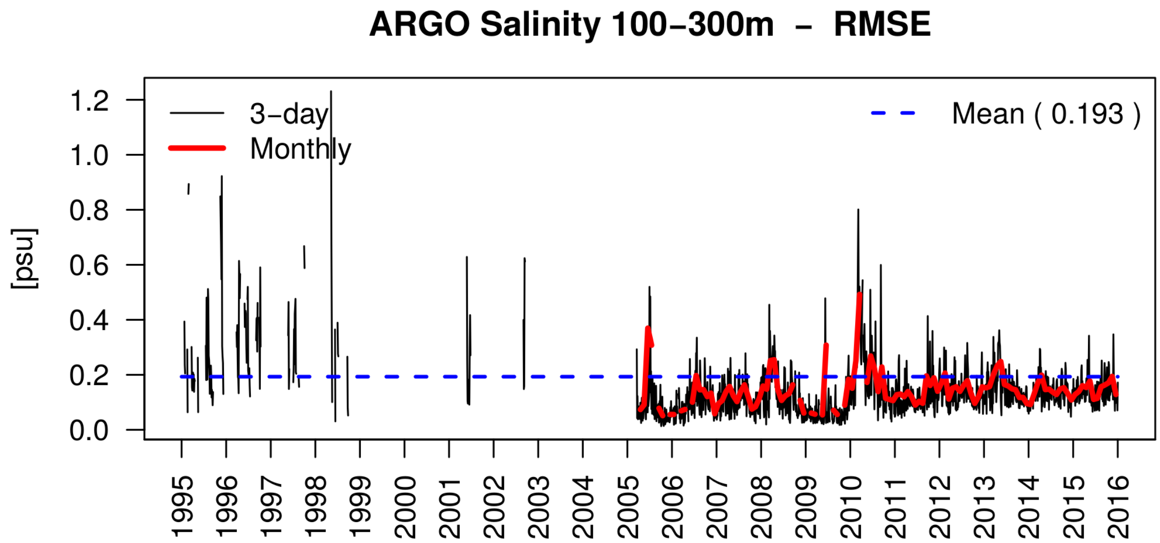

Figure VIII-6. S-CLASS4-RMS-LAYERS computed from misfits of reanalysis product in different layers for time period 1995-2015 (continues in next page).

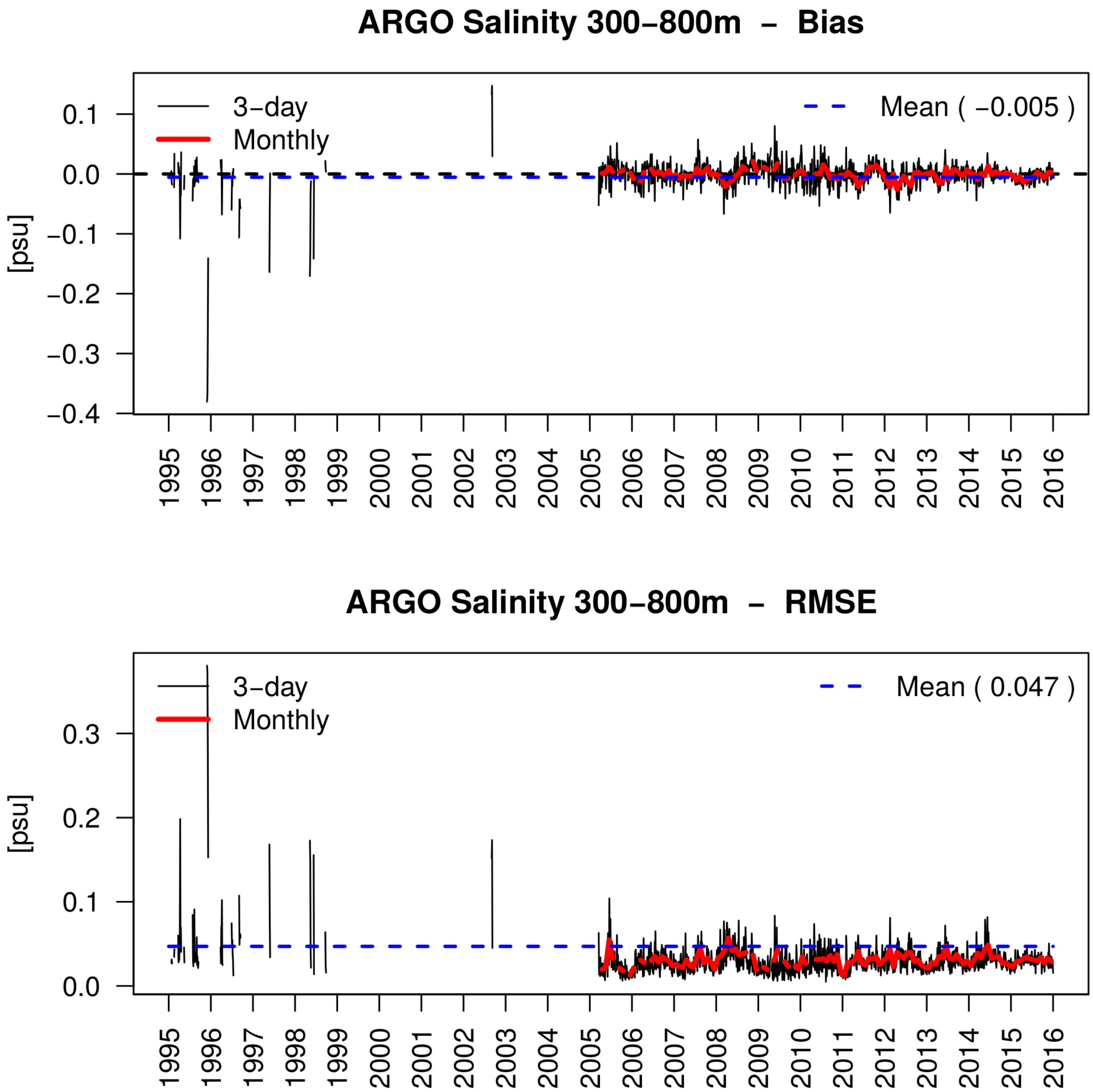

Figure VIII-7. S-CLASS4-RMS-LAYERS computed from misfits of reanalysis product in different layers for time period 1995-2015.

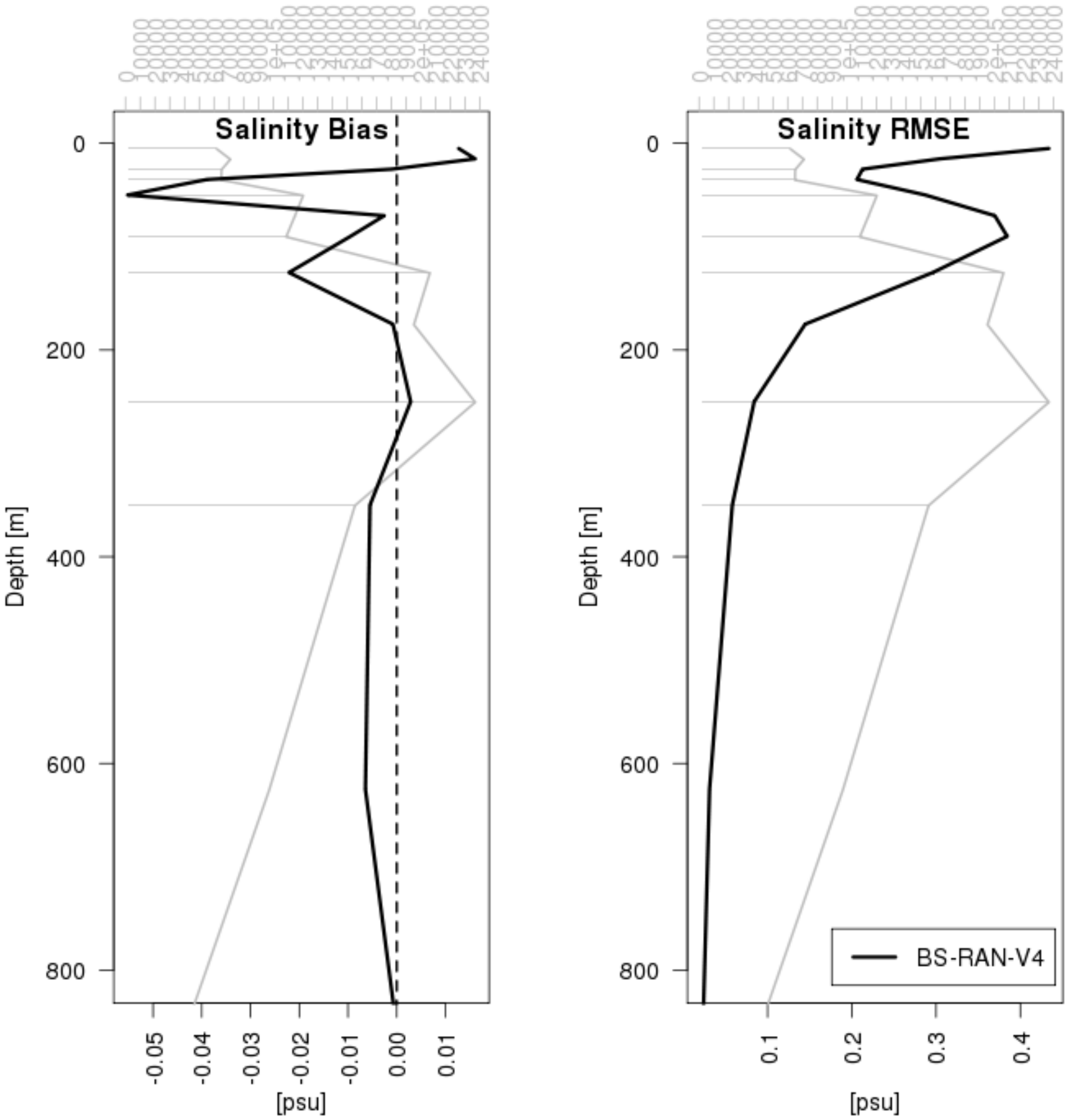

Figure VIII-8. S-CLASS4-BIAS-DEPTH and S-CLASS4-RMS-DEPTH computed from reanalysis misfits for time period 1995-2015. Number of observations is shown in grey.

IX REFERENCES

Adler, R.F., G.J. Huffman, A. Chang, R. Ferraro, P. Xie, J. Janowiak, B. Rudolf, U. Schneider, S. Curtis, D. Bolvin, A. Gruber, J. Susskind, P. Arkin, E. Nelkin 2003: The Version 2 Global Precipitation Climatology Project (GPCP) Monthly Precipitation Analysis (1979-Present). J. Hydrometeor., 4,1147-1167.

Courtier, P., 1997: Variational methods. J. Meteor. Soc. Japan, 75, 211–218.

Dee, Dick P., Bias and data assimilation, Quaterly Journal of the Royal Meteorological Scociety , 2005, Wiley Online Library, Volume 131-613, pp. 3323-3343

Dobricic S.; N. Pinardi, An oceanographic three-dimensional variational data assimilation scheme, OCEAN MODELLING, 2008, 22, pp. 89-105.

Farina, R., Dobricic, S., Storto, A., Masina, S., Cuomo, S. (2015), A revised scheme to compute horizontal covariances in an oceanographic 3D-VAR assimilation system, Journal of Computational Physics, Volume 284, 1 March 2015, Pages 631-647.

Grayek, S., Stanev, E.V. & Kandilarov, R. Ocean Dynamics (2010) 60: 123. doi:10.1007/s10236-009-0249-7

Huffman, G.J, R.F. Adler, D.T. Bolvin, G. Gu 2009: Improving the Global Precipitation Record: GPCP Version 2.1. Geophys. Res. Lett., 36,L17808, doi:10.1029/2009GL040000.

Ludwig W., E. Dumont, M. Meybeck, and S. Heussner, 2009. River discharges of water and nutrients to the Mediterranean and Black Sea: Major drivers for ecosystem changes during past and future decades? Progress in Oceanography, 80, 199-217.

Madec G and the NEMO team (2012) NEMO ocean engine version 3.4. Note du Pole de la Modelisation de l'Insitut Pierre-Simon Laplace No 27 ISSN no 1288-1619.

Peneva, E. L., E. Stanev, V. Belokopytov, and P.Y. Le Traon, 2001. Water transport in the Bosporus Straits estimated from hydro-meteorologycal and altimeter data: Seasonal to decadal variability. J. Mar. Sys., 31, 1-3, 21-35.

Stanev E. and J.M. Beckers, 1999. Barotropic and baroclinic oscillations in strongly stratified ocean basins: Numerical study of the Black Sea. Journal of Marine Systems, 19, 65-112.

Storto, A., S. Dobricic, S. Masina, and P. Di Pietro, 2011: Assimilating along-track altimetric observations through local hydrostatic adjustments in a global ocean reanalysis system. Mon. Wea. Rev. 139, 738-754.

Storto A., Masina S., Dobricic S., 2014. Estimation and impact of non-uniform horizontal correlation length scales for Global Ocean physical analyses. J. Atmos. Ocean. Technol., 31: 2330-2349.